University of Windsor

Scholarship at UWindsor

Electronic Theses and Dissertations

Theses, Dissertations, and Major Papers

2013

Radiative Decay Rates of Metastable Triplet Helium and Heliumlike Ions

Lauren L. Moffatt
University of Windsor

Follow this and additional works at: https://scholar.uwindsor.ca/etd

Radiative Decay Rates of Metastable Triplet Helium and Heliumlike Ions

by

Lauren Moffatt

A Dissertation
Submitted to the Faculty of Graduate Studies
through the Department of Physics in Partial Fulfillment
of the Requirements for the Degree of Doctor of Philosophy at the
University of Windsor

Windsor, Ontario, Canada
2013

Radiative Decay Rates of Metastable Triplet Helium and Heliumlike Ions

by

Lauren Moffatt

APPROVED BY:

T. Kirchner, External Examiner
York University

R. Frost
School of Computer Science

C. Rangan
Department of Physics

W. Kedzierski
Department of Physics

G. W. F. Drake, Advisor
Department of Physics

April 23rd, 2013

Authors Declaration of Originality

I hereby certify that I am the sole author of this thesis and that no part of this thesis has been published or submitted for publication.

I certify that, to the best of my knowledge, my thesis does not infringe upon anyones copyright nor violate any proprietary rights and that any ideas, techniques, quotations, or any other material from the work of other people included in my thesis, published or otherwise, are fully acknowledged in accordance with the standard referencing practices. Furthermore, to the extent that I have included copyrighted material that surpasses the bounds of fair dealing within the meaning of the Canada Copyright Act, I certify that I have obtained a written permission from the copyright owner(s) to include such material(s) in my thesis and have included copies of such copyright clearances to my appendix.

I declare that this is a true copy of my thesis, including any final revisions, as approved by my thesis committee and the Graduate Studies office, and that this thesis has not been submitted for a higher degree to any other University or Institution.

Abstract

The metastable $1s2s\,^3S_1$ state of helium is the longest-lived neutral atomic state with a lifetime of 7859 seconds. This property has important astrophysical applications in the determination of temperature and density conditions in low density sources such as planetary nebulae.

This lifetime is determined by single photon relativistic magnetic dipole (M1) transition rates and is evaluated numerically using large basis size variational Hylleraas wave functions for all the heliumlike ions through the isoelectronic sequence up to Ar^{+16}. The coefficients of a $\frac{1}{Z}$ expansion, based on the results from the variational calculation, are evaluated up to ninth order with the zeroth and first order coefficients being determined analytically. This $\frac{1}{Z}$ expansion is used to evaluate the lowest order M1 transition rates for heliumlike ions through the isoelectronic sequence from K^{+17} to Fm^{+98}. The results for helium are compared with experimental measurements by Moos and Woodsworth(1975), recent experimental results by Hodgman et al.(2009) and high precision numerical calculations by Łach and Pachucki (2001). For heliumlike ions, results are compared with several electron beam ion trap measurements for heliumlike lithium, carbon, oxygen, neon, and sulfur.

This value of the $1s2s\,^3S_1 \rightarrow 1s^2\,^1S_0$ transition rate evaluated in this work is $1.2724255998(6)\times 10^{-4}$ s^{-1}, where the uncertainty in this result is given in parentheses.

This work is dedicated to the people who accepted me for who I am.
Thank you!

Acknowledgements

I would like to thank, first and foremost, my supervisor Dr. Gordon Drake for giving me the opportunity to further my knowledge and career. It is important that he knows how I much appreciate his near infinite patience and understanding. Additionally, I would like to thank him, and the Department of Physics at the University of Windsor, for the financial support I needed to complete my studies.

I would like to extend my appreciation to all the fellow graduate students, past and present, with whom I have had the benefit of working with and learning from. Specifically, I would like to thank the current members of Dr. Drake's research group, Eva Schulhoff, Mike Busuttil, Amirreza Moini, Dr. Atef Titi, and Dr. Qixue "Charles" Wu.

Of course I would like to thank my partner, Dr. Vanessa Chong, for her love and acceptance, and for all that she has had to put up with while this work was being done. Finally, I would like to thank my family and friends, of whom there are too many to be mentioned, for their friendship, support, and acceptance.

Contents

List of Figures

List of Tables

Chapter 1

Introduction

Speculations of interest in atomic theory have been attributed, as far back in history as the Trojan Wars, to a Greek figure known as Mochus of Sidon. As far back as the sixth century BCE, [1] the concept of indivisble bits of matter known as *paramanu* (atoms) had been proposed by the Hindu sage Kanada. A formal atomic theory is first attributed to Leucippus and his student Democritus in ancient Greece during the fifth century BCE. Needless to say, the study of atomic structure, and indeed the nature of matter itself, is not a new concept and has been of interest for thousands of years.

Not until the 20th century, due to the work of physicists such as Bohr and Heisenberg, were theories developed that describe the quantum mechanical world (and have the ability to explain atomic structure and behaviour with any level of accuracy). The simplest quantum mechanical system is the hydrogen atom, which consists of only a proton and an electron. We refer to this type of a system as a two body system, and it is possible, at least in a nonrelativistic approximation, to describe analytically the hydrogen atom or any other two body problem exactly. The second simplest quantum mechanical system is the helium atom, which consists of a single nucleus and two electrons (i.e. helium is a three body quantum

---

[1] The dating of this is under contention and could be closer to second century BCE.

mechanical system). By increasing the number of bodies in our system from two to three we have lost the ability to solve the system analytically. While we have lost mathematical simplicity, we continue to study helium and heliumlike ions because we gain a vast amount of information about the structure of more complicated multielectron atomic systems while maintaining the *second simplest* level of mathematical complexity.

1.1 Metastable States

Metastable states in atomic physics refer to those states which have appreciably long life times, sometimes on the order of seconds and, to be calculated in this work, even up to several thousand seconds. Typically metastable states are those states for which transitions to the ground state are forbidden by the electric dipole ($E1$) selection rules. The use of the word *forbidden* is a misnomer, as these transitions do occur. However they are, for example, two photon ($2E1$) transitions or single photon magnetic dipole ($M1$) transitions.

As an example, the $2P \to 1S$ transition rate for a hydrogen atom can be calculated (see for example *Principles of Quantum Mechanics* by Shankar [2]) This calculation gives the spontaneous emission transition rate

$$A_{2P-2S} = 6.27 \times 10^8 \ \text{s}^{-1},\tag{1.1}$$

and gives a lifetime of the hydrogen $2P$ state to be

$$\tau_{2P} \approx 1.6 \times 10^{-9} \ \text{s}.\tag{1.2}$$

As a comparison, the $2S \to 1S$ transition rate, and the $2S$ lifetime, for a hydrogen atom have been calculated to be [3] [4]

$$A_{2S-1S} = 8.299\text{s}^{-1}\tag{1.3}$$

$$\tau_{2S} \approx 0.12 \ \text{s}.$$

An extensive list of both allowed and forbidden transition rates for hydrogen, helium, and lithium has been compiled by *W. L. Wiese and J. R. Fuhr* [5], based primarily on data

supplied to them by Drake, and it can be seen that metastable transitions do occur on a different timescale than $E1$ allowed transitions.

The focus of this study will be to determine the transition rate from the $1s2s\ ^3S \rightarrow 1s^2\ ^1S$ states of helium and heliumlike ions to a high order of accuracy. The following section will outline a review of experimental measurements and theoretical calculation that have been done up to this point.

1.2 The $1s2s\ ^3S \rightarrow 1s^2\ ^1S$ Transition

In a simple independent-particle approximation, the $1s2s\ ^3S$ state of helium is the lowest lying excited state where one electron is in its ground state and the second electron is excited to the $n = 2$ state. The electrons, being spin $\frac{1}{2}$ fermions, are in a triplet configuration known as orthohelium where their spins are parallel, as opposed to a singlet configuration known as parahelium. As seen in Fig. (1.1) [6], due to the spin configuration of the electrons, the energies of orthohelium states are lower than those of parahelium states [for more details see Appendix (A)].

The energy of the $1s2s\ ^3S$ triplet state for a helium atom, in atomic units, is [7]

$$E_{^3S} = -2.175212 \tag{1.4}$$

and when the atom deexcites from the triplet state to the ground state a photon is emitted with this unique energy, and a corresponding characteristic wavelength

$$\lambda \approx 62.6 \text{ nm.} \tag{1.5}$$

In addition to helium, a similar state, and a similar transition occur for all heliumlike ions such as Li^+, Be^{2+}, B^{3+}, and so on with increasing nuclear charge Z. For each of these ions the two electrons can all form a triplet $1s2s\ ^3S$ state with a unique energy and characteristic wavelength See Fig. (1.2) for a diagrammatic representation of this transition for a helium atom. The $1s2s\ ^3S \rightarrow 1s^2\ ^1S$ transition is a single photon magnetic dipole transition ($M1$) and is considered a *doubly forbidden* transition in that
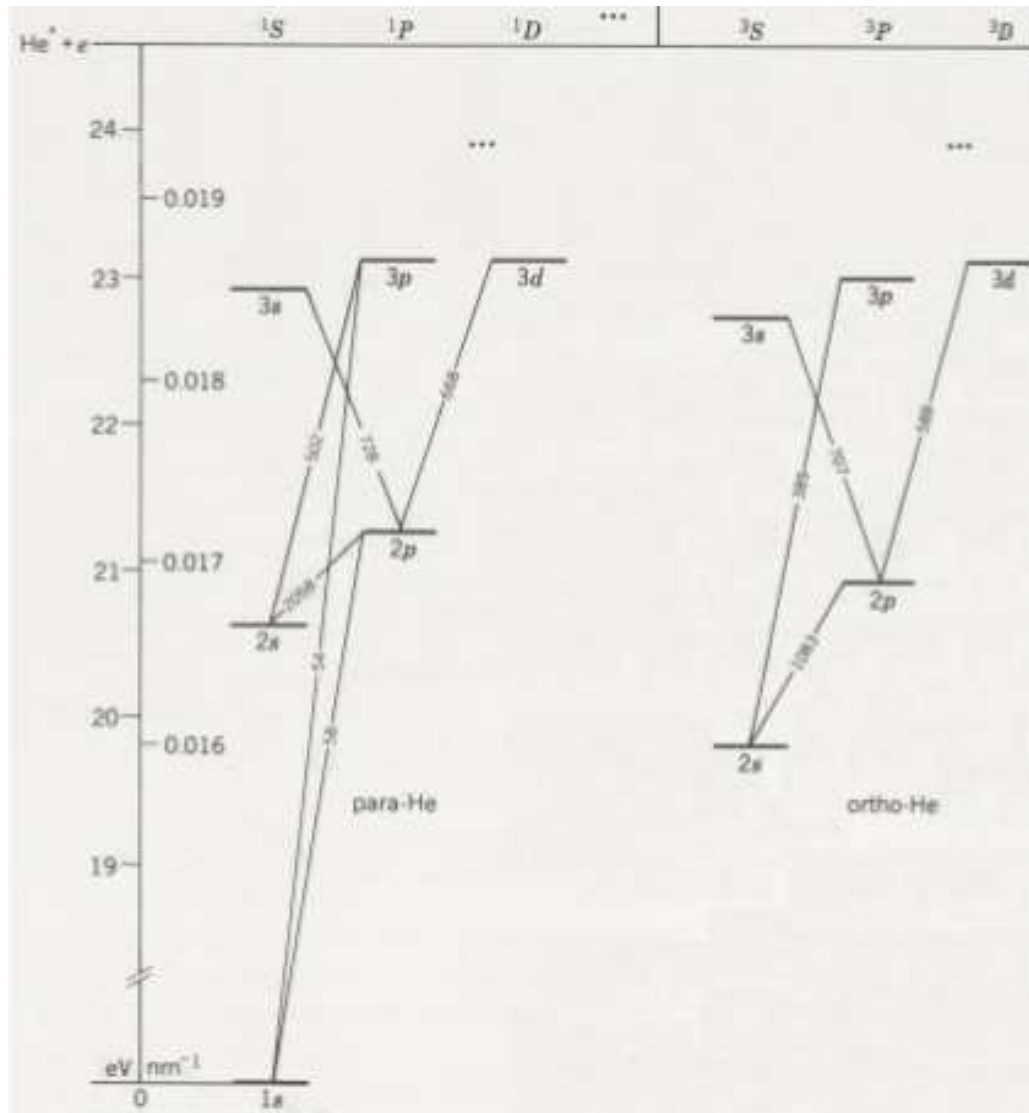
Figure 1.1: The low lying energy levels of both parahelium and orthohelium. The energy levels of orthohelium are slightly lower in comparison to the energy levels of parahelium. Figure is taken from "Introduction to the Structure of Matter" by Brehm and Mullin, p. 470.

1. the excited $1s2s$ ^3S state has the same angular momentum ($l = 0$) as the ground state. This is forbidden from the selection rules stating that the change in angular momentum $\Delta l = \pm 1$ for allowed transitions,

2. due to this being orthohelium, the excited electron has spin parallel to the ground state electron. Therefore a spin flip must occur if the excited electron is to return to the atomic ground state so that the two electrons are in an antiparallel (parahelium) configuration.

The motivation for studying the lifetimes of metastable $1s2s$ ^3S states of helium and heliumlike ions is primarily due to its use in astrophysical observations. As suggested by Gabriel and Jordan (1969) [8], and further developed by Blumenthal, Drake, and Tucker(1972) [9], the relative intensity of the $1s2s$ $^3S \rightarrow 1s^2$ ^1S spectral transition line to the $1s2p$ $^1P \rightarrow 1s^2$ ^1S spectral transition line can be used to estimate electron density in hot plasmas such as gas nebulae (such as the well known Orion Nebula [10][2] shown in Fig. (1.3) [12]), or the corona of the sun and other stars. By measuring the relative intensities of these spectral lines, we can therefore deduce information about the composition, density, and temperature of the object we are observing. This is particularly useful in low density plasmas (such as stellar nebulae) where an electron in the metastable state has a low probability to deexcite due to collisions.

There have been many measurements and calculations of the lifetime of the metastable $1s2s$ ^3S state. One of the earliest calculations by Breit and Teller [13] incorrectly suggested that the metastable state decays by a two photon electric dipole ($2E1$) process, and a calculation of the $M1$ transition rate much slower at about 5×10^{-6} s^{-1}.

Work by Mathis [11] calculated the $2E1$ transition rate to be 2.2×10^{-5} s^{-1}, which would give a lifetime of

$$\tau_{^3S}^{\text{Mathis}} \approx 4.5 \times 10^4 \text{ s.} \tag{1.6}$$

This result was used in astrophysical literature for many years until work by Drake and Dalgarno [14] showed that the work by Mathis was developed upon an incorrect formulation

---

[2]These calculations were based on an incorrect calculation of the metastable $1s2s$ ^3S state lifetime by Mathis [11]

of the problem. Later works by Bely and Faucher [15], and Drake, Victor, and Dalgarno [16] determined the $2E1$ transition rate to be 4×10^{-9} s^{-1}, and a respective lifetime

$$\tau_{^3S}^{\text{DVD/BF}} \approx 2.5 \times 10^8 \text{ s.} \tag{1.7}$$

It was later suggested by Gabriel and Jordan [8] [17], after observations and identification of the $1s2s\,^3S \to 1s^2\,^1S$ transition lines for the C_V to Si_{XIII} heliumlike ions in the spectrum of the solar corona, that the mechanism for the $1s2s\,^3S \to 1s^2\,^1S$ is primarily a single photon magnetic dipole emission.

The $1s2s\,^3S \to 1s^2\,^1S$ transition rate, via the $M1$ mechanism, was first calculated correctly by Drake (1971) [18], using quantum electrodynamics, for helium and heliumlike ions with nuclear charge ranging from 2 to 26. A brief review of this calculation will be discussed in Sec. (1.3), as this will serve as the starting point for this body of work. For helium, the transition rate and lifetime were calculated to be

$$A^{\text{Drake}}(1s2s\,^3S \to 1s^2\,^1S) \quad = \quad 1.272 \times 10^{-4} \text{ s}^{-1} \tag{1.8}$$

$$\text{and}$$

$$\tau_{^3S}^{\text{Drake}} \quad \approx \quad 7.862 \times 10^3 \text{ s.} \tag{1.9}$$

Further work by Drake (1974) [1] showed that the lowest-order QED corrections cancel out for this transition.

Additional theoretical works using quantum electrodynamics have been performed; Feinberg and Sucher (1971) [19] calculated the transition rate and lifetime as

$$A^{\text{Feinberg}}(1s2s\,^3S \to 1s^2\,^1S) \quad = \quad 1.2 \times 10^{-4} \text{ s}^{-1}, \tag{1.10}$$

$$\text{and}$$

$$\tau_{^3S}^{\text{Feinberg}} \quad \approx \quad 8.4 \times 10^3 \text{ s,} \tag{1.11}$$

and Johnson and Lin (1974) [20] obtained the values

$$A^{\text{Johnson,Lin}}(1s2s\,^3S \to 1s^2\,^1S) \quad = \quad 1.253 \times 10^{-4} \text{ s}^{-1}, \tag{1.12}$$

$$\text{and}$$

$$\tau_{^3S}^{\text{Johnson,Lin}} \quad \approx \quad 7.981 \times 10^3 \text{ s,} \tag{1.13}$$

and a later calculation by Johnson et al.(1995) [21], using relativistic many body perturbation theory reported

$$A^{\text{Johnson}}(1s2s\ ^3S \rightarrow 1s^2\ ^1S) \quad = \quad 1.266 \times 10^{-4}\ \text{s}^{-1}, \tag{1.14}$$

$$\text{and}$$

$$\tau^{\text{Johnson}}_{^3S} \quad \approx \quad 7899\ \text{s}. \tag{1.15}$$

In 1986, Krause [22], using screened hydrogenic wave functions, reported the transition rate and lifetime

$$A^{\text{Krause}}(1s2s\ ^3S \rightarrow 1s^2\ ^1S) \quad = \quad 8.737 \times 10^{-5}\ \text{s}^{-1}, \tag{1.16}$$

$$\text{and}$$

$$\tau^{\text{Krause}}_{^3S} \quad \approx \quad 1.145 \times 10^4\ \text{s}. \tag{1.17}$$

It should be stated that the results from Krause are inaccurate due to an inadequate treatment of the correlation between the electrons, and that the results for higher nuclear charge in the isoelectronic sequence are in better agreement.

Most recently, Łach and Pachucki (2001) [23] performed a systematic derivation of the transition matrix elements in quantum electrodynamic theory for low level forbidden transitions in helium and helium like ions, and reported

$$A^{\text{Łach,Pachucki}}(1s2s\ ^3S \rightarrow 1s^2\ ^1S) = 1.272426 \times 10^{-4}\ \text{s}^{-1}, \tag{1.18}$$

which would give

$$\tau^{\text{Łach,Pachucki}}_{^3S} \approx 7.859 \times 10^3\ \text{s}, \tag{1.19}$$

which is in close agreement with the original calculation by Drake (1971).

There have also been a few experiments performed to determine the lifetimes of the metastable $1s2s\ ^3S$ state. However it is interesting to note that, in contrast to other areas of physics, due to the precise nature of these types of calculations, experiments played only a minimal role in the determination of the lifetimes and transition rates.

While there were some experiments that measured the lifetime of the metastable $1s2s\ ^3S$ state for slightly heavier heliumlike ions (see for example Marrus and Schmieder (1972) [24]

for measurements for Ar XVII), the first experimental determination of the $1s2s\ {}^3S$ lifetime was by Moos and Woodworth in 1973 [25], and later a more accurate measurement in 1975 [26]. These experiments were conducted on a plasma discharge which was unstable and therefore difficult to obtain accurate measurements. In addition, the helium lifetimes could have been potentially reduced due to possible deexcitation from collisions since the helium atoms were not isolated in the plasma discharge. The latter, and more accurate, results were

$$A^{\text{Moos,Woodworth}}(1s2s\ {}^3S \to 1s^2\ {}^1S) \quad = \quad 2.4 \times 10^{-4}\ \text{s}^{-1}, \tag{1.20}$$

and

$$\tau_{{}^3S}^{\text{Moos,Woodworth}} \quad \approx \quad 9 \times 10^3\ \text{s}, \tag{1.21}$$

with an experimental error of 30%. While this result had a large degree of uncertainty it did correctly identify the order of magnitude of the transition, and served to give experimental proof that the decay of the $1s2s\ {}^3S$ state was primarily through single photon magnetic dipole emission.

Electron beam ion traps (EBIT) have been used to measure the $1s2s\ {}^3S$ lifetimes for O^{6+} ions [27], Ne^{8+} ions [28], and S^{14+} ions [29]. These EBIT experiments are unsuitable to measure the metastable helium lifetime since they are designed to create and trap highly ionized particles, and helium is not an ion. Heavy ion storage rings (HSR) have also been used to measure the lifetime for C^{4+} ions [30]. As with the EBIT measurements, HSR is not a possible method to measure the $1s2s\ {}^3S$ lifetime for helium. A summary of these techniques for measuring atomic lifetimes of multiply charged ions has been written by Träbert (2010) [31]

Consequently, the only accurate measurement of the $1s2s\ {}^3S$ lifetime for helium was performed by Hodgman et al. [32] (2009). This experiment addressed the issues in Moos and Woodworth's experiments by isolating the helium atoms in vacuum by use of laser cooling. The results of these measurements agree strongly with Drake [18] and other theoretical

calculations. The values they obtained are

$$A^{\text{Hodgman}}(1s2s\ ^3S \to 1s^2\ ^1S) \quad \approx \quad 1.27 \times 10^{-4}\ \text{s}^{-1}, \tag{1.22}$$

and

$$\tau_{^3S}^{\text{Hodgman}} \quad = \quad 7.870 \times 10^3\ \text{s}. \tag{1.23}$$

Table (1.1) summarizes the results of both theoretical and experimental measurements of the metastable $1s2s\ ^3S$ lifetime for helium over the past 56 years.

1.3 Theoretical Background

The foundation of this body of work will be based upon the theoretical calculation of the $M1$ transition operator by Drake (1971) [18]. A brief discussion of the calculation of this operator is presented in this section along with a review of the Foldy-Wouthuysen transformation.

1.3.1 The Dirac Equation and Interaction with the Field

For an accurate calculation including spin and relativistic effects, we begin with the Dirac equation for a spin $\frac{1}{2}$ particle such as an electron

$$i\hbar\frac{\partial}{\partial t}\psi\left(\mathbf{r},t\right) = H_{\text{D}}\psi\left(\mathbf{r},t\right), \tag{1.24}$$

with,

$$H_{\text{D}} = c\bar{\alpha} \cdot \mathbf{p} + \beta mc^2. \tag{1.25}$$

The operators $\vec{\alpha}$, with components α_{x}, α_{y}, and α_{z}, and β are represented by 4×4 matrices with the following definitions

$$\alpha_{\text{x}} = \begin{pmatrix} 0 & 0 & 0 & 1 \\ 0 & 0 & 1 & 0 \\ 0 & 1 & 0 & 0 \\ 1 & 0 & 0 & 0 \end{pmatrix}, \alpha_{\text{y}} = \begin{pmatrix} 0 & 0 & 0 & -i \\ 0 & 0 & i & 0 \\ 0 & -i & 0 & 0 \\ i & 0 & 0 & 0 \end{pmatrix}, \alpha_{\text{z}} = \begin{pmatrix} 0 & 0 & 1 & 0 \\ 0 & 0 & 0 & -1 \\ 1 & 0 & 0 & 0 \\ 0 & -1 & 0 & 0 \end{pmatrix}, \tag{1.26}$$

Year	Transition Rate ($\frac{1}{s}$)	Lifetime (s)	Type	Theory/Exp.	Source
1956	2.2×10^{-5}	4.5×10^4	2E1	Theory	Mathis
1968	4×10^{-9}	2.5×10^9	2E1	Theory	Bely & Faucher
1968	4×10^{-9}	2.5×10^9	2E1	Theory	Drake, Victor, & Dalgarno
1971	1.272×10^{-4}	7.862×10^3	M1	Theory	Drake
1971	1.2×10^{-4}	8.4×10^3	M1	Theory	Feinberg & Sucher
1973		$4 \times 10^3 \pm 300\%$	M1	Exp.	Moos & Woodworth
1974	1.272×10^{-4}	7.862×10^3	M1	Theory	Drake
1974	1.253×10^{-4}	7.981×10^3	M1	Theory	Johnson & Lin
1975		$9 \times 10^3 \pm 30\%$	M1	Exp.	Moos & Woodworth
1986	8.737×10^{-5}	1.145×10^4	M1	Theory	Krause
1995	1.266×10^{-4}	7.899×10^3	M1	Theory	Johnson et al
2001	1.272426×10^{-4}	7.859×10^3	M1	Theory	Łach & Pachucki
2009	1.272×10^{-4}	$7.870 \times 10^3 \pm 6.5\%$	M1	Exp.	Hodgman et $al.$

Table 1.1: A summary of the calculations and measurements of the transition rate and life time of the $1s2s\ ^3S \rightarrow 1s^2\ ^1S$ transition in helium. When available, the uncertainty in the calculations or measurements is given either in parentheses or as a percentage. The result from 1974 by Drake [1] is a confirmation of the previous calculation while explicitly showing the cancellation of lowest-order QED corrections

and

$$\beta = \begin{pmatrix} 1 & 0 & 0 & 0 \\ 0 & 1 & 0 & 0 \\ 0 & 0 & -1 & 0 \\ 0 & 0 & 0 & -1 \end{pmatrix}. \tag{1.27}$$

Or in a more compact notation

$$\bar{\alpha} = \begin{pmatrix} 0 & \sigma \\ \sigma & 0 \end{pmatrix}, \text{ and } \beta = \begin{pmatrix} 1 & 0 \\ 0 & -1 \end{pmatrix}, \tag{1.28}$$

where each entry is itself a 2×2 matrix, and σ are the Pauli matrices [33]. The wave function must then be a 4 component vector

$$\psi(\mathbf{r}, t) = \begin{pmatrix} \psi_1(\mathbf{r}, t) \\ \psi_2(\mathbf{r}, t) \\ \psi_3(\mathbf{r}, t) \\ \psi_4(\mathbf{r}, t) \end{pmatrix} \tag{1.29}$$

which, in the compact notation is written as

$$\psi(\mathbf{r}, t) = \begin{pmatrix} \phi(\mathbf{r}, t) \\ \chi(\mathbf{r}, t) \end{pmatrix} \tag{1.30}$$

where $\phi(\mathbf{r}, t)$ and $\chi(\mathbf{r}, t)$ are both two component spinors respectively known as the *large component* and *small component* of the wave function.

To account for the interaction with a magnetic field, one changes to the canonical momentum

$$\mathbf{p} \to \mathbf{p} - \frac{e}{c}\mathbf{A}, \tag{1.31}$$

where

$$\mathbf{A} = \hat{e}e^{i\mathbf{k}\cdot\mathbf{r}} \tag{1.32}$$

is the vector potential. The Dirac Hamiltonian can be rewritten as

$$\begin{aligned} H_{\mathrm{D}} &= c\bar{\alpha} \cdot \mathbf{p} - e\bar{\alpha} \cdot \mathbf{A} + \beta mc^2 \\ &= c\bar{\alpha} \cdot \left(\mathbf{p} - \frac{e}{c}\mathbf{A}\right) + \beta mc^2 \end{aligned} \tag{1.33}$$

and the interaction with the magnetic field is then due to the interaction term $-e\bar{\alpha} \cdot \mathbf{A}$. It is this term that mixes the large and small components of the wave function, for example a general matrix element of this term would be

$$\langle \Psi_a | \bar{\alpha} \cdot \mathbf{A} | \Psi_b \rangle = \langle \phi_a | \sigma \cdot \mathbf{A} | \chi_b \rangle + \langle \chi_b | \sigma \cdot \mathbf{A} | \phi_a \rangle. \tag{1.34}$$

It can be seen explicitly that there is mixing between ϕ and χ, and these terms are of order $\mathcal{O}\left(Z^2\alpha^2\right)$. These operators are known as *odd* operators, and operators which do not mix the large and small components are known as *even* operators.

The general procedure to obtain relativistic corrections is referred to as the Foldy-Wouthuysen transformation [34]. It has been performed to derive the magnetic dipole operator [18].

1.3.2   Foldy-Wouthuysen Transformation

The Foldy-Wouthuysen transformation is a unitary transformation which can be carried out repeatedly, where each iterative application of the Foldy-Wouthuysen transformation reduces the contributions from the *small* component of the wave function by successive orders of $Z^2\alpha^2$. [35] That is, a single Foldy Wouthysen transformation takes the operators of the Hamiltonian that mix the *large* and *small* components and transform them into an operator that does not mix the components, and a smaller (by order $Z^2\alpha^2$) operator that does mix the components. This process can be repeated until these contributions are reduced to the desired order.

For demonstrative purposes, we now perform a Foldy-Wouthuysen transformation of a single Dirac free particle. For a free particle, the Dirac Hamiltonian, given by Eq. (1.25) is

$$H = c\bar{\alpha} \cdot \mathbf{p} + \beta mc^2,$$

where it is the first term, $\bar{\alpha} \cdot \mathbf{p}$, that we wish to remove. The unitary transformation needed is such that

$$\Psi' = e^{iS}\Psi \tag{1.35}$$

and

$$H' = e^{iS}He^{-iS}, \tag{1.36}$$

where the transformation is time independent[3]. By choosing a unitary transformation of the form

$$e^{iS} = e^{\beta\bar{\alpha}\cdot\hat{p}\theta} = \cos\theta + \beta\bar{\alpha}\cdot\hat{p}\sin\theta, \tag{1.37}$$

where $\hat{p} = \frac{\mathbf{p}}{|\mathbf{p}|}$, then using this transformation yields a tranformed Hamiltion

$$
\begin{aligned}
H' &= (\cos\theta + \beta\bar{\alpha}\cdot\hat{p}\sin\theta)\left(c\bar{\alpha}\cdot\mathbf{p} + \beta mc^2\right)(\cos\theta - \beta\bar{\alpha}\cdot\hat{p}\sin\theta) \\
&= c\bar{\alpha}\cdot\mathbf{p}\left(\cos 2\theta - \frac{m}{|\mathbf{p}|}\sin 2\theta\right) + \beta mc^2\left(\cos 2\theta + \frac{|\mathbf{p}|}{m}\sin 2\theta\right).
\end{aligned}
\tag{1.38}
$$

The $\bar{\alpha}\cdot\mathbf{p}$ can be eliminated by a choice of θ such that $\tan 2\theta = \frac{|\mathbf{p}|}{m}$. This gives a transformed free particle Hamiltonian

$$H' = \beta\sqrt{p^2c^2 + m^2c^4} \tag{1.39}$$

which entirely eliminates any odd operators that mix the large and small components of the wave function after only one application of the Foldy-Wouthuysen transformation.

In general this procedure can be performed on any Hamiltonian; however, there will be some left over operator which still mixes the large and small components. This remaining odd operator will be of order $Z^2\alpha^2$ smaller. By successive applications of this procedure, the remaining odd operators are continually reduced until the desired order is reached.

A multiple Foldy-Wouthuysen transformation is applied to the Dirac Hamiltonian for a two electron atom by Drake (1971) [18], from which the magnetic dipole moment operator is derived. For the specific case of the transition from the $1s2s\ ^3S$ state to the $1s^2\ ^1S$ state, in which the orthogonality of the initial and final spin states greatly reduce the complexity, the magnetic dipole moment operators is

$$
\begin{aligned}
\langle 1s^2\ ^1S|Q_{10}|1s2s\ ^3S\rangle &= \mu_B\langle 1s^2\ ^1S| - \left(\frac{2}{3m^2c^2}\right)\left(p_1^2 - p_2^2\right) \\
&\quad - \frac{1}{6}\left(\frac{\omega}{c}\right)^2\left(r_1^2 - r_2^2\right) \\
&\quad + \left(\frac{Ze^2}{3mc^2}\right)\left(\frac{1}{r_1} - \frac{1}{r_2}\right)|1s2s\ ^3S\rangle.
\end{aligned}
\tag{1.40}
$$

---

[3]In general, if the Hamiltonian is time dependent, then the unitary transformation must be written such that $H \to e^{iS}He^{-iS} - ie^{iS}\frac{\partial}{\partial t}e^{-iS}$

The rate for this transition given by Drake (1971) [18] (based on the definitions in [36] and [37]) is

$$A(1s2s \ ^3S \rightarrow 1s^2 \ ^1S) = \hbar^{-1}\frac{4}{3}\left(\frac{\omega}{c}\right)^3 |\langle 1s^2 \ ^1S|Q_{10}|1s2s \ ^3S\rangle|^2, \qquad (1.41)$$

and the lifetime of the metastable $1s2s \ ^3S$ state is found by taking the inverse of the transition rate. All calculations in this work are based on Eqns. (1.40) and (1.41). The numerical calculation of the transition rate will be explained in full detail in Sec. (3).

$1s2s\ ^3S_1$

$\lambda = 62.6\ \text{nm}$

$1s^2\ ^1S_0$
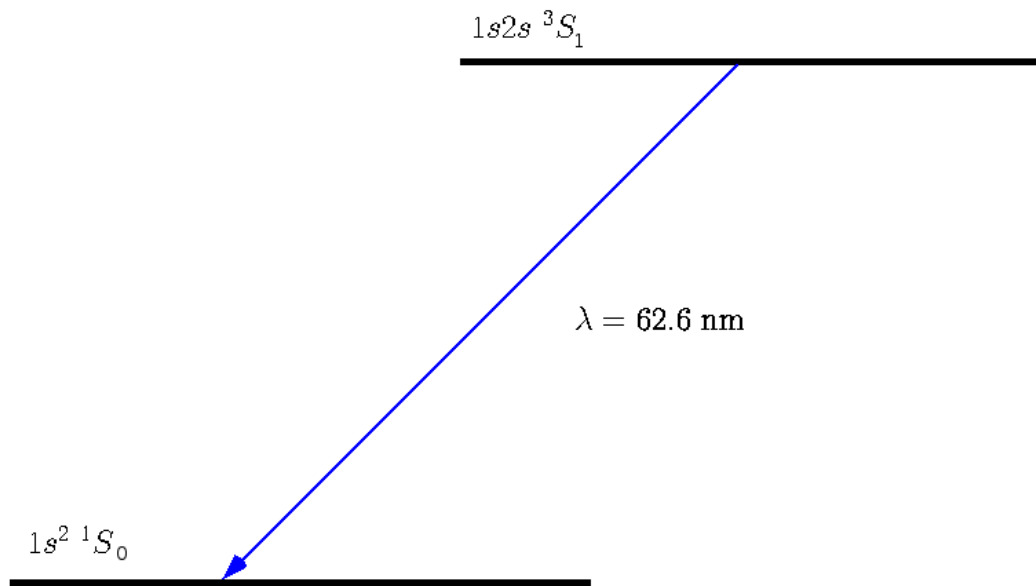
Figure 1.2: A schematic of the transition between the $1s2s\ ^3S$ state and the ground state of helium.

Figure 1.3: The Orion Nebula viewed by the Hubble telescope. The electron density of hot plasmas like the Orion Nebula can be estimated by measuring the relative intensities of atomic transitions. Image courtesy of NASA and the *Astronomy Picture of the Day* website (http://apod.nasa.gov/apod/ap120715.html).

Chapter 2

Methods

This chapter discusses theoretical methods used to calculate radiative transition rates. A general method for calculating transition rates and lifetimes would be to determine the exact wave functions for the systems in question and to use these wave functions to calculate the corresponding matrix elements of the radiative transition operator. These wave functions and their corresponding energies are the eigenfunctions and eigenvalues of the particular Hamiltonian in Schrödinger's equation,

$$H\Psi = E\Psi, \tag{2.1}$$

where H is the Hamiltonian of a quantum mechanical system, Ψ are the eigenfunctions, and E are the corresponding energy eigenvalues.

This section will discuss the methods and techniques used in this thesis to obtain these wave functions, as well as the methods used to calculate matrix elements needed to determine the transition rates and lifetimes of helium like ions.

2.1 The Helium Hamiltonian

To begin, we need to have a description of the system, which can be expressed in terms of the Hamiltonian of the system. A heliumlike ion is a three body quantum mechanical system and, in general, has a three body nonrelativistic Hamiltonian which can be written as

$$
\begin{aligned}
H = \quad - \quad & \frac{\hbar^2}{2m_N}\nabla^2_{R_N} - \frac{\hbar^2}{2m_e}\nabla^2_{R_{e_1}} - \frac{\hbar^2}{2m_e}\nabla^2_{R_{e_2}} \\
- \quad & \frac{Ze^2}{|\vec{R}_N - \vec{R}_{e_1}|} - \frac{Ze^2}{|\vec{R}_N - \vec{R}_{e_2}|} + \frac{e^2}{|\vec{R}_{e_1} - \vec{R}_{e_2}|},
\end{aligned}
\tag{2.2}
$$

where $\vec{R}_N$, $\vec{R}_{e_1}$, and $\vec{R}_{e_2}$ are vectors, with an arbitrary inertial frame of reference (see Fig. (2.1)), respectively corresponding to the positions of the nucleus, and the two electrons, M is nuclear mass, m is the electron mass, Ze is the nuclear charge of the helium-like ion, and e is the electronic charge. The first three terms correspond to the kinetic energies of the particles. The fourth and fifth terms correspond to the potential energies from the interaction between the nucleus and the electrons. The final term is the interaction potential energy between the two electrons. It is the sixth term that prevents us from solving the Schrödinger equation analytically. If the sixth term did not appear in the above equation, the solution would simply be the product of two non-interacting hydrogenlike wave functions.

It is possible to rewrite this equation, through a change of coordinates to a centre of mass reference frame (see Fig. (2.2)), using the the new coordinates

$$
\vec{R} \quad = \quad \frac{M\vec{R}_N + m\vec{R}_{e_1} + m\vec{R}_{e_2}}{M + 2m} \tag{2.3}
$$

$$
\vec{r}_1 \quad = \quad \vec{R}_{e_1} - \vec{R}_N \tag{2.4}
$$

$$
\vec{r}_2 \quad = \quad \vec{R}_{e_2} - \vec{R}_N. \tag{2.5}
$$

These new centre of mass and relative coordinates vector allow us to transform Eq. (2.2) into a new differential equation using the new wavefucntions, $\Psi(\vec{r}_1, \vec{r}_2, \vec{R})$, and differential operators, ∇_1, ∇_2, and ∇_R. Through application of the chain rule, we can write the fixed
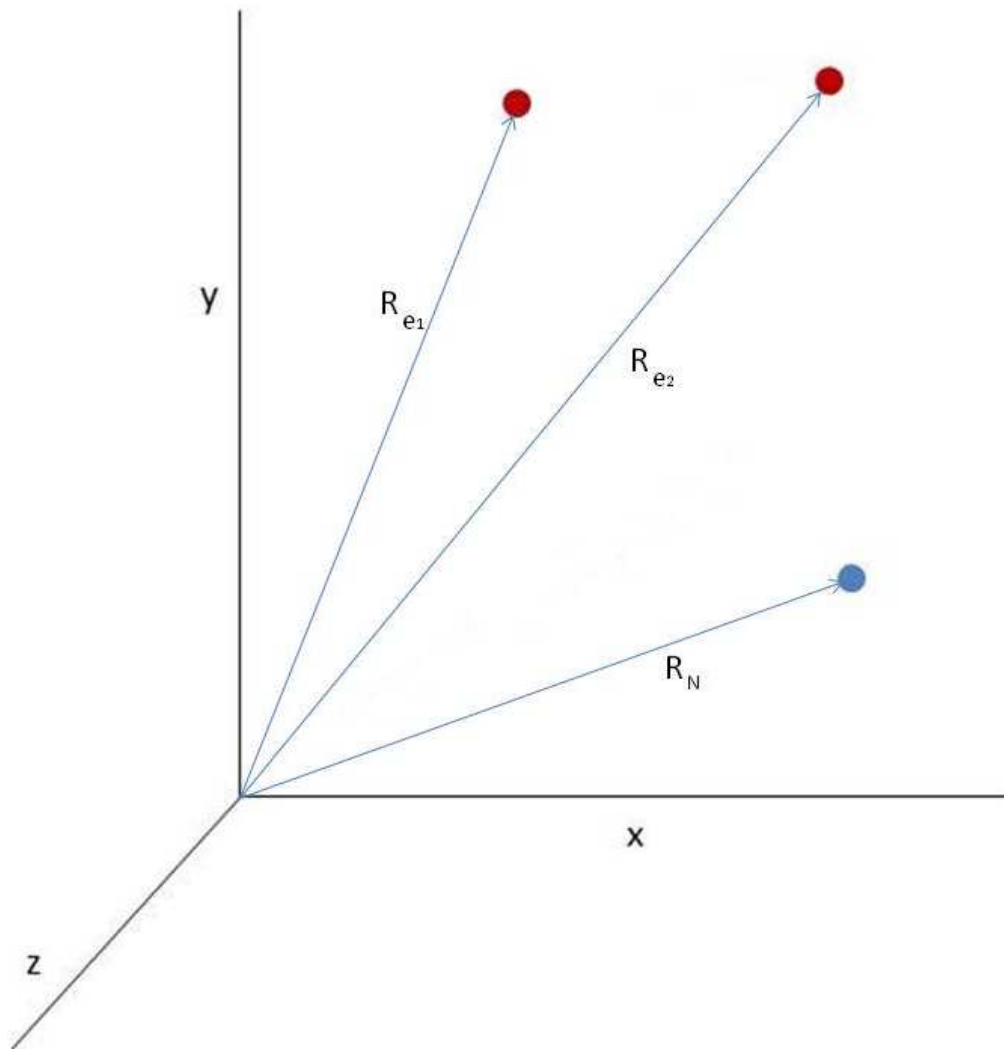
Figure 2.1: Coordinates for a three particle system in an arbitrarily located inertial frame of reference.
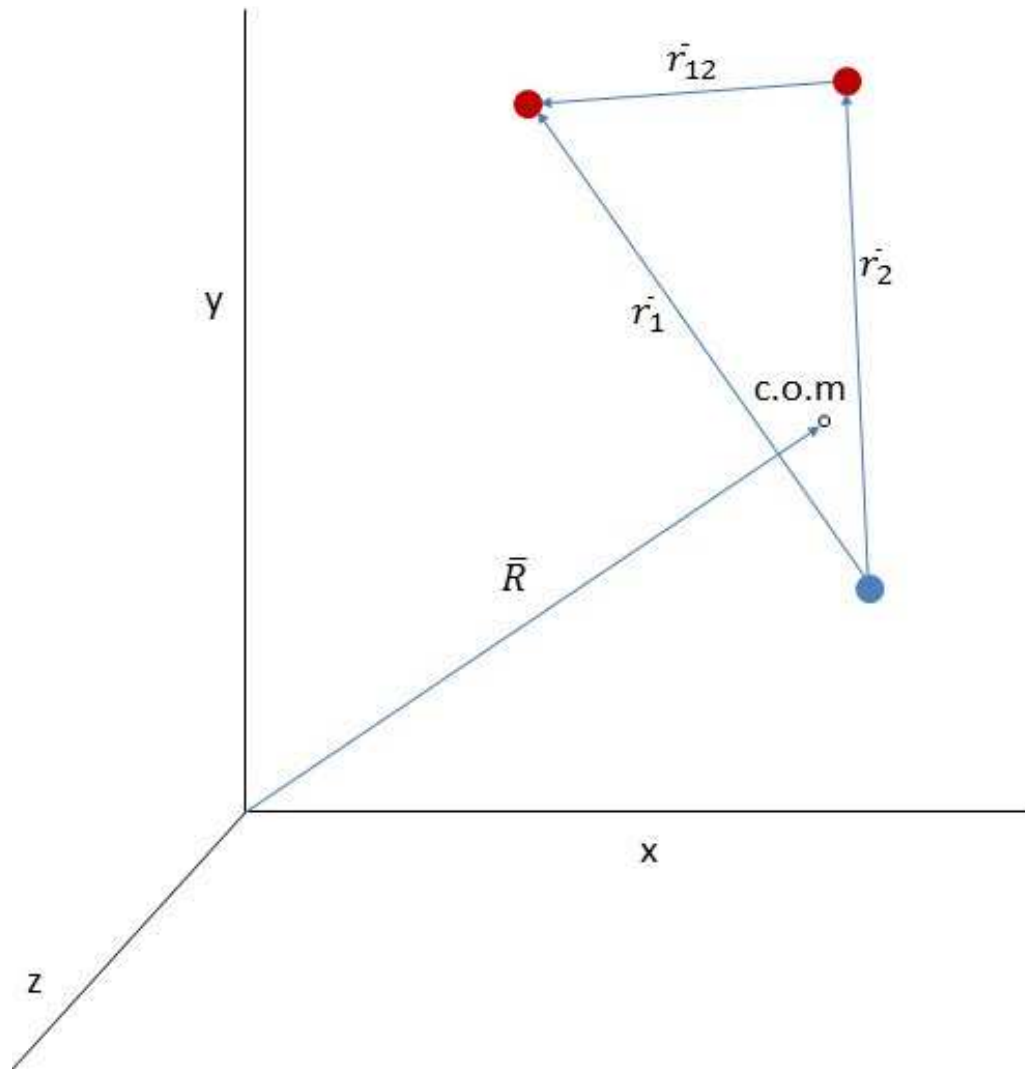
Figure 2.2: Centre of mass coordinates for an arbitrary three particle system with an arbitrarily located inertial frame of reference.

coordinate frame operators in terms of the centre of mass coordinates as

$$\nabla_{R_{e_1}} = \nabla_{r_1} + \frac{m}{M+2m}\nabla_R \tag{2.6}$$

$$\nabla_{R_{e_2}} = \nabla_{r_2} + \frac{m}{M+2m}\nabla_R \tag{2.7}$$

$$\nabla_{R_N} = -\nabla_{r_1} - \nabla_{r_2} + \frac{M}{M+2m}\nabla_R. \tag{2.8}$$

From these equations we write the square of those operators

$$\nabla_{r_1}^2 = \nabla_{r_1}^2 + \left(\frac{m}{M+2m}\right)^2\nabla_R^2 + \frac{2m}{M+2m}\nabla_{r_1}\cdot\nabla_R \tag{2.9}$$

$$\nabla_{r_2}^2 = \nabla_{r_2}^2 + \left(\frac{m}{M+2m}\right)^2\nabla_R^2 + \frac{2m}{M+2m}\nabla_{r_2}\cdot\nabla_R \tag{2.10}$$

$$\nabla_{R_N}^2 = \nabla_{r_1}^2 + \nabla_{r_2}^2 + \left(\frac{M}{M+2m}\right)^2\nabla + R^2 + 2\nabla_{r_1}\cdot\nabla_{r_2} \tag{2.11}$$

$$-\frac{M}{M+2m}\left(\nabla_{r_1}+\nabla_{r_2}\right)\cdot\nabla_R.$$

The Hamiltonian, Eq. (2.2), can now be written as

$$H = -\frac{\hbar^2}{2m}\left[\nabla_{r_1}^2 + \left(\frac{m}{M+2m}\right)^2\nabla_R^2 + 2\frac{m}{M+2m}\nabla_{r_1}\cdot\nabla_R\right] \tag{2.12}$$

$$-\frac{\hbar^2}{2m}\left[\nabla_{r_2}^2 + \left(\frac{m}{M+2m}\right)^2\nabla_R^2 + 2\frac{m}{M+2m}\nabla_{r_2}\cdot\nabla_R\right]$$

$$-\frac{\hbar^2}{2M}\left[\nabla_{r_1}^2 + \nabla_{r_2}^2 + \left(\frac{M}{M+2m}\right)^2\nabla_R^2 + 2\nabla_{r_1}\cdot\nabla_{r_2}\right.$$

$$\left.-2\frac{M}{M+2m}\left(\nabla_{r_1}+\nabla_{r_2}\right)\cdot\nabla_R\right] - \frac{Ze^2}{r_1} - \frac{Ze^2}{r_2} + \frac{e^2}{|\vec{r_1}-\vec{r_2}|}.$$

By introducing the reduced mass notation, μ, with the definition

$$\frac{1}{\mu} = \frac{1}{m} + \frac{1}{M}, \tag{2.13}$$

or

$$\mu = \frac{mM}{m+M}, \tag{2.14}$$

and the total mass $\mathcal{M} = M + 2m$, we can re-write Eq. (2.12) as

$$H = -\frac{\hbar^2}{2\mathcal{M}}\nabla_R^2 - \frac{\hbar^2}{2\mu}\nabla_{r_1}^2 - \frac{\hbar^2}{2\mu}\nabla_{r_2}^2 - \frac{\hbar^2}{2M}\nabla_{r_1}\cdot\nabla_{r_2} \tag{2.15}$$

$$-\frac{Ze^2}{r_1} - \frac{Ze^2}{r_2} + \frac{e^2}{|\vec{r_1}-\vec{r_2}|}.$$

The first term in Eq. (2.15) is the kinetic energy of the centre of mass motion of the system. Since the total Hamiltonian is not a function of the centre of mass position, $\vec{R}$, i.e. the potential energy is only a function of relative distances, there is no net force on the atom and the centre of mass motion is constant[1] [38]. This means that the first term in Eq. (2.15) can be considered ignorable, and we are free to leave it out of the Hamiltonian.

For convenience, we can choose a dimensionless representation by introducing the coordinate

$$\rho_i = \frac{r_i}{a_\mu} \tag{2.16}$$

where

$$a_\mu = \frac{m}{\mu} a_0 \tag{2.17}$$

is the reduced mass Bohr radius, and

$$a_0 = \frac{\hbar^2}{me^2} \tag{2.18}$$

is the Bohr radius, and i is an index for the two electrons. With this coordinate choice, we can write the Schrödinger equation as

$$\left[-\frac{1}{2}\nabla_{\rho_1}^2 - \frac{1}{2}\nabla_{\rho_2}^2 - \frac{\mu}{M}\nabla_{\rho_1} \cdot \nabla_{\rho_2} - \frac{Z}{\rho_1} - \frac{Z}{\rho_2} + \frac{1}{\rho_{12}} \right] \psi(\rho_1, \rho_2) = E\psi(\rho_1, \rho_2), \tag{2.19}$$

with the simplified notation

$$\rho_{12} = |\vec{\rho}_1 - \vec{\rho}_2|. \tag{2.20}$$

The cross term, $-\frac{\mu}{M}\nabla_{\rho_1} \cdot \nabla_{\rho_2}$, on the left hand side of Eq. (2.19) can be neglected in the limit $\frac{\mu}{M} \ll 1$ to first order approximation when the nuclear mass is treated as infinite. In

---

[1]This is actually a specific case of Noether's Theorem which states that for any quantity, q_i, that does not appear in the Hamiltonian (or the Langrangian), its associated canonical mometum is a constant of the motion. That is, the for the Lagrange equations

$$\frac{d}{dt}\frac{\partial L}{\partial \dot{q}_i} - \frac{\partial L}{\partial q_i} = 0,$$

if L has no q_i dependence, then

$$\frac{d}{dt}\frac{\partial L}{\partial \dot{q}_i} = 0.$$

With the definition of the canonical momentum $p_i = \frac{\partial L}{\partial \dot{q}_i}$, this implies that the canonical momentum is a constant of the motion.

this case, a_μ would reduce to a_0 and the cross term would vanish. If we neglect this finite mass term we introduce an uncertainty of the order $\frac{m_e}{m_p} \approx 10^{-4}$ to any future calculations.

By rescaling the radial coordinates according to, $\rho \rightarrow Z\rho$, we can again rewrite the Schrödinger equation in a simpler notation as

$$\left[-\frac{1}{2}\nabla_{\rho_1}^2 - \frac{1}{2}\nabla_{\rho_2}^2 - \frac{\mu}{M}\nabla_{\rho_1} \cdot \nabla_{\rho_2} - \frac{1}{\rho_1} - \frac{1}{\rho_2} + \frac{1}{Z}\frac{1}{\rho_{12}} \right] \psi\left(\rho_1, \rho_2\right) = \mathcal{E}\psi\left(\rho_1, \rho_2\right), \qquad (2.21)$$

or in the infinite nuclear mass limit,

$$\left[-\frac{1}{2}\nabla_{\rho_1}^2 - \frac{1}{2}\nabla_{\rho_2}^2 - \frac{1}{\rho_1} - \frac{1}{\rho_2} + \frac{1}{Z}\frac{1}{\rho_{12}} \right] \psi\left(\rho_1, \rho_2\right) = \mathcal{E}\psi\left(\rho_1, \rho_2\right), \qquad (2.22)$$

where $\mathcal{E} = \frac{a_\mu}{Z^2 e^2}E$ is the Z-scaled energy.

2.2   The Variational Principle

As stated in the previous section, helium and heliumlike ions are three body systems. Because of the interaction term, $\frac{1}{r_{12}}$, we cannot determine exact analytic solutions to the Schrödinger equation, Eq. (2.21), or any atomic system other than hydrogen (or a similar two body system). This requires us to find approximate solutions to Eq. (2.21). The method we will apply is the Variational Method.

For a general Hamiltonian with eigenfunction $|\psi\rangle$, and corresponding energy eigenvalue E, we can write the Schrödinger equation

$$H|\psi\rangle = E|\psi\rangle. \qquad (2.23)$$

By multiplying both sides of Eq. (2.23) by $\langle\psi|$, we can solve for the energy eigenvalue

$$E = \frac{\langle\psi|H|\psi\rangle}{\langle\psi|\psi\rangle}. \qquad (2.24)$$

It is possible to construct a normalizable trial function, $|\psi_{tr}\rangle$, which is to be used as an approximation to the exact wave function, with an associated trial energy defined as

$$E_{\text{tr}} = \frac{\langle\psi_{tr}|H|\psi_{tr}\rangle}{\langle\psi_{tr}|\psi_{tr}\rangle}. \qquad (2.25)$$

We can write the trial function as a series expansion of a complete set of basis eigenfunctions $|\psi_0\rangle$, $|\psi_1\rangle$, $|\psi_2\rangle$, ..., which are exact, but unknown eigenvectors of the Hamiltonian

H. These basis eigenfunctions have corresponding energy eigenvalues E_0, E_1, E_2, ..., such that $E_0 < E_1 < E_2 < \cdots$, where E_0 is the ground state. This allows us to write the trial function as

$$|\psi_{tr}\rangle = \sum_{n=0}^{\infty} c_n |\psi_n\rangle, \tag{2.26}$$

with expansion coefficients c_n. By requiring the trial function to be normalized, we can write the identity

$$
\begin{aligned}
1 &= \langle \psi_{tr} | \psi_{tr} \rangle \\
&= \sum_{m,n=0}^{\infty} \langle \psi_m | \psi_n \rangle c_m^* c_n \\
&= \sum_{n=0}^{\infty} |c_n|^2,
\end{aligned}
\tag{2.27}
$$

given that $\langle \psi_m | \psi_n \rangle = \delta_{m,n}$, Eq. (2.25) can be re-written as

$$
\begin{aligned}
E_{\mathrm{tr}} &= \langle \psi_{tr} | H | \psi_{tr} \rangle \\
&= \sum_{m,n=0}^{\infty} \langle \psi_m | H | \psi_n \rangle c_m^* c_n \\
&= \sum_{m,n=0}^{\infty} \langle \psi_m | E_n | \psi_n \rangle c_m^* c_n \\
&= \sum_{n=0}^{\infty} \langle \psi_n | E_n | \psi_n \rangle |c_n|^2 \\
&= |c_0|^2 E_0 + |c_1|^2 E_1 + |c_2|^2 E_2 + \ldots \\
&= \left(1 - |c_1|^2 - |c_2|^2 - \ldots \right) E_0 + |c_1|^2 E_1 + |c_2|^2 E_2 + \ldots \\
&= E_0 + (E_1 - E_0) E_1 + (E_2 - E_0) E_2 + \ldots \\
&\geq E_0,
\end{aligned}
\tag{2.28}
$$

where we have used the identity, Eq. (2.27) in the form $|c_0|^2 = 1 - \sum_{n=1} |c_n|^2$, in the second to last line of Eq. (2.28). This gives the well known result that the trial energy for an arbitrary trial function is guaranteed to be an upper bound to the ground state energy. This is a powerful result since it is possible, by judicious choice of trial wave functions, to minimize the difference between the trial energy and the ground state eigenvalue.

The standard procedure behind the variational method is then to choose a trial wave function

$$\psi_{tr} = \sum_{n=1}^{N} c_n |\varphi_n\rangle, \tag{2.29}$$

that can be written as a function of variational parameters, where the basis set (the functions φ_n) become complete only in the limit $N \to \infty$. These variational parameters can then be adjusted so that the associated variational energy, E_{tr} is a minimum. For the case of linear variational coefficients, as in Eq. (2.26), the energy can be written as

$$
\begin{aligned}
E_{\mathrm{tr}} &= \frac{\langle \psi_{tr}|H|\psi_{tr}\rangle}{\langle \psi_{tr}|\psi_{tr}\rangle} \\
&= \frac{\sum_{m,n}\langle c_m\varphi_m|H|c_n\varphi_n\rangle}{\sum_{m,n,}\langle c_m\varphi_m|c_n\varphi_n\rangle} \\
&= \frac{\sum_{m,n}\langle c_m^* c_n\langle\varphi_m|H|\varphi_n\rangle}{\sum_{m,n}\langle c_m^* c_n\langle\varphi_m|\varphi_n\rangle} \\
&= \frac{\sum_{m,n} c_m^* c_n H_{mn}}{\sum_{m,n} c_m^* c_n O_{mn}},
\end{aligned}
\tag{2.30}
$$

with the definitions,

$$
\begin{aligned}
H_{mn} &= \langle\varphi_m|H|\varphi_n\rangle, \\
O_{mn} &= \langle\varphi_m|\varphi_n\rangle.
\end{aligned}
\tag{2.31}
$$

Minimizing E_{tr} it is then equivalent to solving the following set of N equations

$$\frac{\partial E_{\mathrm{tr}}}{\partial c_n} = 0, \ \text{for all } n = 1, 2, \ldots, N. \tag{2.32}$$

By use of Eq. (2.30), an expression for the left hand side of Eq. (2.32) can be derived.

$$
\begin{aligned}
\frac{\partial E_{\mathrm{tr}}}{\partial c_n} &= \frac{\left(\sum_m c_m^* H_{mn}\right)\left(\sum_{m,n} c_m^* c_n O_{mn}\right)}{\left(\sum_{m,n} c_m^* c_n O_{mn}\right)^2} \\
&\quad - \frac{\left(\sum_{m,n} c_m^* c_n H_{mn}\right)\left(\sum_m c_m^* O_{mn}\right)}{\left(\sum_{m,n} c_m^* c_n O_{mn}\right)^2} \\
&= \frac{\sum_m c_m^* H_{mn}}{\sum_{m,n} c_m^* c_n O_{mn}} - \frac{\left(\sum_{m,n} c_m^* c_n H_{mn}\right)\left(\sum_m c_m^* O_{mn}\right)}{\left(\sum_{m,n} c_m^* c_n O_{mn}\right)^2} \\
&= \frac{\sum_m c_m^* H_{mn}}{\sum_{m,n} c_m^* c_n O_{mn}} - \frac{E_{\mathrm{tr}}\sum_m c_m^* O_{mn}}{\sum_{m,n} c_m^* c_n O_{mn}}.
\end{aligned}
\tag{2.33}
$$

Since $\frac{\partial E_{\text{tr}}}{\partial c_n} = 0$, we have the set of N equations (after multiplying through by the denominator of Eq (2.33)

$$\sum_n^N c_n \left(H_{nm} - E_{\text{tr}} O_{nm} \right) = 0, \tag{2.34}$$

where we have relabeled the summation over the index n, and have used the fact that H_{mn}, O_{mn}, and E_{tr} are real.

Eq. (2.34) must be true for all values of m, and can be expressed algebraically in matrix form as

$$\begin{pmatrix} H_{11} & H_{12} & \cdots & H_{1N} \\ H_{21} & H_{22} & \cdots & H_{2N} \\ \vdots & & \ddots & \\ H_{N1} & H_{N2} & \cdots & H_{NN} \end{pmatrix} \begin{pmatrix} c_1 \\ c_2 \\ \vdots \\ c_N \end{pmatrix} = E_{\text{tr}} \begin{pmatrix} O_{11} & O_{12} & \cdots & O_{1N} \\ O_{21} & O_{22} & \cdots & O_{2N} \\ \vdots & & \ddots & \\ O_{N1} & O_{N2} & \cdots & O_{NN} \end{pmatrix} \begin{pmatrix} c_1 \\ c_2 \\ \vdots \\ c_N \end{pmatrix}, \tag{2.35}$$

or more compactly as

$$\mathbf{Hc} = E_{\text{tr}} \mathbf{Oc}, \tag{2.36}$$

where $\mathbf{H}$ is the Hamiltonian matrix, $\mathbf{O}$ is the overlap matrix, with matrix elements as described in Eq. (2.31) respectively, and $\mathbf{c}$ is a column vector of coefficients c_n. Diagonialization of $\mathbf{H}$ results in N eigenvalues $(E_{\text{tr}}^0, E_{\text{tr}}^1, E_{\text{tr}}^2, \ldots, E_{\text{tr}}^{N-1})$, and the lowest of these eigenvalues is an upper bound to the exact ground state eigenvaule E_0. For each of these eigenvalues there is a corresponding eigenvector that represents the trial wave function written in the chosen basis set.

2.2.1   Excited States

The upper bound of the ground state energy can be generalized to the excited state energies via the Hylleraas-Undheim-MacDonald theorem [39, 40]. Each excited state energy, $E_1, E_2, \ldots, E_{N-1}$, is itself bounded above by the eigenvalues $E_{\text{tr}}^1, E_{\text{tr}}^2, \ldots, E_{\text{tr}}^{N-1}$. The Hylleraas-Undheim-MacDonald theorem is a result of the matrix interleaving theorem, that says that if we add a row and column to the matrices in Eq. (2.36) (increasing the dimension), the $k-th$ *old* eigenvalue, E_{tr}^k, that is calculated with matrices with dimension N, will lie between the new E_{tr}^k and E_{tr}^{k+1} eigenvalues when calculated with dimension $N+1$. Since

these trial eigenvalues become the exact eigenvalues in the limit $N \to \infty$, and the system is bounded from below, it follows that the trial eigenvalues can never be lower than the exact eigenvalues. Thus as N is increased, the eigenvalues progress toward the exact eigenvalues. The progression of these eigenvalues is illustrated in Fig. (2.3).

2.3   Hylleraas Basis Set

Since the Schrödinger equation, Eq. (2.21), is not separable, which is a consequence of the $\frac{1}{r_{12}}$ term, it is important to include in any useful basis set the variable r_{12} . Following the form of Eq. (2.26), we choose our basis functions of the form

$$|\psi_{tr}\rangle = \sum_n^N c_n |\chi_n\rangle, \tag{2.37}$$

where

$$\chi_n = r_1^i r_2^j r_{12}^k e^{-\alpha r_1 - \beta r_2}, \tag{2.38}$$

and now n labels sets of distinct triples of positive definite integer values of the exponents i, j, and k. The variables α and β are two additional, but nonlinear, variational parameters that determine the distance scales involved in the system we are studying.

A basis set constructed in this form using the functions from Eq. (2.38), and directly including the electron-electron separation r_{12}, is called a Hylleraas basis set [41, 42]. This can be generalized to include angular momentum. For a state with total angular momentum L, our trial function can be written as

$$
\begin{aligned}
|\psi_{tr}\rangle &= \sum_{l_1=0}^{L/2} \sum_n C_{n,l_1} |\chi_n\rangle r_1^{l_1} r_2^{l_2} \mathcal{Y}_{l_1 L - l_1 L}^M(\hat{\mathbf{r}}_1, \hat{\mathbf{r}}_2) \\
&\quad \pm \text{ exchange term}
\end{aligned} \tag{2.39}
$$

with

$$\mathcal{Y}_{l_1 l_2 L}^M(\hat{\mathbf{r}}_1, \hat{\mathbf{r}}_2) = \sum_{m_1, m_2} Y_{l_1 m_1}(\hat{\mathbf{r}}_1) Y_{l_2 m_2}(\hat{\mathbf{r}}_2) \langle l_1 l_2 m_1 m_2 | LM \rangle \tag{2.40}$$

being the vector coupled product of the angular momenta l_1 and l_2 for the two electrons, m_1 and m_2 are the z components of the angular momenta for the two electrons, and M
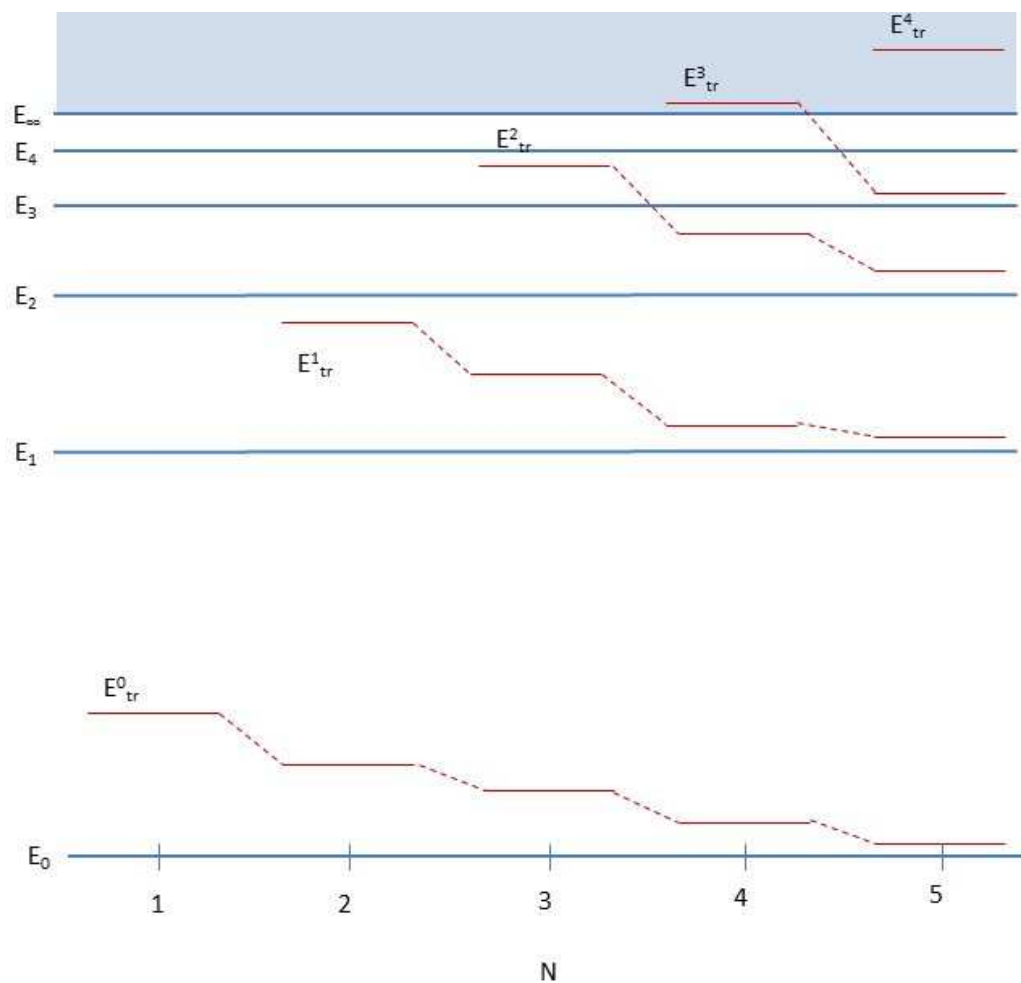
Figure 2.3: Diagram illustrating the Hylleraas-Undheim-MacDonald theorem. The eigenvalues E_{tr}^p, with $p = 0, 1, 2, \ldots, N$, for an N dimensional basis set are shown in comparison to E_i, the exact energy eigenvalues of H. This shows that, as the basis size is increased, the trial energies approach the exact eigenvalues from above.

is the total z component of the angular momentum of the state. The sum over n in Eq. (2.39) is over all terms within a *Pekeris shell* [43] of radius Ω, where Ω is an integer with $i + j + k \leq \Omega$. The total number of basis functions os given by

$$N = \frac{1}{6} (\Omega + 1) (\Omega + 2) (\Omega + 3).$$ (2.41)

The nonlinear coefficients α and β are determined by numerically minimizing the trial energy with respect to the nonlinear coefficients,

$$\frac{\partial E_{\text{tr}}}{\partial \alpha} = 0$$ (2.42)
$$\frac{\partial E_{\text{tr}}}{\partial \beta} = 0.$$

The trial functions used in this thesis will include a second set of terms similar to Eq. (2.39) with new linear variational coefficients and two new additional nonlinear coefficients. The trial functions of this *double basis set* method, developed by Drake [43], are

$$\begin{aligned}
\Psi_{\text{tr}} (\mathbf{r}_1, \mathbf{r}_2) &= \sum_{ijk} c_{ijk}^{(1)} r_1^i r_2^j r_{12}^k e^{-\alpha_1 r_1 - \beta_1 r_2} \mathcal{Y}_{l_1 l_2 L}^M (\hat{r}_1, \hat{r}_2) \\
&+ \sum_{ijk} c_{ijk}^{(2)} r_1^i r_2^j r_{12}^k e^{-\alpha_2 r_1 - \beta_2 r_2} \mathcal{Y}_{l_1 l_2 L}^M (\hat{r}_1, \hat{r}_2) \\
&\pm \text{ exchange terms.}
\end{aligned}$$ (2.43)

In this trial wave function, the basis has been doubled by introducing a second set of terms with two new nonlinear variational parameters α_2 and β_2. The inclusion of these two new parameters increases the accuracy of the wave functions by orders of magnitude while simultaneously simplifying the calculation by reducing the overall needed size of the basis set. In addition, when using a single set of non linear variational parameters, as the basis size becomes large there are errors introduced due to numerical cancellation as the basis set becomes linearly dependent. It is also possible to introduce more nonlinear variational parameters if needed and triple or quadruple the basis set.

Optimization of the α and β parameters in a doubled basis set leads naturally to a separation of the wave function into two regions with distinct physical interpretations. The parameters α_1 and β_1 describe the asymptotic form of the wave function where their values

are close to the screened hydrogenic values, $\alpha_1 \approx Z$, and $\beta_1 \approx \frac{Z-1}{n}$, where n is the principal quantum number of the outer electron. The second set of parameters, α_2 and β_2, correspond to the region close to the nucleus where the correlation effects are more significant [43].

This method can be extended further by creating a tripled basis set, or a quadrupled basis set, and the determination of these nonlinear parameters is accomplished in the same manner as Eq. (2.42).

2.4   Calculation of the Matrix Elements

Once the wave functions have been determined, the calculation of any matrix element requires the evaluation of a large number of integrals. The general procedure for calculating the matrix elements is an application of the methods explained in the *Atomic, Molecular, and Optical Physics Handbook* (p. 202-205) [44].

Construction of the overlap matrix $\mathbf{O}$ and the Hamiltonian matrix $\mathbf{H}$ requires, in general, the evaluation of integrals of the form

$$\int_{\mathcal{V}} d\tau \, \psi_{\text{tr}}^* \left(\mathbf{r}_1, \mathbf{r}_2 \right) \psi_{\text{tr}} \left(\mathbf{r}_1, \mathbf{r}_2 \right) \tag{2.44}$$

and

$$\int_{\mathcal{V}} d\tau \, \psi_{\text{tr}}^* \left(\mathbf{r}_1, \mathbf{r}_2 \right) H \psi_{\text{tr}} \left(\mathbf{r}_1, \mathbf{r}_2 \right). \tag{2.45}$$

The volume element, $d\tau$, in any integral we wish to calculate, can be expressed in Cartesian coordinates as $d\tau = dx_1 dy_1 dz_1 dx_2 dy_2 dz_2$. However, because the trial wave function includes the electron-electron separation variable r_{12}, it is more convenient to write the volume element using six independent variables known as Hylleraas coordinates. These variables are $r_1, r_2, r_{12}, \theta_1, \phi_1$, and χ, as shown in Figure (2.4). The radial variables r_1, r_2, and r_{12} are the same variables we have been using previously. The angular variables θ_1, and ϕ_1, are respectively the spherical polar, and azimuthal angles for the radial vector $\mathbf{r}_1$, and χ is the angle of rotation about r_1 of the plane described by the rigid triangle formed by r_1, r_2, and r_{12}. In these coordinates, the volume element can be written as [45]

$$d\tau \;\; = \;\; r_1 r_2 r_{12} \sin\theta_1 dr_1 dr_2 dr_{12} d\theta_1 d\phi_1 d\chi \tag{2.46}$$
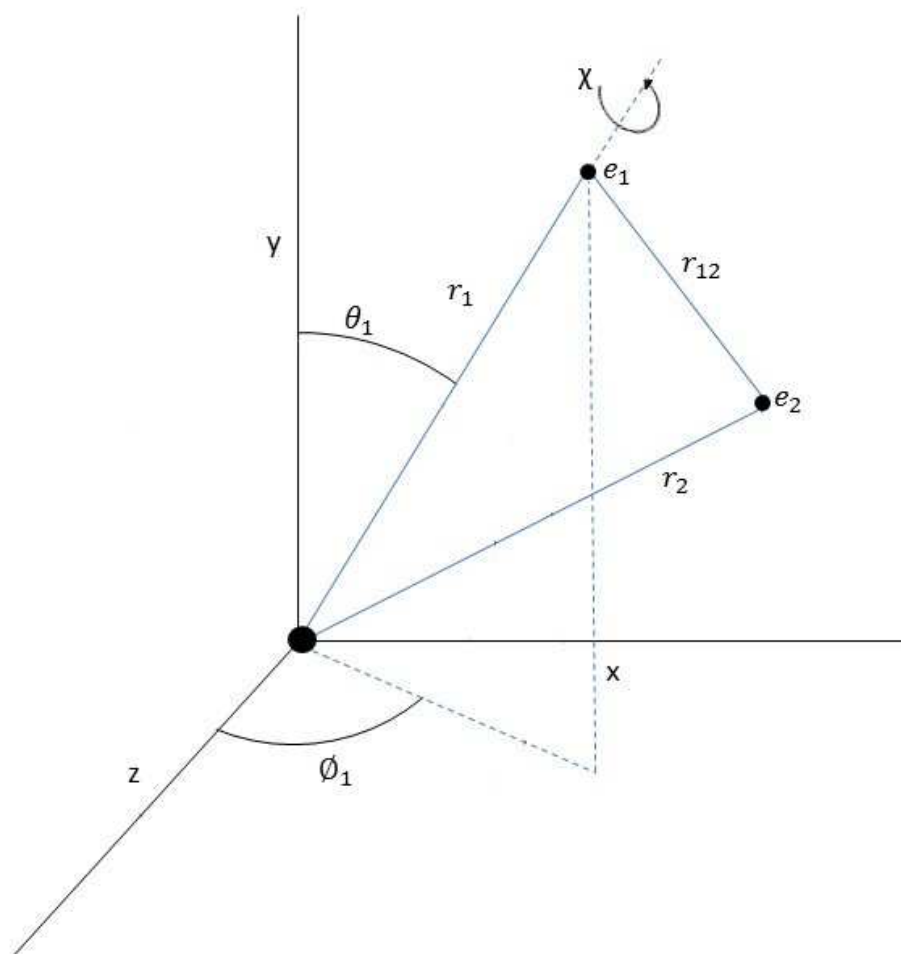
Figure 2.4: Hylleraas coordinates for a helium atom with the origin centered at the nucleus.

Integration of this volume element over all space can be written explicitly, showing the limits of integration, as

$$\int_{\mathcal{V}} d\tau = \int_0^\infty r_1 dr_1 \int_0^\infty r_2 dr_2 \int_{|r_1-r_2|}^{r_1+r_2} r_{12} dr_{12} \int_0^\pi \sin\theta_1 d\theta_1 \int_0^{2\pi} d\phi_1 \int_0^{2\pi} d\chi. \qquad (2.47)$$

The trial wave function, Eq. (2.39), can be separated into a radial and angular parts

$$\psi_{\text{tr}}(\mathbf{r}_1, \mathbf{r}_2) = R_{nl}(r_1, r_2, r_{12})\, \mathcal{Y}_{l_1 l_2 L}^{M}(\hat{r}_1, \hat{r}_2), \qquad (2.48)$$

which allows the radial and angular components of these integrals to be analyzed and calculated separately.

2.4.1 Radial Integrals

The general form of the radial component of the integrals can be illustrated by looking at the overlap integral between two different states,

$$\int_{\mathcal{V}} \psi_{\text{tr}}^{*\,\prime} \psi_{\text{tr}} d\tau = \int_{\mathcal{V}} R_{n'l'}(r_1, r_2, r_{12})\, \mathcal{Y}_{l_1' l_2' L'}^{M'}(\hat{r}_1, \hat{r}_2)\, R_{nl}(r_1, r_2, r_{12})\, \mathcal{Y}_{l_1 l_2 L}^{M}(\hat{r}_1, \hat{r}_2)\, d\tau. \qquad (2.49)$$

The radial component of Eq. (2.49) can be expressed in its most general form as

$$
\begin{aligned}
I_0(a,b,c;\alpha,\beta) &= \int_0^\infty r_1 dr_1 \int_0^\infty r_2 dr_2 \int_{|r_1-r_2|}^{r_1+r_2} r_{12} dr_{12}\, r_1^a r_2^b r_{12}^c e^{-\alpha r_1 - \beta r_2} \qquad (2.50) \\
&= \int_0^\infty r_1 dr_1 \int_{r_1}^\infty r_2 dr_2 \int_{r_2-r_1}^{r_1+r_2} r_{12} dr_{12}\, r_1^a r_2^b r_{12}^c e^{-\alpha r_1 - \beta r_2} \\
&+ \int_{r_2}^\infty r_1 dr_1 \int_0^\infty r_2 dr_2 \int_{r_1-r_2}^{r_1+r_2} r_{12} dr_{12}\, r_1^a r_2^b r_{12}^c e^{-\alpha r_1 - \beta r_2}
\end{aligned}
$$

where $a = i' + i, b = j' + j, c = k' + k$, are the summation of the exponents of the r_1, r_2, and r_{12} terms respectively. Integrating over the electron-electron separation, r_{12} gives

$$
\begin{aligned}
I_0 &= \frac{1}{c+2} \int_0^\infty dr_1 \int_{r_1}^\infty dr_2 [(r_2+r_1)^{c+2} - (r_2-r_1)^{c+2}] r_1^{a+1} r_2^{b+1} e^{-\alpha r_1 - \beta r_2} \qquad (2.51) \\
&+ \frac{1}{c+2} \int_{r_2}^\infty dr_1 \int_0^\infty dr_2 [(r_2+r_1)^{c+2} - (r_1-r_2)^{c+2}] r_1^{a+1} r_2^{b+1} e^{-\alpha r_1 - \beta r_2}
\end{aligned}
$$

These general integrals can be written more conveniently by using the binomial theorem

as

$$I_0 = \frac{2}{c+2} \sum_{s=0}^{[[(c+\frac{1}{2})]]} \begin{pmatrix} c+2 \\ 2s+1 \end{pmatrix} \ [\ \int_0^\infty dr_1 \int_{r_1}^\infty dr_2 r_1^p r_2^q e^{-\alpha r_1 - \beta r_2} \tag{2.52}$$

$$+ \int_0^\infty dr_2 \int_{r_2}^\infty dr_1 r_1^{p'} r_2^{q'} e^{-\alpha r_1 - \beta r_2}],$$

where the term in the round brackets is a binomial coefficient

$$\begin{pmatrix} n \\ k \end{pmatrix} = \frac{n!}{k!\,(n-k)!}, \text{ for integers n, and k,} \tag{2.53}$$

the square bracket notation used in the upper limit of the summation, $[[x]]$, means the largest integer value in x, and $p = a + 2s$, $p' = b + 2s$, $q = b + c - 2s$, and $q' = a + c - 2s$, for some value of the index s. The individual integrals within the summation of Eq. (2.52) can be expressed analytically in terms of Gamma functions and Incomplete Gamma functions [46],

$$\Gamma(n) = \int_0^\infty t^{n-1} e^{-t} dt, \text{ n= 1,2,3,\dots} \tag{2.54}$$

$$\Gamma(a,x) = \int_x^\infty t^{a-1} e^{-t} dt$$

$$\Gamma(n,x) = (n-1)! e^{-x} \sum_{s=0}^{n-1} \frac{x^s}{s!}, \text{ n = 1,2,3,\dots,}$$

to obtain

$$I_0 = \frac{2}{c+2} \sum_{s=0}^{[[(c+\frac{1}{2})]]} \begin{pmatrix} c+2 \\ 2s+1 \end{pmatrix} [F_{p,q}(\alpha,\beta) + F_{p',q'}(\alpha,\beta)], \tag{2.55}$$

where

$$F_{p,q}(\alpha,\beta) = \begin{cases} \frac{q!}{(\alpha+\beta)^{p+1}\beta^{q+1}} \sum_{l=0}^q \frac{(p+l)!}{l!} \left(\frac{\beta}{\alpha+\beta}\right)^l & q \geq 0, p \geq 0 \\ \frac{p!}{\alpha^{p+q+2}} \sum_{l=p+q+1}^\infty \frac{l!}{(l-q)!} \left(\frac{\alpha}{\alpha+\beta}\right)^{l+1} & q < 0, p \geq 0 \\ 0 & p < 0 \end{cases} \tag{2.56}$$

This general radial integral, Eq. (2.55), for the overlap matrix is valid for $a, b \geq -1$, and $c \geq -1$. While only the overlap integral was analyzed, to calculate matrix elements with arbitrary powers of r_1, r_2, and r_{12} the above result can be extended to any integral of this form by adjusting the exponents a, b, and c accordingly. An extensive list of these integrals can be found in the *Atomic, Molecular, and Optical Physics Handbook* [44].

2.4.2 Angular Integrals

The angular component of the integrals in Eq. (2.49) will now be studied. Again, for simplicity we will look at the general form of these integrals for the case of the calculation of the overlap matrix. Instead of breaking the basic integral up into a radial and angular components as we did in the previous section, we retain the radial components of the wave function, but focus on the angular portion. As an example to study we investigate a simple angular integral which illustrates the technique that is applied generally

$$I = \int_{\mathcal{V}} d\tau \, R'R Y_{l_1}^{m_1*}(\theta_1, \phi_1) \, Y_{l_2}^{m_2}(\theta_2, \phi_2) \,, \tag{2.57}$$

with the radial function defined as before, $R = r_1^i r_2^j r_{12}^k exp\left(-\alpha r_1 - \beta r_2\right)$, and $a = i' + i$, $b = j' + j$, and $c = k' + k$.

To begin, we write the spherical harmonic of the first electron as

$$Y_{l_1}^{m_1*}(\theta_1, \phi_1) = \sqrt{\frac{2l_1 + 1}{4\pi}} \mathcal{D}_{m_1,0}^{l_1}(\phi_1, \theta_1, \chi) \,. \tag{2.58}$$

Due to our change of variables to Hylleraas coordinates, the polar angles θ_2, and ϕ_2, of $\mathbf{r}_2$ are no longer independent. As a consequence, we must write the spherical harmonic for the second electron in terms of a rotation matrix

$$Y_{l_2}^{m_2}(\theta_2, \phi_2) = \sum_{M} \mathcal{D}_{m_2,M}^{l_2*}(\phi_1, \theta_1, \chi) \, Y_{l_2}^{M}(\theta, \phi) \,, \tag{2.59}$$

where we define the angles θ, and ϕ, as the polar and azimuthal angles of the vector $\mathbf{r}_2$ relative to the radial vector $\mathbf{r}_1$.

The basic integral Eq. (2.57) can then be rewritten by using the orthogonality relation of rotation matrices [33], Eqs. (2.58) and (2.59), and then integrating over the angular

variables

$$I = \int_{\mathcal{V}} d\tau \, R' R Y_{l_1}^{m_1*} (\theta_1, \phi_1) \, Y_{l_2}^{m_2} (\theta_2, \phi_2) \tag{2.60}$$

$$= \int_{\mathcal{V}} d\tau \, R' R \sum_M \mathcal{D}_{m_2 M}^{l_2*} (\phi_1, \theta_1, \chi) \, Y_{l_2}^M (\theta, \phi) \sqrt{\frac{2l_2 + 1}{4\pi}} \mathcal{D}_{m_1 0}^{l_1} (\phi_1, \theta_1, \chi)$$

$$= \int_{\mathcal{V}} d\tau_R \, R' R \frac{\delta_{l_2 l_1} \delta_{M 0} \delta_{m_2 m_2} 8\pi^2}{2l_2 + 1} Y_{l_2}^M (\theta, \phi) \sqrt{\frac{2l_2 + 1}{4\pi}}$$

$$= \frac{8\pi^2 \delta_{l_2 l_1} \delta_{m_2 m_2}}{2l_2 + 1} \int_{\mathcal{V}_{\mathcal{R}}} d\tau_R \, R' R \sqrt{\frac{2l_2 + 1}{4\pi}} P_{l_2} (\cos\theta) \sqrt{\frac{2l_2 + 1}{4\pi}}$$

$$= 2\pi \delta_{l_2 l_1} \delta_{m_2 m_1} \int_{\mathcal{V}_{\mathcal{R}}} d\tau_R \, R' R P_{l_2} (\cos\theta),$$

where the remaining integration should be taken over the radial space $\mathcal{V}_{\mathcal{R}}$ with the corresponding volume element $d\tau_R$. The definition of the Legendre polynomial in terms of spherical harmonics (see for example *Introduction to Quantum Mechanics* [47])

$$P_{l_2} (\cos\theta) = \sqrt{\frac{2l_2 + 1}{4\pi}} Y_{l_2}^0 (\theta, \phi) \tag{2.61}$$

has been used as well.

Because of the choice of independent variables of integration, θ is not an independent variable, but is uniquely determined by the triangle formed by the independent variables r_1, r_2, and r_{12} according to

$$\cos\theta = \frac{r_1^2 + r_2^2 - r_{12}^2}{2r_1 r_2} = \frac{r_1}{2r_2} + \frac{r_2}{2r_2} - \frac{r_{12}^2}{2r_1 r_2}, \tag{2.62}$$

thus we must include the Legendre polynomial, $P_{l_2} (\cos\theta)$, which is consequently a purely radial function, in the calculation of the radial integrals.

We can extend this to a more general integral, that includes vector coupled spherical harmonics, of the form,

$$I (a, b, c; l_1, m_1, l_2, m_2; \alpha, \beta) = \int_{\mathcal{V}} d\tau \, R' R \mathcal{Y}_{l_1' l_2' L'}^{M'} (\hat{\mathbf{r}}_1, \hat{\mathbf{r}}_2) \, \mathcal{Y}_{l_1 l_2 L}^M (\hat{\mathbf{r}}_1, \hat{\mathbf{r}}_2), \tag{2.63}$$

with

$$\mathcal{Y}_{l_1 l_2 L}^M (\hat{\mathbf{r}}_1, \hat{\mathbf{r}}_2) = \sum_{m_1 m_2} \langle l_1 l_2 m_1 m_2 | LM \rangle Y_{l_1}^{m_1} (\hat{r}_1) \, Y_{l_2}^{m_2} (\hat{r}_2). \tag{2.64}$$

This integral can be evaluated by use of the following properties of spherical harmonics [33],

$$Y_{l_1}^{m_1}(\hat{r}_1) Y_{l_2}^{m_2}(\hat{r}_2) = \sum_{lm} \left(\frac{(2l_1+1)(2l_2+1)(2l+1)}{4\pi} \right)^{\frac{1}{2}} \tag{2.65}$$

$$\times \begin{pmatrix} l_1 & l_2 & l \\ m_1 & m_2 & m \end{pmatrix} \begin{pmatrix} l_1 & l_2 & l \\ 0 & 0 & 0 \end{pmatrix} \times Y_l^{m*}(\hat{r}),$$

and

$$Y_L^{M*}(\hat{r}) = (-1)^M Y_L^{-M}(\hat{r}). \tag{2.66}$$

Using Eq. (2.65) allows the product of two spherical harmonics to be rewritten as a sum, and the general angular integral, Eq. (2.63), can be rewritten as

$$
\begin{aligned}
I &= \int_{\mathcal{V}} d\tau \, R'R \left[\sum_{m_1' m_2'} \langle l_1' l_2' m_1' m_2' | L'm' \rangle Y_{l_1'}^{m_1'}(\hat{r}_1) Y_{l_2'}^{m_2'}(\hat{r}_2) \right] \\
&\quad \times \left[\sum_{m_1 m_2} \langle l_1 l_2 m_1 m_2 | Lm \rangle Y_{l_1}^{m_1}(\hat{r}_1) Y_{l_2}^{m_2}(\hat{r}_2) \right] \\
&= \int_{\mathcal{V}} d\tau \, R'R \sum_{m_1' m_2'} \sum_{m_1 m_2} \langle l_1' l_2' m_1' m_2' | L'm' \rangle \langle l_1 l_2 m_1 m_2 | Lm \rangle \\
&\quad \times \sum_{\Lambda M} \sum_{\Lambda' M'} \left[\frac{(2l_1'+1)(2l_1+1)(2\Lambda+1)(2l_2'+1)(2l_2+1)(2\Lambda'+1)}{4\pi} \right]^{\frac{1}{2}} \\
&\quad \times (-1)^{m_1'+m_2'+M'+M} \left[Y_{\Lambda}^{-M}(\hat{r}_1) \right] \left[Y_{\Lambda'}^{-M'}(\hat{r}_2) \right] \\
&\quad \times \begin{pmatrix} l_1' & l_1 & \Lambda \\ -m_1' & m_1 & M \end{pmatrix} \begin{pmatrix} l_1' & l_1 & \Lambda \\ 0 & 0 & 0 \end{pmatrix} \begin{pmatrix} l_2' & l_2 & \Lambda' \\ -m_2' & m_2 & M' \end{pmatrix} \begin{pmatrix} l_2' & l_2 & \Lambda' \\ 0 & 0 & 0 \end{pmatrix} \\
&= \int_{\mathcal{V}} d\tau \, R'R \sum_{m_1' m_2'} \sum_{m_1 m_2} \sum_{\Lambda' M'} \sum_{\Lambda M} (\cdots) \left[\sqrt{\frac{2\Lambda+1}{4\pi}} \mathcal{D}_{M,0}^{\Lambda*}(\theta_1, \phi_1, \chi) \right] \\
&\quad \times \left[\sum_N \mathcal{D}_{M',N}^{\Lambda'}(\theta_1, \phi_1, \chi) Y_{\Lambda'}^N(\theta, \phi) \right] \\
&= \int_{\mathcal{V}_R} d\tau_R \sum_{m_1' m_2'} \sum_{m_1 m_2} \sum_{\Lambda' M'} \sum_{\Lambda M} (\cdots) \delta_{M,M'} \delta_{\Lambda,\Lambda'} P_{\Lambda}(\cos\theta) \\
&= \int_{\mathcal{V}_R} d\tau_R \, R'R \sum_{\Lambda} C_{\Lambda} P_{\Lambda}(\cos\theta),
\end{aligned}
$$

$$\tag{2.67}$$

where the constant, C_Λ is defined as [48]

$$
\begin{aligned}
C_\Lambda &= \frac{1}{2} \left[\frac{(2l_1' + 1)(2l_1 + 1)(2l_2' + 1)(2l_2 + 1)}{4\pi} \right]^{\frac{1}{2}} \\
&\quad \times (-1)^{\Lambda+L} (2\Lambda + 1) \\
&\quad \times \begin{pmatrix} l_1' & l_1 & \Lambda \\ 0 & 0 & 0 \end{pmatrix} \begin{pmatrix} l_2' & l_2 & \Lambda \\ 0 & 0 & 0 \end{pmatrix} \begin{Bmatrix} L & l_1 & l_2 \\ \Lambda & l_2' & l_1' \end{Bmatrix}.
\end{aligned}
\tag{2.68}
$$

Therefore, the general angular integral, Eq. (2.63), can be written as a summation of radial integrals which can be calculated using the methods described in Sec. (2.4.1)

$$
I(a, b, c; l_1, m_1, l_2, m_2; \alpha, \beta) = \sum_\Lambda C_\Lambda \int_{\mathcal{V}_R} d\tau_R \, R' R P_\Lambda(\cos\theta).
\tag{2.69}
$$

2.5 Pseudostates

In this section, the method of using a pseudostate spectrum to determine the solution to perturbation equations. will be explained further. The advantage of the pseudostate method is that it replaces the actual spectrum of infinitely many bound states plus a continuum by a finite pseudospectrum that is entirely discrete, and becomes complete in the limit of an infinite basis set. A pseudostate spectrum will be used in Sec. (3.3) as a numerical tool for the calculation of first order correction in a $\frac{1}{Z}$ expansion method. As an example, pseudostates will be used to calculate the dipole polarizability of hydrogen in Sec. (2.5.1). This sample calculation illustrates how powerful using a pseudostate method can be by showing that exact analytic solution to the first order perturbed wave function can be found with only two pseudostates in the spectrum.

To construct a pseudostate spectrum, we choose set of basis functions, $|\chi_p\rangle$, that diagonalize the Hamiltionian H. The matrix elements in this basis set are then

$$
\langle \chi_p | H | \chi_q \rangle = E_p \delta_{pq},
\tag{2.70}
$$

$$
\langle \chi_p | \chi_q \rangle = \delta_{pq},
\tag{2.71}
$$

where the eigenvectors $|\chi_p\rangle$, with corresponding eigenvalues E_p, form a discrete variational representation of the true spectrum of the system spanning both the the bound and continuous regions.

To calculate these pseudostates, we begin by orthonormalizing the basis set by forming linear combinations

$$|\chi_p\rangle = \sum_q \varphi_q R_{\mathrm{pq}} \tag{2.72}$$

subject to Eq. (2.71). This is done by finding an $N \times N$ orthogonal transformation matrix $\mathbf{T}$ such that

$$\mathbf{T}^{\mathrm{T}}\mathbf{OT} = \mathbf{I} = \begin{pmatrix} I_1 & 0 & \cdots & 0 \\ 0 & I_2 & & \vdots \\ \vdots & & \ddots & \\ 0 & & \cdots & I_{\mathrm{N}} \end{pmatrix}, \tag{2.73}$$

where $\mathbf{O}$ is the overlap matrix with matrix elements

$$O_{\mathrm{pq}} = \langle \varphi_p | \varphi_q \rangle, \tag{2.74}$$

and following with the application of a scale change matrix

$$\mathbf{S} = \begin{pmatrix} \frac{1}{I_1^{1/2}} & 0 & \cdots & 0 \\ 0 & \frac{1}{I_2^{1/2}} & & \vdots \\ \vdots & & \ddots & \\ 0 & & \cdots & \frac{1}{I_{\mathrm{N}}^{1/2}} \end{pmatrix} = \mathbf{S}^{\mathrm{T}}. \tag{2.75}$$

This gives us the result

$$\begin{aligned} \mathbf{S}^{\mathrm{T}}\mathbf{T}^{\mathrm{T}}\mathbf{OTS} &= \mathbf{R}^T\mathbf{OR}^{\mathrm{T}} \\ &= \mathbb{I}, \end{aligned} \tag{2.76}$$

where we have

$$\mathbf{R} = \mathbf{TS} \tag{2.77}$$

and

$$\mathbf{R}^{\mathrm{T}} = \mathbf{S}^{\mathrm{T}}\mathbf{T}^{\mathrm{T}}. \tag{2.78}$$

The columns in the transformation matrix $\mathbf{T}$ are the eigenvectors that diagonalize the overlap matrix, and the diagonal elements, $I_1, I_2, \ldots, I_N$, are the corresponding eigenvalues.

These can be found either analytically or computationally by using algorithms such as the Jacobi method.

A given Hamiltonian matrix $\mathbf{H}$, with matrix elements

$$\mathbf{H}_{\mathrm{pq}} = \langle \varphi_p | H | \varphi_q \rangle, \tag{2.79}$$

can be expressed in terms of the $|\chi_p\rangle$ basis set as

$$\mathbf{H}' = \mathbf{R}^{\mathrm{T}} \mathbf{H} \mathbf{R}. \tag{2.80}$$

Diagonalization of the transformed Hamiltonian $\mathbf{H}'$ is accomplished by finding another orthogonal transformation matrix $\mathbf{W}$, with the property

$$\begin{aligned} \mathbf{W}^{\mathrm{T}} \mathbf{H}' \mathbf{W} &= \mathbf{\Lambda} \\ &= \begin{pmatrix} \lambda_1 & 0 & \cdots & 0 \\ 0 & \lambda_2 & & \vdots \\ \vdots & & \ddots & \\ 0 & & \cdots & \lambda_{\mathrm{N}} \end{pmatrix}. \end{aligned} \tag{2.81}$$

In the new basis, the nth eigenvector is

$$\begin{aligned} \Psi^{(\mathrm{n})} &= \sum_{\mathrm{p,q}} |\chi_p\rangle W_{\mathrm{p,n}} \\ &\quad \sum_{\mathrm{p,p'}} \varphi_{\mathrm{p'}} R_{\mathrm{p'p}} W_{\mathrm{p,n}}. \end{aligned} \tag{2.82}$$

2.5.1 Example: Polarizability of Hydrogen

As an example of the use of pseudostates, the calculation of the dipole polarizability of hydrogen will be shown. The Hamiltonian for a hydrogen atom in its ground state subject to an electric field $\vec{F} = eF\hat{z}$, is

$$\begin{aligned} H &= H^{(0)} + H^{(1)} \\ &= H^{(0)} + eFz \\ &= H^{(0)} + eFr\cos\theta \end{aligned} \tag{2.83}$$

By treating the $eFr\cos\theta$ term as a perturbation we can write the Hamiltonian in the general form

$$H = H^{(0)} + \lambda V, \tag{2.84}$$

where $V = eFr\cos\theta$ is the perturbation, and λ is a perturbation constant that will be set to 1 at the end of the calculation. It is used only to keep track of order. Then, using perturbation theory we expand the wave function and energies as

$$\Psi = \Psi^{(0)} + \lambda\Psi^{(1)} + \lambda^2\Psi^{(2)} + \dots \tag{2.85}$$

$$E = E^{(0)} + \lambda E^{(1)} + \lambda^2 E^{(2)} + \dots \tag{2.86}$$

The exact first order solution, with perturbation $eFr\cos\theta$, which is calculated analytically in Appendix (C), is [49]

$$\Psi^{(1)} = -\frac{1}{\sqrt{3}}\left(2r + r^2\right)e^{-r}Y_1^0\left(\vec{\mathbf{r}}\right). \tag{2.87}$$

It is readily apparent that the perturbation, which is proportional to $\cos\theta$, is of odd parity. This gives the immediate result that the first order correction to the energy is

$$E^{(1)} = \frac{\langle\Psi^{(0)}|V|\Psi^{(0)}\rangle}{\langle\Psi^{(0)}|\Psi^{(0)}\rangle} \tag{2.88}$$
$$= 0.$$

Therefore, it is at second order that the first contribution to the energy expansion occurs. From perturbation theory, the expression for the second order energy is

$$E^{(2)} = \frac{\langle\Psi^{(0)}|V - E^{(0)}|\Psi^{(1)}\rangle}{\langle\Psi^{(0)}|\Psi^{(0)}\rangle} \tag{2.89}$$
$$= \frac{\langle\Psi^{(0)}|V|\Psi^{(1)}\rangle}{\langle\Psi^{(0)}|\Psi^{(0)}\rangle},$$

or in terms of the pseodostate spectrum

$$E^{(2)} = \sum_{p=1}^{N}{}' \frac{|\langle\chi_p|V|\Psi^{(0)}\rangle|^2}{E^{(0)} - E_p}, \tag{2.90}$$

where the primed notation denotes that we are omitting, if present, states with $E_p = E^{(0)}$. This can be done, without loss of generality, by imposing the orthogonality condition

$$\langle\Psi^{(0)}|\chi_p\rangle = 0. \tag{2.91}$$

The advantage of Eq. (2.90) is that it doesn't require the explicit calculation of the first order wave function.

From the second order correction to the energy, the dipole polarizbility can be found from the definition [2]

$$\alpha_d \equiv -2E^{(2)} \tag{2.92}$$

$$= \frac{9}{2}a_0^3, \tag{2.93}$$

where a_0 is the Bohr radius.

While the analytic result is known, a variational wave function of the form

$$\Psi_{\text{tr}}^{(1)} = -\frac{1}{\sqrt{3}} \sum_{n=0}^{N} b_n r^n e^{-\lambda r} Y_1^0(\hat{\mathbf{r}}), \tag{2.94}$$

where the coeffients b_n are linear variational parameters, and λ is an additional nonlinear variational parameter, can be used to solve for the second order correction to the energy. Additionally, since we know a priori that Eq. (2.87) does not include an r^0 term, it is sufficient to choose the variational solution

$$\Psi_{\text{tr}}^{(1)} = -\frac{1}{\sqrt{3}} \sum_{n=1}^{N} b_n r^n e^{-\lambda r} Y_1^0(\hat{\mathbf{r}}), \tag{2.95}$$

In this form, the solution is written in an N-dimensional basis set, and for any value of λ the basis set provides the best possible variational representation of $\Psi^{(1)}$. For the specific situation where $\lambda = 1$, the exact solution (2.87), is recovered.

Figure (2.5) shows the value of the dipole polarizability as a function of the nonlinear variational parameter λ for different basis sizes. The exact solution is found by locating where the dipole polarizability is a global maximum (when the second order correction

---

[2] By writing the electric dipole moment as an expansion about the electric field as a perturbation

$$p = p^{(0)} + \alpha_{\text{d}} F + \beta F^2 + \dots,$$

the change in energy can be calculated, by integrating over the electric field, to first nonvanishing order, to be

$$\Delta E = -\frac{1}{2}\alpha_{\text{d}} E^{(2)} F^2.$$

Comparing this result to Eq. (2.86) with $\lambda = F$, yields Eq. (2.92).

to the energy is a minimum). As seen in Figure (2.5), the region around $\lambda = 1$ remains
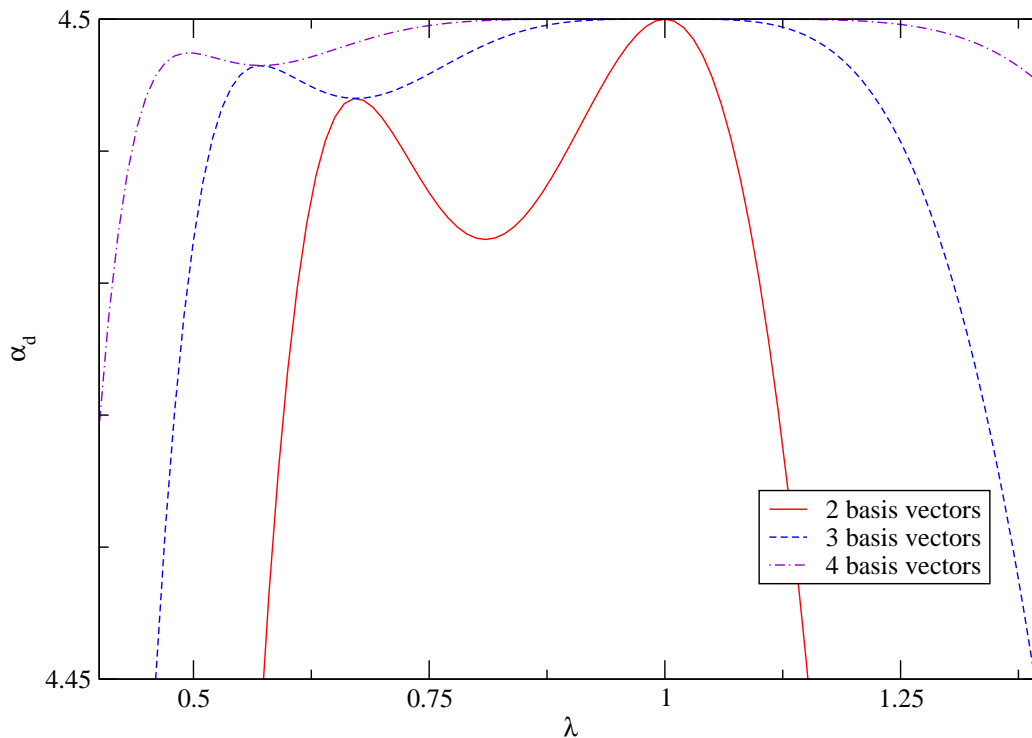
Figure 2.5: Variational polarizability, α_d, of hydrogen in units of a_0^3. Three sets of data are shown for basis sizes of $N = 2, 3, 4$. The exact value of the polarizability $\alpha_d = 4.5a_0^3$ occurs, in all cases (with $N > 1$), when the variational parameter $\lambda = 1$

shown more explicitly in Fig. (2.6), is that as the number of basis functions is increased, the lower local maximum and local minimum occur with higher values (though always lower than the global maximum corresponding to the correct value of α_d) and at lower values of the variational parameter λ. Specifically, the location of the local maximum with N basis vectors always occurs at the the precise location of the local minimum for the case with $N + 1$ basis vectors. This is even true for the case when there is only a single basis vector, though this particular case does not yeild the correct answer for the dipole polarizability α_d.
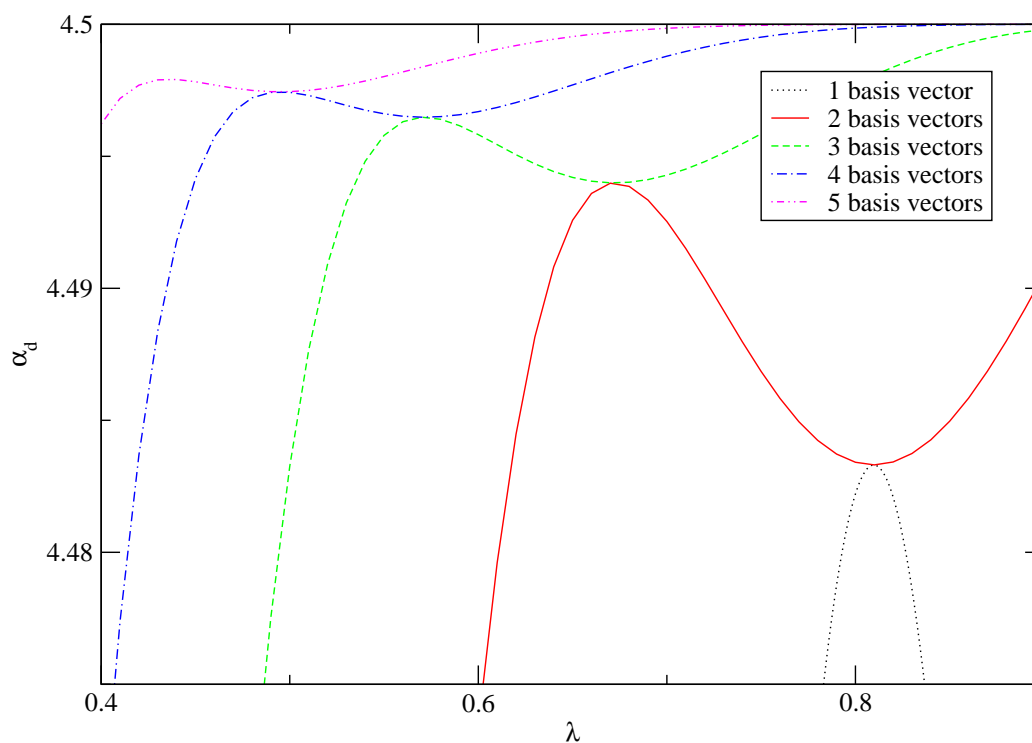
Figure 2.6: The variational polarizability α_d, of hydrogen in units of a_0^3 at the points of local minima and maxima. The location of the local maximum with N basis vectors always occurs at the the precise location of the local minimum with $N + 1$ basis vectors. The special case with $N = 1$ is included to show that it continues this trend even though with only one basis vector the correct value for the dipole polarizability is not found.

2.6 $\frac{1}{Z}$ Expansion

For larger values of the atomic charge Z, it is possible to make an expansion in terms of powers of $\frac{1}{Z}$. That is, we want to calculate the matrix element of an operator $\mathcal{A}$,

$$A = \langle \Psi_i | \mathcal{A} | \Psi_f \rangle, \tag{2.96}$$

in terms of an infinite power series expansion as

$$\begin{aligned} A &= \langle \Psi_i | \mathcal{A} | \Psi_f \rangle \\ &= Z^n (A_0 + A_1 \frac{1}{Z} + A_2 \frac{1}{Z^2} + A_3 \frac{1}{Z^3} + \ldots), \end{aligned} \tag{2.97}$$

where n is determined by the $Z-$scaling of A. In practice this infinite series is truncated to

$$A = Z^n (A_0 + A_1 \frac{1}{Z} + A_2 \frac{1}{Z^2} + A_3 \frac{1}{Z^3} + \ldots + A_M \frac{1}{Z^M}), \tag{2.98}$$

for some integer value M.

To accomplish this, we treat the interaction term in the Schrödinger equation (2.21) as a perturbation,

$$H = H_0 + \frac{1}{Z} \frac{1}{r_{12}}, \tag{2.99}$$

where r_{12} is the electron-electron separation. By performing a scale change such that

$$\mathbf{r}_i \to \frac{\mathbf{r}_i}{Z}, \tag{2.100}$$

where $i = 1, 2$ denotes the electron label, gives

$$\mathbf{r}_{12} \to \frac{\mathbf{r}_{12}}{Z} \tag{2.101}$$

$$\nabla_i \to Z \nabla_i \tag{2.102}$$

$$H \to Z^2 H \tag{2.103}$$

$$A \to Z^{-2} A. \tag{2.104}$$

With this scale change, the wave function and energy can be expanded in powers of $\frac{1}{Z}$ as

$$\begin{aligned} \Psi &= \Psi^{(0)} + \frac{1}{Z} \Psi^{(1)} + \frac{1}{Z^2} \Psi^{(2)} + \ldots \end{aligned} \tag{2.105}$$

$$\begin{aligned} E &= E^{(0)} + \frac{1}{Z} E^{(1)} + \frac{1}{Z^2} E^{(2)} + \ldots, \end{aligned} \tag{2.106}$$

with

$$\langle \Psi^{(0)} | \Psi^{(1)} \rangle = 0, \tag{2.107}$$

such that

$$\left(H_0 + \frac{1}{Z} \frac{1}{r_{12}} \right) \left(\Psi^{(0)} + \frac{1}{Z} \Psi^{(1)} + \dots \right) = \left(E^{(0)} + \frac{1}{Z} E^{(1)} + \dots \right) \left(\Psi^{(0)} + \frac{1}{Z} \Psi^{(1)} + \dots \right) \tag{2.108}$$

with $\Psi^{(0)}$ being the exact solution, with energy $E^{(0)}$, to the unperturbed equation

$$H_0 \Psi^{(0)} = E^{(0)} \Psi^{(0)} \tag{2.109}$$

The scale changed expansion of the wave function Eq. (2.105) yields the form of the expansion of the matrix element A in Eq. (2.97). Expanding and collecting the first order terms in Eq. (2.108) yields the first order equation (Eq. (2.109) being the zeroth order equation)

$$H_0 \Psi^{(1)} + \frac{1}{r_{12}} \Psi^{(0)} = E^{(0)} \Psi^{(1)} + E^{(1)} \Psi^{(0)}, \tag{2.110}$$

or more conveniently written

$$\left(H_0 - E^{(0)} \right) \Psi^{(1)} + \frac{1}{r_{12}} \Psi^{(0)} = E^{(1)} \Psi^{(0)}. \tag{2.111}$$

We can then substitute Eq. (2.105) into Eq. (2.96) to find expressions for the expansion coefficients

$$
\begin{aligned}
A &= \langle \Psi^{(0)} + \frac{1}{Z} \Psi^{(1)} + \dots | \mathcal{A} | \Psi^{(0)} + \frac{1}{Z} \Psi^{(1)} + \dots \rangle \\
&= \langle \Psi^{(0)} | \mathcal{A} | \Psi^{(0)} \rangle + \frac{1}{Z} 2 \langle \Psi^{(1)} | \mathcal{A} | \Psi^{(0)} \rangle + \mathcal{O} \left(\frac{1}{Z^2} \right),
\end{aligned}
\tag{2.112}
$$

such that the first two expansion coefficients can be written as

$$
\begin{aligned}
A_0 &= \langle \Psi^{(0)} | \mathcal{A} | \Psi^{(0)} \rangle \\
A_1 &= 2 \langle \Psi^{(1)} | \mathcal{A} | \Psi^{(0)} \rangle,
\end{aligned}
\tag{2.113}
$$

where we have assumed the initial and final state in Eq. (2.96) are identical and that we are calculating diagonal matrix elements. For a discussion regarding the calculation of off-diagonal elements see Appendix (D).

The solutions to Eq. (2.109) are the product of two noninteracting hydrogen wave functions, and the solutions to Eq. (2.111) are not solvable analytically. Therefore, the zeroth order coefficient A_0 can be calculated in a straightforward manner since the hydrogen wave functions are well known. While we do not know the solutions $\Psi^{(1)}$, it is possible to use an alternative method to calculate A_1, as discussed in the following section.

2.6.1 The Dalgarno Interchange Theorem

Because we cannot directly solve for analytic solutions to the first order perturbation equation (2.111), we cannot directly calculate the first order coefficient A_1. It is, however, possible, by use of the Dalgarno Interchange Theorem [50] [51] [52] to calculate A_1 by finding an equivalent matrix element that we can calculate directly if A is a one-electron operator.

By treating the operator $\mathcal{A}$ as a perturbation to the unperturbed Hamiltonian H_0, we can follow a similar perturbation calculation as we did with the $\frac{1}{r_{12}}$ perturbation

$$(H_0 + \lambda \mathcal{A})\chi = \varepsilon \chi. \tag{2.114}$$

where λ is some constant which is included primarily to keep track of terms. We make the expansions

$$\chi = \chi^{(0)} + \lambda \chi^{(1)} + \lambda^2 \chi^{(2)} + \ldots \tag{2.115}$$

$$\varepsilon = \varepsilon^{(0)} + \lambda \varepsilon^{(1)} + \lambda^2 \varepsilon^{(2)} + \ldots \tag{2.116}$$

with

$$\langle \chi^{(0)} | \chi^{(1)} \rangle = 0. \tag{2.117}$$

The zeroth order equation will remain unchanged, and the zeroth order solutions to this new perturbation equation will again be products of two hydrogen wave functions and we will have

$$\chi^{(0)} = \Psi^{(0)} \tag{2.118}$$

$$\varepsilon^{(0)} = E^{(0)}.$$

The first order equation is then

$$\left(H_0 - E^{(0)}\right)\chi^{(1)} + \mathcal{A}\Psi^{(0)} = \varepsilon^{(1)}\Psi^{(0)}, \tag{2.119}$$

and as long as the operator $\mathcal{A}$ is not a function of r_{12}, i.e. $\mathcal{A}$ is a function of single electron operators, this equation can be solved.

If we multiply Eq. (2.111) from the left by $\langle\chi^{(1)}|$, and multiply Eq. (2.119) from the left by $\langle\Psi^{(1)}|$ we obtain

$$\langle\chi^{(1)}|\left(H_0 - E^{(0)}\right)|\Psi^{(1)}\rangle + \langle\chi^{(1)}|\frac{1}{r_{12}}|\Psi^{(0)}\rangle = \langle\chi^{(1)}|E^{(1)}|\Psi^{(0)}\rangle \tag{2.120}$$

$$\langle\Psi^{(1)}|\left(H_0 - E^{(0)}\right)|\chi^{(1)}\rangle + \langle\Psi^{(1)}|\mathcal{A}|\chi^{(0)}\rangle = \langle\Psi^{(1)}|\varepsilon^{(1)}\chi^{(0)}\rangle. \tag{2.121}$$

Subtracting Eq. (2.120) from Eq. (2.121)

$$\langle\chi^{(1)}|H_0 - E^{(0)}|\Psi^{(1)}\rangle - \langle\Psi^{(1)}|H_0 - E^{(0)}|\chi^{(1)}\rangle \tag{2.122}$$

$$+\langle\chi^{(1)}|\frac{1}{r_{12}}|\Psi^{(0)}\rangle - \langle\Psi^{(1)}|\mathcal{A}|\Psi^{(0)}\rangle = E^{(1)}\langle\chi^{(1)}|\Psi^{(0)}\rangle - \varepsilon^{(1)}\langle\Psi^{(1)}|\Psi^{(0)}\rangle.$$

By the orthogonality conditions, Eq. (2.107) and Eq. (2.117), the right hand side of Eq. (2.122) is zero. We are not keeping terms higher than first order, and therefore the first two terms in Eq. (2.122) are dropped leaving the result

$$\langle\chi^{(1)}|\frac{1}{r_{12}}|\Psi^{(0)}\rangle = \langle\Psi^{(1)}|\mathcal{A}|\Psi^{(0)}\rangle, \tag{2.123}$$

or

$$A_1 = \langle\chi^{(1)}|\frac{1}{r_{12}}|\Psi^{(0)}\rangle. \tag{2.124}$$

This result is the Dalgarno interchange theorem, and it allows us to calculate the matrix element on the right hand side of Eq. (2.123), which is not possibile to calculate directly, by an equivalent matrix element.

It now remains to find a way to determine the solution to Eq. (2.119). In general we can use the following procedure (where I have switched to a bra-ket notiation for the wave

functions),

$$\begin{aligned}
|\chi^{(1)}\rangle &= \frac{1}{H_0 - E^{(0)}} \left(\varepsilon^{(1)} - \mathcal{A} \right) |\Psi^{(0)}\rangle \\
&= \frac{1}{H_0 - E^{(0)}} \sum_{n \neq 0} |\phi_n\rangle\langle\phi_n| \left(\varepsilon^{(1)} - \mathcal{A} \right) |\Psi^{(0)}\rangle \\
&= \sum_{n \neq 0} \frac{1}{E_n - E^{(0)}} |\phi_n\rangle\langle\phi_n| \left(\varepsilon^{(1)} - \mathcal{A} \right) |\Psi^{(0)}\rangle
\end{aligned} \tag{2.125}$$

where we have, in the second line of Eq. (2.125), introduced the resolution of the identity

$$\mathbb{I} = \sum_{n \neq 0} |\phi_n\rangle\langle\phi_n|, \tag{2.126}$$

with the set of functions $|\phi_n\rangle$ being a complete set of states that we can choose at our convenience. The $n = 0$ state is not included in order to remove any singularities that would occur due to the denominator in Eq. (2.125) being equal to zero. The exclusion of the $n = 0$ state is consistent with our choice of orthogonalization, Eq. (2.107) and the fact that we will be investigating matrix elements of first order.

Chapter 3

Calculation of Transition Rates

Now that there exists an established method for calculating high precision wave functions for the ground and excited states of helium and helium like ions, those wave functions can be used to calculate various matrix elements, and eventually the transition rates we wish to determine.

This chapter will discuss the calculation of the magnetic dipole transition matrix elements via variational Hylleraas wave functions for helium and helium like ions nuclear charge $Z = 3$ to $Z = 18$.

For heavier ions with nuclear charge $Z > 18$, a $\frac{1}{Z}$ expansion can be performed utilizing the results from the above calculation, and the Dalgarno interchange theorem, to fit the coefficients of the expansion. The leading two terms of this expansion can be calculated analytically. This expansion procedure will also be discussed in this chapter.

All calculations in this study were performed in quadruple precision using computational resources allocated from the Shared Hierarchical Academic Research Computing Network (SHARCNet) consortium.

3.1   Magnetic Dipole Matrix Element

The emission probability, or transition rate, for the $1s2s\,^3S_1 \to 1s^2\,^1S_0$ transition of helium is

$$A(1s2s\,^3S_1 \to 1s^2\,^1S) = \hbar^{-1}\frac{4}{3}\left(\frac{\omega}{c}\right)^3|\langle 1s^2\,^1S_0|Q_{10}|1s2s\,^3S_1\rangle|^2, \tag{3.1}$$

where Q_{10} is the $M = 0$ component of the nonrelativisitc magnetic dipole transition operator and its matrix element can be written in terms of the momentum and position operators of the electrons

$$
\begin{aligned}
\langle 1s^2\,^1S_0|Q_{10}|1s2s\,^3S_1\rangle &= \mu_B\langle 1s^2\,^1S_0| - \left(\frac{2}{3m^2c^2}\right)\left(p_1^2 - p_2^2\right) \\
&\quad -\frac{1}{6}\left(\frac{\omega}{c}\right)^2\left(r_1^2 - r_2^2\right) \\
&\quad +\left(\frac{Ze^2}{3mc^2}\right)\left(\frac{1}{r_1} - \frac{1}{r_2}\right)|1s2s\,^3S_1\rangle,
\end{aligned}
\tag{3.2}
$$

where μ_B is the Bohr magneton, and with the spin parts of the wave functions having been omitted. Therefore, to determine the transition rate, it is necessary to calculate the energy difference between the $1s2s\,^3S$ state and the $1s^2\,^1S_0$ ground state, and the following matrix elements

$$
\begin{aligned}
\langle\frac{1}{r}\rangle &= \langle 1s^2\,^1S_0|\frac{1}{r}|1s2s\,^3S_1\rangle, \tag{3.3} \\
\langle r^2\rangle &= \langle 1s^2\,^1S_0|r^2|1s2s\,^3S_1\rangle, \\
&\text{and} \\
\langle p^2\rangle &= \langle 1s^2\,^1S_0|p^2|1s2s\,^3S_1\rangle,
\end{aligned}
$$

where the notation $\frac{1}{r} = \frac{1}{r_1} - \frac{1}{r_2}$, $r^2 = r_1^2 - r_2^2$, and $p^2 = p_1^2 - p_2^2$ has been used for the operators.

This operator in Eq. (3.2) does not include the next higher order relativistic corrections of relative order $(\alpha Z)^2$. As discussed by Drake [1], and Feinberg and Sucher [19], corrections of order α, and $\alpha\log\alpha$ vanish.

3.2 Variational Calculation of Matrix Elements

To determine the matrix elements of the magnetic dipole transition operator, trial wave functions, of the form described in Sec. (2.3), were used to calculate numerically these matrix elements. To estimate the accuracy of the results the calculation was performed multiple times with increasing basis size. As the basis size increases, the value of the matrix elements converges towards the exact value [53]. For a matrix element $\langle A \rangle$, the uncertainty in the calculation is estimated as

$$\delta \langle A \rangle_n = \frac{\langle A \rangle_n - \langle A \rangle_{n-1}}{2}, \tag{3.4}$$

where the subscript n denotes an iteration of the calculation with a particular basis size, and $n-1$ denotes the immediately previous iteration and has a smaller basis size. For all calculations, the uncertainty decreases and approaches zero asymptotically as the basis size is increased.

As an example, the logarithmic difference between the transition rate and the asymptotic value of the $1s2s\ ^3S_1 \rightarrow 1s^2\ ^1S_0$ transition rate for helium is plotted as a function of the number of basis functions in the $1s^2\ ^1S_0$ wave function in Fig (3.1). It can be seen that the value of the transition rate rapidly converges to the exact value as the basis size is increased.

The final results of these calculations, for $Z = 2$ were performed with the groundstate, $|1s^2\ ^1S\rangle$ being formed by 1262 basis functions, and the metastable state $\langle 1s2s\ ^3S|$ formed by 981 basis functions. For $Z > 2$ these calculations were performed with the ground state, $|1s^2\ ^1S\rangle$ being formed by 1262 basis functions, and the metastable state $\langle 1s2s\ ^3S|$ formed by 705 basis functions. Tables (3.1) and (3.2) shows the results of these calculations for nuclear charge $Z = 2$ through $Z = 18$.

Generating variational wave functions for nuclear charge $Z > 18$ can be accomplished, however these calculations continually increase in numerical complexity as Z increases. For $Z > 18$ a $\frac{1}{Z}$ expansion of the wave functions, as described in Sec. (2.6), will be performed to calculate the nonrelativistic M1 transition rate.
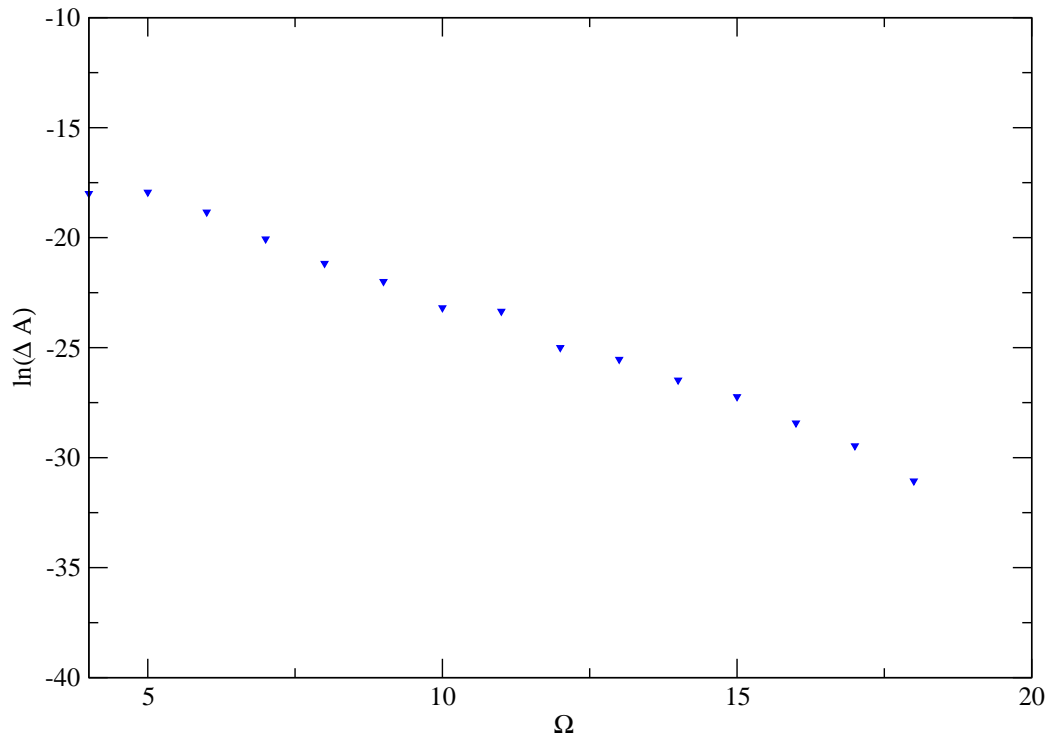
Figure 3.1: The logarithmic difference between the transition rate and the asymptotic value of the $1s2s\ ^3S_1 \rightarrow 1s^2\ ^1S_0$ transition rate for helium, $\ln\left(A_{asymptotic} - A_\Omega\right)$, as a function of the number of basis functions in terms of the Pekeris shell radius $\Omega = (i + j + k)_{\mathrm{max}}$.

Z	$\Delta E/Z^2$ (a.u)	$\frac{p^2}{Z^2}$	$Z^2 r^2$
2	0.7284949987973282(1)	0.43836731951(2)	$-7.488842007(9)$
3	2.16918604009856559(5)	0.49287942257(1)	$-6.072997363(4)$
4	4.3583996486459711(1)	0.518357459836(9)	$-5.509541022(3)$
5	7.2970742314285457(4)	0.533363374191(9)	$-5.207742253(3)$
6	10.98549069959057649(4)	0.543293282712(8)	$-5.019842003(3)$
7	15.42376341128167339(8)	0.550360650931(8)	$-4.891642835(4)$
8	20.61194780267291033(9)	0.555650885487(6)	$-4.798608427(2)$
9	26.5500740344411860(1)	0.559760854596(5)	$-4.728022194(2)$
10	33.2381599309641830(6)	0.563046548305(3)	$-4.672637308(1)$
11	40.6762167052039888(7)	0.565733659982(2)	$-4.6280221929(4)$
12	48.8642517650440361(7)	0.567972280880(1)	$-4.59131479897(7)$
13	57.80227020158881949(4)	0.5698661444277(6)	$-4.5605844261(1)$
14	67.4902756294097809(4)	0.5714892571867(3)	$-4.5344814579(3)$
15	77.92827068575445875(4)	0.57289584354168(2)	$-4.5120340860(4)$
16	89.1162573400083288(2)	0.5741265457263(1)	$-4.4925247751(4)$
17	101.0542370925539328(1)	0.5752124281724(4)	$-4.4754122174(4)$
18	113.7422111065596288(2)	0.5761776433054(3)	$-4.4602803669(4)$

Table 3.1: The energy difference, and the $\langle p^2 \rangle$ and $\langle r^2 \rangle$ transition matrix elements from the $1s2s\ ^3S$ state to the $1s^2\ ^1S_0$ state transition. All results are recorded in atomic units unless otherwise specified. The uncertainty in these calculations is given in parentheses for each individual calculation.

Z	$\frac{1}{Zr}$	$A\left(1s2s\ {}^3S_1 \rightarrow 1s^2\ {}^1S_0\right)\ (\text{s}^{-1})$	$A\left(1s2s\ {}^3S_1 \rightarrow 1s^2\ {}^1S_0\right)\frac{10^6}{Z^{10}}\ (\text{s}^{-1})$
2	0.27405791074(1)	0.00012724255998(6)	0.12426031
3	0.285306600610(7)	0.020400700108(8)	0.34548765
4	0.289022960814(6)	0.5620600596(2)	0.53602224
5	0.290863550971(7)	6.697205120(2)	0.68579380
6	0.291961006446(6)	48.56837371(2)	0.80323210
7	0.292689575252(7)	253.3040299(2)	0.89673000
8	0.293208449833(5)	1044.2379879(4)	0.97252241
9	0.293596768137(4)	3608.898317(1)	1.03502193
10	0.293898301389(2)	10873.542056(2)	1.08735420
11	0.294139221855(1)	29355.093908(2)	1.13176595
12	0.2943361390665(6)	72437.2377658(6)	1.16990183
13	0.2945001015767(1)	165842.147292(5)	1.20298826
14	0.2946387445078(1)	356348.96351(2)	1.23195585
15	0.2947575132788(4)	725150.67141(5)	1.25752221
16	0.2948603961091(4)	1407648.5317(1)	1.28024888
17	0.2949503809127(6)	2621963.7255(2)	1.30058118
18	0.2950297504261(4)	4709005.4077(3)	1.31887652

Table 3.2: The $\langle\frac{1}{r}\rangle$ transition matrix element, and the M1 transition rate from the $1s2s\ {}^3S$ state to the $1s^2\ {}^1S_0$ state. All results are recorded in atomic units unless otherwise specified. The uncertainty in these calculations is given in parentheses for each individual calculation. The final column illustrates the Z^10 scaling of the transition rate.

3.3 $\frac{1}{Z}$ Expansion of the Matrix Elements

By treating the $\frac{1}{r_{12}}$ term in the Hamiltonian as a perturbation, the unperturbed Hamiltonian is the sum of two independent hydrogen Hamiltonians

$$
\begin{aligned}
H &= H_0 + \lambda \frac{1}{r_{12}} \\
&= h(r_1) + h(r_2) + \lambda \frac{1}{r_{12}},
\end{aligned}
\tag{3.5}
$$

where $hr_i)$ is the single electron hydrogen Hamiltonian for i-th electron.

The unperturbed wave functions used in this study, which are functions of both r_1 and r_2, are separable products of single electron hydrogen wave functions. The spatial part of the unperturbed $1s^2\ ^1S_0$ ground state is the product of two hydrogen ground state wave functions

$$
\begin{aligned}
|\Psi^{(0)}_{1s^2\ ^1S}\rangle &= \frac{1}{\sqrt{\pi}} e^{-r_1} \frac{1}{\sqrt{\pi}} e^{-r_2} \\
&= \psi_{1s}(r_1)\psi_{1s}(r_2),
\end{aligned}
\tag{3.6}
$$

and the spatial part of the unperturbed $1s2s\ ^3S$ excited state is the antisymmetric combination of the form

$$
|\Psi^{(0)}_{1s2s\ ^3S}\rangle = \frac{1}{\sqrt{2}} \left[\psi_{1s}(r_1)\psi_{2s}(r_2) - \psi_{1s}(r_2)\psi_{2s}(r_1) \right],
\tag{3.7}
$$

with

$$
\psi_{1s}(r) = \frac{1}{\sqrt{\pi}} e^{-r}
\tag{3.8}
$$

and

$$
\psi_{2s}(r) = \frac{1}{\sqrt{32\pi}} (2 - r) e^{-r/2}.
\tag{3.9}
$$

As discussed in Sec. (2.6), the matrix elements can then be expanded, in Z-scaled atomic units, as

$$
\begin{aligned}
\langle p^2 \rangle &= \langle p^2 \rangle^{(0)} + \frac{1}{Z} \langle p^2 \rangle^{(1)} + \frac{1}{Z^2} \langle p^2 \rangle^{(2)} + \frac{1}{Z^3} \langle p^2 \rangle^{(3)} + \ldots \\
\langle r^2 \rangle &= \langle r^2 \rangle^{(0)} + \frac{1}{Z} \langle r^2 \rangle^{(1)} + \frac{1}{Z^2} \langle r^2 \rangle^{(2)} + \frac{1}{Z^3} \langle r^2 \rangle^{(3)} + \ldots \\
\langle \frac{1}{r} \rangle &= \langle \frac{1}{r} \rangle^{(0)} + \frac{1}{Z} \langle \frac{1}{r} \rangle^{(1)} + \frac{1}{Z^2} \langle \frac{1}{r} \rangle^{(2)} + \frac{1}{Z^3} \langle \frac{1}{r} \rangle^{(3)} + \ldots,
\end{aligned}
\tag{3.10}
$$

where the superscript outside the angular bracket denotes the order of the expansion.

3.3.1 Zeroth Order Expansion Coefficient

The zeroth order expansion coefficients of Eq. (3.10) can be analytically calculated as they involve only integrals consisting of the unperturbed wave functions. They are

$$
\begin{aligned}
\langle p^2 \rangle^{(0)} &= \langle \Psi^{(0)}_{1s2s\ ^3S} | p_1^2 - p_2^2 | \Psi^{(0)}_{1s^2\ ^1S} \rangle \\
&= \int\int \sin\theta_1 \sin\theta_2 d\theta_1 d\theta_2 \int\int d\phi_1 d\phi_2 \int\int dr_1 dr_2 r_1^2 r_2^2 (p_1^2 - p_2^2) \\
&\quad \times \frac{1}{\sqrt{2}} \psi_{1s}(r_1)\psi_{1s}(r_2) \left[\psi_{1s}(r_1)\psi_{2s}(r_2) - \psi_{1s}(r_2)\psi_{2s}(r_1) \right] \\
&= \frac{16}{27} \\
&\approx 0.5925925926,
\end{aligned}
\tag{3.11}
$$

$$
\begin{aligned}
\langle r^2 \rangle^{(0)} &= \langle \Psi^{(0)}_{1s2s\ ^3S} | r_1^2 - r_2^2 | \Psi^{(0)}_{1s^2\ ^1S} \rangle \\
&= \int\int \sin\theta_1 \sin\theta_2 d\theta_1 d\theta_2 \int\int d\phi_1 d\phi_2 \int\int dr_1 dr_2 r_1^2 r_2^2 (r_1^2 - r_2^2) \\
&\quad \times \frac{1}{\sqrt{2}} \psi_{1s}(r_1)\psi_{1s}(r_2) \left[\psi_{1s}(r_1)\psi_{2s}(r_2) - \psi_{1s}(r_2)\psi_{2s}(r_1) \right] \\
&= -\frac{1024}{243} \\
&\approx -4.2139917695,
\end{aligned}
\tag{3.12}
$$

and

$$
\begin{aligned}
\langle \frac{1}{r} \rangle^{(0)} &= \langle \Psi^{(0)}_{1s2s\ ^3S} | \frac{1}{r_1} - \frac{1}{r_2} | \Psi^{(0)}_{1s^2\ ^1S} \rangle \\
&= \int\int \sin\theta_1 \sin\theta_2 d\theta_1 d\theta_2 \int\int d\phi_1 d\phi_2 \int\int dr_1 dr_2 r_1^2 r_2^2 \left(\frac{1}{r_1} - \frac{1}{r_2}\right) \\
&\quad \times \frac{1}{\sqrt{2}} \psi_{1s}(r_1)\psi_{1s}(r_2) \left[\psi_{1s}(r_1)\psi_{2s}(r_2) - \psi_{1s}(r_2)\psi_{2s}(r_1) \right] \\
&= \frac{8}{27} \\
&\approx 0.2962962963.
\end{aligned}
\tag{3.13}
$$

Using the results from Sec. (3.2), the matrix elements $\langle r^2 \rangle$, $\langle p^2 \rangle$, and $\langle \frac{1}{r} \rangle$, plotted as functions of the nuclear charge, are shown respectively in Figures (3.2), (3.3), and (3.4). In each of these figures the zeroth order coefficient in the expansion of the corresponding matrix element is included. In the limit of infinite nuclear charge, the expansion will be

dominated by the zeroth order term and the the plots in Figures (3.2), (3.3), and (3.4) converge towards the zeroth order expansion coefficient.

3.3.2 First Order Expansion Coefficient

It is also possible, by using the Dalgarno interchange theorem described in Sec. (2.6.1) and Appendix (D.2), to calculate the first order expansion coefficient for single electron operators. Since the matrix elements are off-diagonal, the first order expansion coefficients to be calculated are

$$\langle p^2 \rangle^{(1)} = \langle \Psi^{(0)}_{1s2s\ ^3S}|p_1^2 - p_2^2|\Psi^{(1)}_{1s^2\ ^1S}\rangle + \langle \Psi^{(1)}_{1s2s\ ^3S}|p_1^2 - p_2^2|\Psi^{(0)}_{1s^2\ ^1S}\rangle, \qquad (3.14)$$

$$\langle r^2 \rangle^{(1)} = \langle \Psi^{(0)}_{1s2s\ ^3S}|r_1^2 - r_2^2|\Psi^{(1)}_{1s^2\ ^1S}\rangle + \langle \Psi^{(1)}_{1s2s\ ^3S}|r_1^2 - r_2^2|\Psi^{(0)}_{1s^2\ ^1S}\rangle, \qquad (3.15)$$

$$\langle \frac{1}{r} \rangle^{(1)} = \langle \Psi^{(0)}_{1s2s\ ^3S}|\frac{1}{r_1} - \frac{1}{r_2}|\Psi^{(1)}_{1s^2\ ^1S}\rangle + \langle \Psi^{(1)}_{1s2s\ ^3S}|\frac{1}{r_1} - \frac{1}{r_2}|\Psi^{(0)}_{1s^2\ ^1S}\rangle \qquad (3.16)$$

To calculate the first order expansion coefficients as written in the form above, the first order correction to the wave functions is required. As discussed in Sec. (2.6.1), the first order perturbation equation, with perturbation $\frac{1}{r_{12}}$, is not analytically solvable. Instead, the Dalgarno Interchange theorem will be used to calculate first order corrections to wave functions using p^2, r^2, and $\frac{1}{r}$ as perturbations. This procedure is based on the method performed by Dalgarno and Parkinson(1967) [54] for the $1s^2\ ^1S_0 \rightarrow 1snp\ ^1P$ transition in the helium sequence.

The first order corrections to the wave functions are written as

$$|\Psi^{(1)}_{1s^2\ ^1S}\rangle = |\Psi^{(1)}_{1s^2\ ^1S}\rangle_s + |\Psi^{(1)}_{1s^2\ ^1S}\rangle_d, \qquad (3.17)$$

$$|\Psi^{(1)}_{1s2s\ ^3S}\rangle = |\Psi^{(1)}_{1s2s\ ^3S}\rangle_s + |\Psi^{(1)}_{1s2s\ ^3S}\rangle_d,$$

where the subscript s denotes single excitations where only one electron has been excited from its initial state, and the subscript d denotes double excitations where both electrons can be excited from their inital state. For single excitations,

$$|\Psi^{(1)}_{1s^2\ ^1S}\rangle_s = \sum_{n \neq 1} \frac{1}{E_1^{(0)} - E_n^{(0)}} |\psi_{ns}(r_1)\psi_{1s}(r_2) + \psi_{1s}(r_1)\psi_{ns}\rangle \qquad (3.18)$$

$$\times \ \langle \psi_{ns}(r_1)\psi_{1s}(r_2) + \psi_{1s}(r_1)\psi_{ns}(r_2)|\frac{1}{r_{12}}|\psi_{1s}(r_1)\psi_{1s}(r_2)\rangle,$$
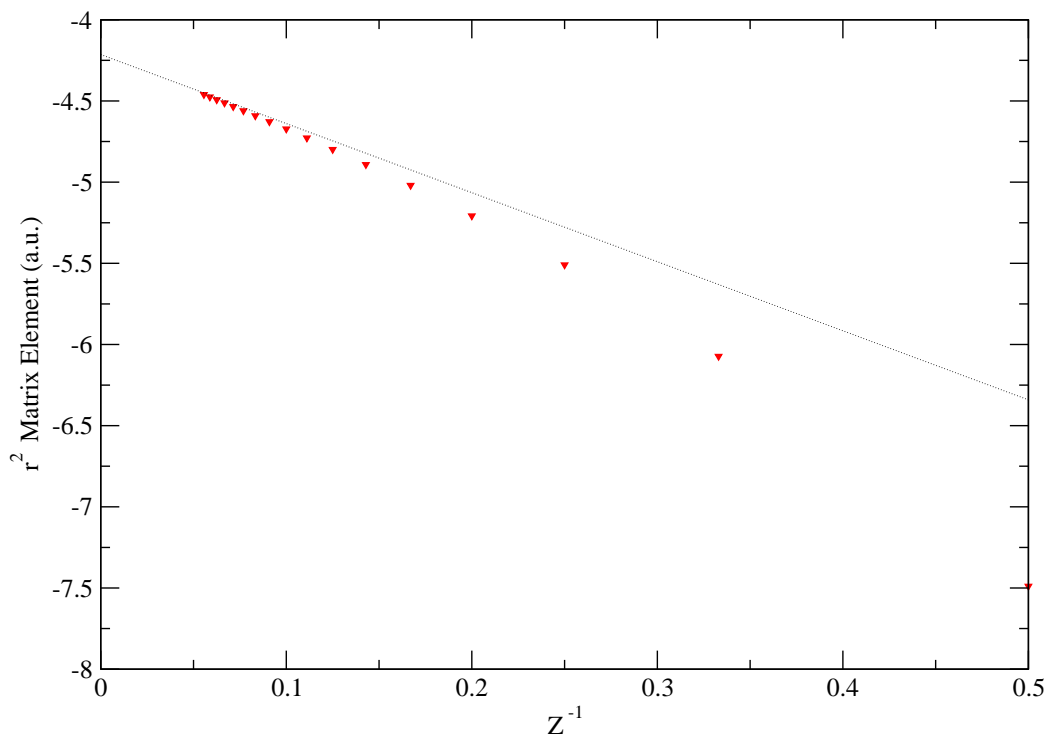
Figure 3.2: The $\langle r^2 \rangle$ matrix element (in atomic units) plotted as a function of the inverse of the nuclear charge Z through the isoelectronic sequence from $Z = 2$ to $Z = 18$. The intercept of the dotted line is the zeroth order expansion coefficient of the $\langle r^2 \rangle$ matrix element. The slope of the dotted line is the first order expansion coefficient which will be calculated in the following section. As expected, $\langle r^2 \rangle$ approaches $\langle r^2 \rangle^{(0)}$ as $Z \to \infty$.
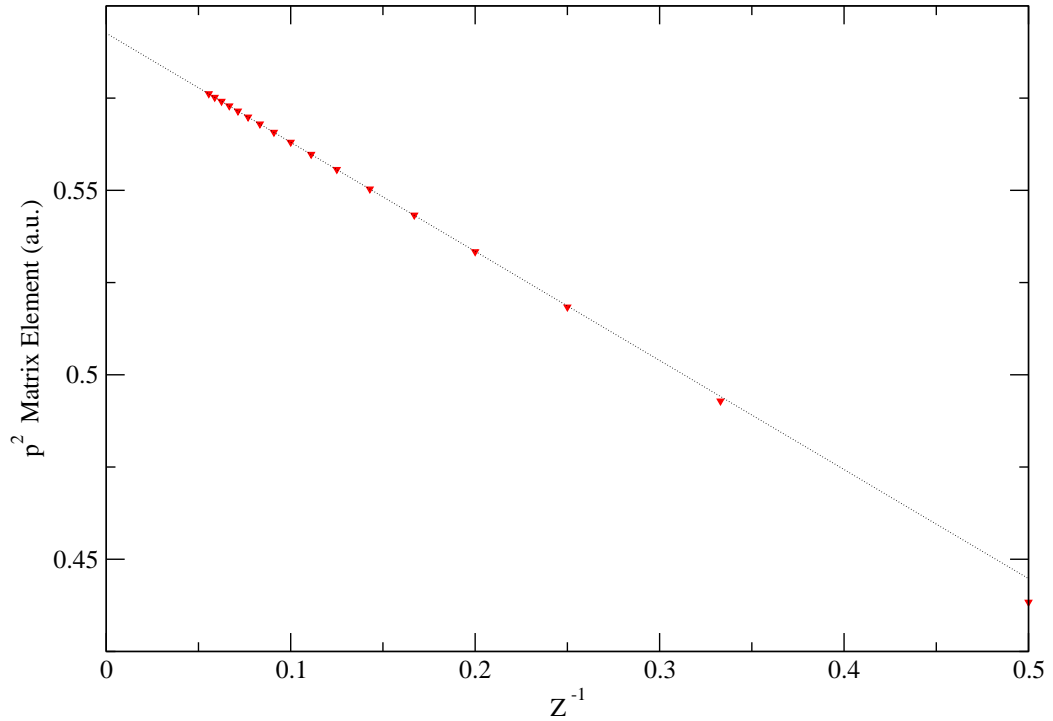
Figure 3.3: The $\langle p^2 \rangle$ matrix element (in atomic units) plotted as a function of the inverse of the nuclear charge Z through the isoelectronic sequence from $Z = 2$ to $Z = 18$. The intercept of the dotted line is the zeroth order expansion coefficient of the $\langle p^2 \rangle$ matrix element. The slope of the dotted line is the first order expansion coefficient which will be calculated in the following section. As expected, $\langle p^2 \rangle$ approaches $\langle p^2 \rangle^{(0)}$ as $Z \to \infty$.
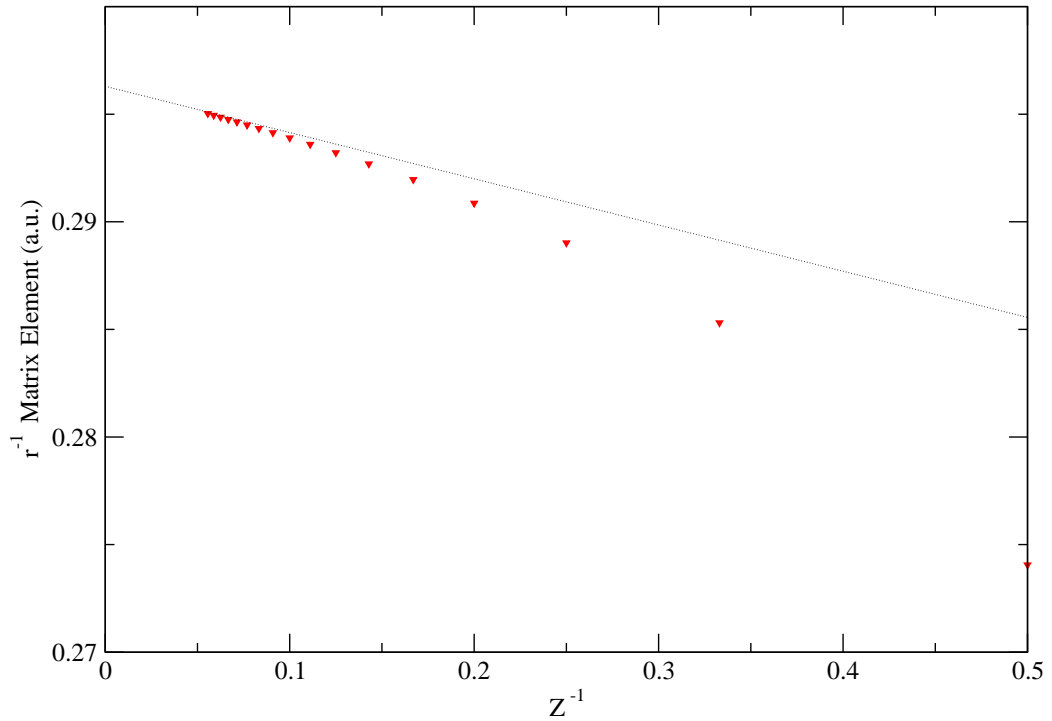
Figure 3.4: The $\langle\frac{1}{r}\rangle$ matrix element (in atomic units) plotted as a function of the inverse of the nuclear charge Z through the isoelectronic sequence from $Z = 2$ to $Z = 18$. The intercept of the dotted line is the zeroth order expansion coefficient of the $\langle\frac{1}{r}\rangle$ matrix element. The slope of the dotted line is the first order expansion coefficient which will be calculated in the following section. As expected, $\langle\frac{1}{r}\rangle$ approaches $\langle\frac{1}{r}\rangle^{(0)}$ as $Z \to \infty$.

$$
\begin{aligned}
|\Psi^{(1)}_{1s2s\ ^3S}\rangle_s \ = \ & \frac{1}{2\sqrt{2}} \sum_{n \neq 1} \frac{1}{E_1^{(0)} - E_n^{(0)}} |\psi_{ns}(r_1)\psi_{2s}(r_2) - \psi_{2s}(r_1)\psi_{ns}(r_2)\rangle \quad (3.19) \\
\times \ & \langle \psi_{ns}(r_1)\psi_{2s}(r_2) - \psi_{2s}(r_1)\psi_{ns}(r_2)| \frac{1}{r_{12}} | \\
\times \ & |\psi_{1s}(r_1)\psi_{2s}(r_2) - \psi_{2s}(r_1)\psi_{1s}(r_2)\rangle \\
+ \ & \frac{1}{2\sqrt{2}} \sum_{n \neq 1} \frac{1}{E_1^{(0)} - E_n^{(0)}} |\psi_{1s}(r_1)\psi_{ns}(r_2) - \psi_{ns}(r_1)\psi_{1s}(r_2)\rangle \\
\times \ & \langle \psi_{1s}(r_1)\psi_{ns}(r_2) - \psi_{ns}(r_1)\psi_{1s}(r_2)| \frac{1}{r_{12}} | \\
\times \ & |\psi_{1s}(r_1)\psi_{2s}(r_2) - \psi_{2s}(r_1)\psi_{1s}(r_2)\rangle,
\end{aligned}
$$

and for double excitations,

$$
\begin{aligned}
|\Psi^{(1)}_{1s^2\ ^1S}\rangle_d \ = \ & \sum_n \frac{1}{2E_1^{(0)} - E_2^{(0)} - E_n^{(0)}} |\psi_{ns}(r_1)\psi_{2s}(r_2) + \psi_{2s}(r_1)\psi_{ns}(r_2)\rangle \quad (3.20) \\
\times \ & \langle \psi_{ns}(r_1)\psi_{2s}(r_2) + \psi_{2s}(r_1)\psi_{ns}(r_2)| \frac{1}{r_{12}} |\psi_{1s}(r_1)\psi_{1s}(r_2)\rangle,
\end{aligned}
$$

and

$$
\begin{aligned}
|\Psi^{(1)}_{1s2s\ ^3S}\rangle_d \ = \ & \frac{1}{2\sqrt{2}} \sum_{n \neq 2} \frac{1}{E_1^{(0)} + E_2^{(0)} - E_1^{(0)} - E_n^{(0)}} \quad (3.21) \\
\times \ & |\psi_{ns}(r_1)\psi_{1s}(r_2) - \psi_{1s}(r_1)\psi_{ns}(r_2)\rangle \\
\times \ & \langle \psi_{ns}(r_1)\psi_{1s}(r_2) - \psi_{1s}(r_1)\psi_{ns}(r_2)| \frac{1}{r_{12}} | \\
\times \ & |\psi_{1s}(r_1)\psi_{2s}(r_2) - \psi_{2s}(r_1)\psi_{1s}(r_2)\rangle \\
+ \ & \frac{1}{2\sqrt{2}} \sum_{n \neq 1} \frac{1}{E_1^{(0)} + E_2^{(0)} - E_2^{(0)} - E_n^{(0)}} \\
\times \ & |\psi_{2s}(r_1)\psi_{ns}(r_2) - \psi_{ns}(r_1)\psi_{2s}(r_2)\rangle \\
\times \ & \langle \psi_{2s}(r_1)\psi_{ns}(r_2) - \psi_{ns}(r_1)\psi_{2s}(r_2)| \frac{1}{r_{12}} | \\
\times \ & |\psi_{1s}(r_1)\psi_{2s}(r_2) - \psi_{2s}(r_1)\psi_{1s}(r_2)\rangle.
\end{aligned}
$$

In the double excitation terms, only those contributions with $n = 2$ have been included since all other terms will not contribute to the summation. Any doubly excited state with $n > 2$ will be orthogonal to the unperturbed wave functions which only have $n = 1$ and $n = 2$.

The first order coefficient in the $\frac{1}{Z}$ expansion of $\langle \frac{1}{r} \rangle$ is then divided into four terms

$$
\langle \frac{1}{r} \rangle^{(1)} = T_{1,s} + T_{2,s} + T_{1,d} + T_{2,d}. \quad (3.22)
$$

Using Eqs. (3.6), (3.7), (3.16), (3.18), (3.19), (3.20), and (3.21), the terms on the right side of Eq. (3.22) are, after simplification,

$$
\begin{aligned}
T_{1,s} &= \langle \Psi^{(0)}_{1s2s\ ^3S} | \frac{1}{r_1} - \frac{1}{r_2} | \Psi^{(1)}_{1s^2\ ^1S} \rangle_s \\
&= -\frac{4}{\sqrt{2}} \langle \chi'_1(r_1)\psi_{1s}(r_2) | \frac{1}{r_{12}} | \psi_{1s}(r_1)\psi_{1s}(r_2) \rangle \\
&\quad + \frac{4}{\sqrt{2}} \frac{\langle \psi_{1s}(r_1) | \frac{1}{r_1} | \psi_{1s}(r_1) \rangle}{E^{(0)}_1 - E^{(0)}_2} \\
&\quad \times \langle \psi_{1s}(r_1)\psi_{2s}(r_2) | \frac{1}{r_{12}} | \psi_{1s}(r_1)\psi_{1s}(r_2) \rangle,
\end{aligned}
\tag{3.23}
$$

$$
\begin{aligned}
T_{2,s} &= \langle \Psi^{(0)}_{1s^2\ ^1S} | \frac{1}{r_1} - \frac{1}{r_2} | \Psi^{(1)}_{1s2s\ ^3S} \rangle_s \\
&= -\sqrt{2} \langle \psi_{1s}(r_1)\chi'_2(r_2) | \frac{1}{r_{12}} | \psi_{1s}(r_1)\psi_{2s}(r_2) - \psi_{2s}(r_1)\psi_{1s}(r_2) \rangle,
\end{aligned}
\tag{3.24}
$$

$$
\begin{aligned}
T_{1,d} &= \langle \Psi^{(0)}_{1s2s\ ^3S} | \frac{1}{r_1} - \frac{1}{r_2} | \Psi^{(1)}_{1s^2\ ^1S} \rangle_d \\
&= \frac{4}{\sqrt{2}} \langle \chi''_1(r_1)\psi_{2s}(r_2) | \frac{1}{r_{12}} | \psi_{1s}(r_1)\psi_{1s}(r_1) \rangle \\
&\quad + \frac{4}{\sqrt{2}} \frac{\langle \psi_{2s}(r_1) | \frac{1}{r_1} | \psi_{2s}(r_1) \rangle}{E^{(0)}_1 - E^{(0)}_2} \\
&\quad \times \langle \psi_{1s}(r_1)\psi_{2s}(r_2) | \frac{1}{r_{12}} | \psi_{1s}(r_1)\psi_{1s}(r_2) \rangle,
\end{aligned}
\tag{3.25}
$$

and

$$
\begin{aligned}
T_{2,d} &= \langle \Psi^{(0)}_{1s^2\ ^1S} | \frac{1}{r_1} - \frac{1}{r_2} | \Psi^{(1)}_{1s2s\ ^3S} \rangle_d \\
&= -\sqrt{2} \langle \psi_{1s}(r_1)\chi'_2(r_2) | \frac{1}{r_{12}} | \psi_{1s}(r_1)\psi_{2s}(r_2) - \psi_{2s}(r_1)\psi_{1s}(r_2) \rangle \\
&= T_{2,s},
\end{aligned}
\tag{3.26}
$$

where $|\chi'_1\rangle$, $|\chi'_2\rangle$, and $|\chi''_1\rangle$ are defined as

$$
|\chi'_1(r_i)\rangle = \sum_{n \neq 1} \frac{1}{E^{(0)}_1 - E^{(0)}_n} |\psi_{ns}(r_i)\rangle \langle \psi_{ns}(r_i) | \frac{1}{r_i} | \psi_{2s}(r_i) \rangle,
\tag{3.27}
$$

$$
|\chi'_2(r_i)\rangle = \sum_{n \neq 2} \frac{1}{E^{(0)}_2 - E^{(0)}_n} |\psi_{ns}(r_i)\rangle \langle \psi_{ns}(r_i) | \frac{1}{r_i} | \psi_{1s}(r_i) \rangle,
\tag{3.28}
$$

and

$$|\chi_1''(r_i)\rangle = \sum_n \frac{1}{2E_1^{(0)} - E_2^{(0)} - E_n^{(0)}} |\psi_{ns}(r_i)\rangle\langle\psi_{ns}(r_i)|\frac{1}{r_i}|\psi_{1s}(r_i)\rangle. \tag{3.29}$$

The $\langle p^2\rangle^{(1)}$, and $\langle r^2\rangle^{(1)}$ matrix expansion coefficients are derived in an identical manner where the only difference is the single electron operators appearing between the bra and ket states.

The purpose of the use of the Dalgarno interchange theorem is that we cannot solve the perturbation equation directly for the first order corrections $|\Psi_{1s^2\ ^1S}^{(1)}\rangle$ or $|\Psi_{1s2s\ ^3S}^{(1)}\rangle$ because of the presence of the electron-electron interaction term, $\frac{1}{r_{12}}$ in the differential equation. Instead, the matrix elements are written in terms of the solutions to solvable first order perturbation equations and integrals of the electron-electron interaction. While the interaction term prevents us from solving its own perturbation equation, its integration with known functions is straight forward. The interaction term can be replaced by the summation

$$\frac{1}{r_{12}} = \sum_{l=0}^{\infty} \left(\frac{r_<^l}{r_>^{l+1}}\right) P_l\left(\cos\theta\right), \tag{3.30}$$

where $P_l\left(\cos\theta\right)$ are Legendre polynomials, θ describes the angle between r_1 and r_2, and $r_<$, and $r_>$ correspond to the smaller and larger of r_1 and r_2. The analytical calculation of these integrals was performed using the functions defined in the Handbook of Atomic, Molecular, and Optical Physics (pages 203-205) [44].

The states defined in Eqs. (3.27), (3.28), and (3.29), were evaluated using a pseudostate spectrum to represent the $|\psi_{ns}\rangle$ basis using the methods described in Sec. (2.5). The number of basis functions in the pseudostate spectrum was varied and the calculation of the first order expansion coefficients of the matrix elements was performed iteratively until convergence was obtained. Convergence was obtained after including 9 terms in the pseudostate basis and numerical cancellation occurred for larger bases. The resulting first order

expansion coefficients, in Z-scaled atomic units, are

$$\langle p^2 \rangle^{(1)} = -0.295700550063(2), \tag{3.31}$$

$$\langle r^2 \rangle^{(1)} = -4.25418477972(2), \tag{3.32}$$

and

$$\langle \frac{1}{r} \rangle^{(1)} = -0.021483174894(5). \tag{3.33}$$

These values can be directly compared with the values obtained by Drake [18], which were obtained from $\frac{1}{Z}$ expanded wave functions, given below

$$\langle p^2 \rangle^{(1)}_{\text{Drake}} = -0.29569, \tag{3.34}$$

$$\langle r^2 \rangle^{(1)}_{\text{Drake}} = -4.2602, \tag{3.35}$$

and

$$\langle \frac{1}{r} \rangle^{(1)}_{\text{Drake}} = -0.02147. \tag{3.36}$$

As an example, the convergence of $\langle \frac{1}{r} \rangle^{(1)}$ as a function of basis size is shown in Table (3.3) where it can be seen that $\langle \frac{1}{r} \rangle^{(1)}$ rapidly approaches the correct value after including only a small number of basis functions in the pseudospectrum.

Basis Size	$\langle \frac{1}{Zr} \rangle^{(1)}$
2	-0.010802024546
3	-0.021466170856
4	-0.021482928135
5	-0.021483178513
6	-0.021483175259
7	-0.021483174920
8	-0.021483174905
9	-0.021483174894

Table 3.3: The first order correction to the $\langle \frac{1}{Zr} \rangle$ matrix element calculated using a pseudospectrum of varying basis size. Convergence was achieved with 9 basis functions.

3.3.3   Higher Order Expansion Coefficients

It is not possible to use the Dalgarno Interchange theorem to calculate higher order coefficients of the $\frac{1}{Z}$ expansion of matrix elements. To obtain them, a least squares fitting of the data, along with the exact value of the zeroth order expansion coefficient and the calculated value of the first order expansion coefficient, to a polynomial of order M was performed. All calculations in the following section were performed in double precision since all the numerical data used were the results of the previous sections, which could be represented accurately in double precision.

The matrix elements are

$$\langle p^2 \rangle \approx \langle p^2 \rangle_{\exp} \;\; = \;\; \langle p^2 \rangle^{(0)} + \frac{1}{Z}\langle p^2 \rangle^{(1)} + \sum_{m=2}^{M} \frac{1}{Z^m}\langle p^2 \rangle^{(m)}, \tag{3.37}$$

$$\langle r^2 \rangle \approx \langle r^2 \rangle_{\exp} \;\; = \;\; \langle r^2 \rangle^{(0)} + \frac{1}{Z}\langle r^2 \rangle^{(1)} + \sum_{m=2}^{M} \frac{1}{Z^m}\langle r^2 \rangle^{(m)},$$

$$\langle \frac{1}{r} \rangle \approx \langle \frac{1}{r} \rangle_{\exp} \;\; = \;\; \langle \frac{1}{r} \rangle^{(0)} + \frac{1}{Z}\langle \frac{1}{r} \rangle^{(1)} + \sum_{m=2}^{M} \frac{1}{Z^m}\langle \frac{1}{r} \rangle^{(m)},$$

where the zeroth and first order coefficients have been determined in Secs. (3.3.2) and (3.3.1) respectively. The subscript "exp" is to denote that these values correspond to the $\frac{1}{Z}$ approximation of the matrix elements. The value of M corresponding to the most accurate expansion is determined by successively performing the expansion for progressively larger values of M until the error associated with the expansion ceases to decrease with increasing M.

An eight parameter least squares fitting of the data obtained in Sec. (3.2), after being adjusted by subtracting the zeroth and first order terms, was performed. The values of these coefficients are listed in Table (3.4).

The error associated with each expansion coefficient $\langle A \rangle^{(i)}$ is the standard error of polynomial regression [55], and is given by

$$\delta\langle A \rangle^{(i)} = s_\epsilon \sqrt{C_{ii}^{-1}}, \tag{3.38}$$

where s_ϵ is the standard deviation of the residuals[1] defined by

$$s_\epsilon^2 = \frac{\sum_Z^{18}(\langle A(Z)\rangle - \langle A(Z)\rangle_{\exp})^2}{10},$$
(3.39)

and C_{ii}^{-1} are the diagonal elements of the inverse of the matrix of sums and cross products defined as

$$\mathbf{C} = \mathbf{X}^T\mathbf{X},$$
(3.40)

where $\mathbf{X}^T$ is the transpose of the matrix $\mathbf{X}$, with

$$\mathbf{X} = \begin{bmatrix} x_2^2 & x_2^3 & \dots & x_2^k \\ x_3^2 & x_3^3 & \dots & x_3^k \\ \vdots & & \ddots & \vdots \\ x_n^2 & x_n^3 & \dots & x_n^k \end{bmatrix},$$
(3.41)

where x_i is being used to denote the value of $\frac{1}{Z}$ with $Z = i$.

With the higher order coefficients calculated, Eq. (3.37) can be used to estimate the values of $\langle p^2\rangle$, $\langle r^2\rangle$, and $\langle\frac{1}{r}\rangle$ for ions with nuclear charge $Z > 18$. The associated uncertainty of those values is estimated by using standard propagation of error techniques. Since the expansion is being performed in orders of $\frac{1}{Z}$, the contributions of the higher order terms decreases as Z increases. Initially, at $Z = 19$, the correction due to the second order term is only 2.8% (with higher orders contributing a smaller and smaller correction). This is expected because at higher Z, the electron-electron interaction contribution is suppressed by a factor of $\frac{1}{Z}$.

Including these statistical uncertainties, the values of all the coefficients in the $\frac{1}{Z}$ expansion of the matrix elements are listed in Table (3.4)

The quality of this fitting can be seen by calculating the residual difference between the matrix elements as calculated with the variational method from Sec. (3.2) and those calculated via the $\frac{1}{Z}$ expansion, and finding the residual standard deviation from Eq. (3.39). The

---

[1] The 10 in the denominator of Eq. (3.39) is the number of degrees of freedom normally defined as $n - M$, with n being the number of points in the sample data, and M equal to the highest order of the polynomial we are fitting.

In this calculation, the zeroth and first order coefficients have already been determined and are not being calculated via polynomial regression. This increases the degrees of freedom by 2.

residual standard deviation gives, on average, how close the $\frac{1}{Z}$ expanded matrix elements are to matrix elements as calculated from the variational method. The residual standard deviations are

$$s_\epsilon(\langle p^2 \rangle) \;=\; 8.26 \times 10^{-13}, \tag{3.42}$$

$$s_\epsilon(\langle r^2 \rangle) \;=\; 1.63 \times 10^{-10}, \tag{3.43}$$

$$s_\epsilon(\langle p^2 \rangle) \;=\; 7.19 \times 10^{-13}, \tag{3.44}$$

and as an example of the expansion, the $\langle \frac{1}{r} \rangle$ matrix element is plotted using the expansion of Eq. (3.37) with the coefficients from Table (3.4) in Fig. (3.5).
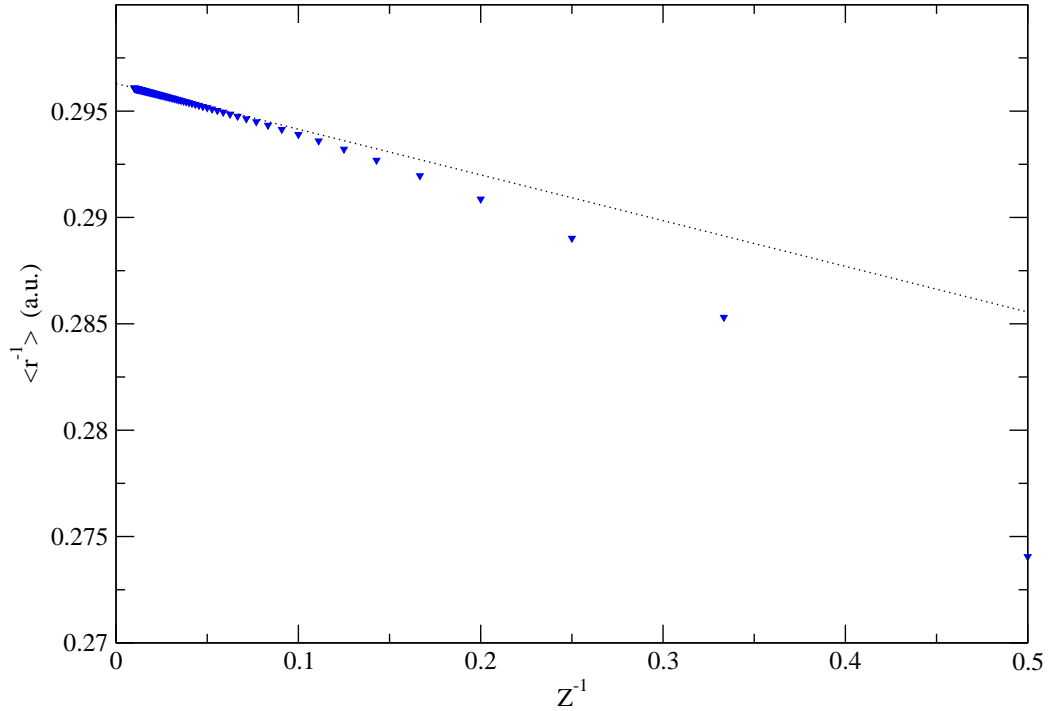
Figure 3.5: The $\langle\frac{1}{r}\rangle_{\exp}$ matrix element (in atomic units), as calculated as a $\frac{1}{Z}$ expansion with coefficients given in Table (3.4), plotted as a function of the inverse of the nuclear charge Z through the isoelectronic sequence from $Z = 2$ to $Z = 100$. The intercept of the dotted line is the zeroth order expansion coefficient of the $\langle\frac{1}{r}\rangle$ matrix element. The slope of the dotted line is the first order expansion coefficient of the $\langle\frac{1}{r}\rangle$ matrix element. As expected, $\langle\frac{1}{r}\rangle_{\exp}$ approaches $\langle\frac{1}{r}\rangle^{(0)}$ as $Z \to \infty$.

$\mathcal{O}(\frac{1}{Z})$	$\langle p^2 \rangle$	$\langle r^2 \rangle$	$\langle \frac{1}{r} \rangle$
0	0.5925925926	-4.2139917695	0.2962962963
1	0.295700550063(2)	4.25418477972(2)	-0.021483174894(5)
2	0.006165760(7)	-3.104598(1)	-0.022190783(6)
3	-0.0341073(3)	-2.040656(6)	-0.0250888(3)
4	-0.032135(6)	-1.318(1)	-0.024269(5)
5	-0.03036(5)	-0.78(1)	-0.02363(4)
6	-0.0171(3)	-0.82(6)	-0.0130(3)
7	-0.0596(9)	1.1(2)	-0.0501(8)
8	0.064(1)	-3.0(3)	0.056(1)
9	0.1089(9)	3.1(2)	-0.0930(8)

Table 3.4: The results of a $\frac{1}{Z}$ expansion of the $\langle p^2 \rangle$, $\langle r^2 \rangle$, and $\langle \frac{1}{r} \rangle$ matrix elements. The zeroth order coefficient was calculated analytically and has no uncertainty associated with the values listed in this table.

Chapter 4

Results and Conclusions

Large basis nonrelativistic Hylleraas wave functions of the form Eq. (2.43) were used to calculate numerically the following transition matrix elements from the metastable $1s2s\,{}^3S_1$ state to the $1s^2\,{}^1S_0$ state of helium and heliumlike ions through the isoelectronic sequence up to nuclear charge $Z = 18$,

$$
\begin{aligned}
\langle p^2 \rangle &= \langle 1s^2\,{}^1S_0 | p_1^2 - p_2^2 | 1s2s\,{}^3S_1 \rangle, \qquad\qquad (4.1)\\
\langle r^2 \rangle &= \langle 1s^2\,{}^1S_0 | r_1^2 - r_2^2 | 1s2s\,{}^3S_1 \rangle,\\
&\text{and}\\
\langle \frac{1}{r} \rangle &= \langle 1s^2\,{}^1S_0 | \frac{1}{r_1} - \frac{1}{r_2} | 1s2s\,{}^3S_1 \rangle.
\end{aligned}
$$

These transition matrix elements are used to evaluate the relativisitc magnetic dipole moment (M1) operator

$$
\begin{aligned}
\langle 1s^2\,{}^1S | Q_{10} | 1s2s\,{}^3S \rangle = \; & \mu_B \langle 1s^2\,{}^1S | - \left(\frac{2}{3m^2c^2} \right) \left(p_1^2 - p_2^2 \right) \\
& - \frac{1}{6} \left(\frac{\omega}{c} \right)^2 \left(r_1^2 - r_2^2 \right) \\
& + \left(\frac{Ze^2}{3mc^2} \right) \left(\frac{1}{r_1} - \frac{1}{r_2} \right) | 1s2s\,{}^3S \rangle,
\end{aligned}
$$

which is derived by taking multiple Foldy-Wouthuysen transformations of the helium Hamil-
tonian (as described in Sec. (1.3.2)). The corresponding decay rate from the metastable
triplet state to the ground state is

$$A(1s2s\ ^3S \to 1s^2\ ^1S) = \hbar^{-1}\frac{4}{3}\left(\frac{\omega}{c}\right)^3 |\langle 1s^2\ ^1S|Q_{10}|1s2s\ ^3S\rangle|^2.$$

Both the decay rate and the magnetic dipole moment operator are derived in full detail by
Drake(1971) [18]. The main result of the calculation from this thesis yields, for helium, a
nonrelativistic transition rate of

$$A(1s2s\ ^3S_1 \to 1s^2\ ^1S_0) = 1.2724255998(6) \times 10^{-4}\ \text{s}^{-1}, \tag{4.2}$$

and a lifetime of

$$\tau = 7.8590056673(4) \times 10^3\ \text{s}, \tag{4.3}$$

where the number quoted in the parentheses gives the uncertainty in the calculation at that
decimal value.

The values of the matrix elements of Eq. (4.1) are presented in Tables (3.1) and (3.2).
The transition rates and corresponding lifetimes are given in Table (4.1).

By treating the interaction term, $\frac{1}{r_{12}}$, in the helium Hamiltonian as a perturbation,
the nonrelativistic matrix elements of Eq. (4.1) were written as a $\frac{1}{Z}$ expansion in Sec. (2.6).
The zeroth order expansion coefficients are easily evaluated analytically as they involve only
integrals with unperturbed hydrogen wave functions. The first order expansion coefficients
are derived analytically by using the Dalgarno Interchange theorem in Sec. (3.3.2). The
higher order expansion coefficients were calculated by performing a least squares fitting to
the data obtained through the variational calculation. The expansion was taken to ninth
order at which point the error associated with the fitting was optimally minimized. The
expansion coefficients for the transition matrix elements are given in Table (3.4).

This expansion becomes highly accurate for large values of the nuclear charge Z. As Z
increases, the higher order terms in the expansion contribute less, and the zeroth and first
order terms, which were derived analytically, dominate the expansion. However, these are
lowest order nonrelativistic approximations.

Z	$A\left(1s2s\ ^3S \to 1s^2\ ^1S\right)$ (s^{-1})	τ (s)
2	$1.2724255998(6) \times 10^{-4}$	$7.8590056673(4) \times 10^{3}$
3	$2.0400700108(8) \times 10^{-2}$	$4.9017925596(2) \times 10^{1}$
4	$5.620600596(2) \times 10^{-1}$	$1.77916929502(6) \times 10^{0}$
5	$6.697205120(2) \times 10^{0}$	$1.4931601796(5) \times 10^{-1}$
6	$4.856837371(2) \times 10^{1}$	$2.05895302563(9) \times 10^{-2}$
7	$2.533040299(2) \times 10^{2}$	$3.9478250717(3) \times 10^{-3}$
8	$1.0442379879(4) \times 10^{3}$	$9.5763610555(4) \times 10^{-4}$
9	$3.608898317(1) \times 10^{3}$	$2.77092872163(8) \times 10^{-4}$
10	$1.0873542056(2) \times 10^{4}$	$9.1966352349(2) \times 10^{-5}$
11	$2.9355093908(2) \times 10^{4}$	$3.40656379140(2) \times 10^{-5}$
12	$7.24372377658(6) \times 10^{4}$	$1.380505429035(1) \times 10^{-5}$
13	$1.65842147292(5) \times 10^{5}$	$6.02983027131(2) \times 10^{-6}$
14	$3.5634896351(2) \times 10^{5}$	$2.80623799253(2) \times 10^{-6}$
15	$7.2515067141(5) \times 10^{5}$	$1.37902375248(1) \times 10^{-6}$
16	$1.4076485317(1) \times 10^{6}$	$7.10404605610(5) \times 10^{-7}$
17	$2.6219637255(2) \times 10^{6}$	$3.81393529695(3) \times 10^{-7}$
18	$4.7090054077(3) \times 10^{6}$	$2.12359068088(1) \times 10^{-7}$

Table 4.1: The M1 transition rate from the $1s2s\ ^3S_1$ state to the $1s^2\ ^1S_0$ state, and the lifetime, τ, of the metastable $1s2s\ ^3S_1$ state for nuclear charge $Z = 2$ through $Z = 18$ as calculated using large basis variational wavefunctions. The uncertainty in these calculations is given in parentheses for each individual calculation.

The values of the transition matrix elements of Eq. (4.1) for heliumlike ions through the isoelectronic sequence from $Z = 19$ through $Z = 100$ are given in Tables (4.2), (4.3), (4.4), and (4.5). These transition matrix elements were then used to evaluate the lowest order nonrelativistic $1s2s\ ^3S_1 \to 1s^2\ ^1S_0$ transition rates, and the $1s2s\ ^3S_1$ lifetimes for heliumlike ions through the isoelectronic sequence from $Z = 19$ through $Z = 100$, and are given in Tables (4.6), (4.7), (4.8), and (4.9).

4.1 Comparison with Experimental Measurements

In order to compare to experimental results, it should be clarified that these calculations are correct only up to order $(Z\alpha)^2$. This approximation becomes less valid with increasing nuclear charge as the relativistic effects increase and become nonnegligible. By comparison with experimental work, it should be possible to determine when these relativistic effects become important in determining the transition rate for the $1s2s\ ^3S_1 \to 1s^2\ ^1S_0$ transition. For the rest of this section, all current calculations, when compared with experimental values will be expressed only to order $(Z\alpha)^2$. Specifically, the largest source of uncertainty in these results will come from the estimation of the uncertainty in the corrections to the energy in a one-electron hydrogenic approximation. The leading relativistic correction to the energy for an electron with principal quantum number n and total angular momentum $\vec{j} = \vec{l} + \vec{s}$, is, from Bethe and Salpeter [37] (page 61),

$$\delta E = -\frac{\alpha^2 Z^4}{2n^3} \left(\frac{1}{j + 1/2} - \frac{3}{4n} \right).\tag{4.4}$$

For the ground state $n = 1$ and $j = \frac{1}{2}$ this gives

$$\delta E^{1s} = -\frac{1}{4}\frac{\alpha^2 Z^4}{2},\tag{4.5}$$

which gives a total energy for the $1s$ electron of

$$E_{\text{tot}}^{1s} = -\frac{Z^2}{2} \left[1 + \frac{1}{4}\alpha^2 Z^2 \right].\tag{4.6}$$

Similarly for the $2s$ electron, the energy is

$$E_{\text{tot}}^{2s} = -\frac{Z^2}{8} \left[1 + \frac{5}{16}\alpha^2 Z^2 \right].\tag{4.7}$$

Z	$\frac{p^2}{Z^2}$	$\frac{r^2}{Z^2}$	$\frac{1}{Zr}$
19	0.5770412535(7)	-4.4468041(1)	0.2951002787(6)
20	0.5778185055(6)	-4.4347261(1)	0.2951633652(5)
21	0.5785217396(5)	-4.4238392(1)	0.2952201289(4)
22	0.5791610513(4)	-4.41397570(8)	0.2952714751(4)
23	0.5797447795(4)	-4.40499769(7)	0.2953181441(3)
24	0.5802798728(3)	-4.39679109(6)	0.2953607473(3)
25	0.5807721675(3)	-4.38926058(6)	0.2953997938(2)
26	0.5812266020(2)	-4.38232592(5)	0.2954357111(2)
27	0.5816473827(2)	-4.37591909(4)	0.2954688611(2)
28	0.5820381154(2)	-4.36998204(4)	0.2954995517(2)
29	0.5824019080(2)	-4.36446493(3)	0.2955280468(2)
30	0.5827414543(2)	-4.35932472(3)	0.2955545739(1)
31	0.5830591004(1)	-4.35452408(3)	0.2955793300(1)
32	0.5833568992(1)	-4.35003044(3)	0.2956024869(1)
33	0.5836366547(1)	-4.34581525(2)	0.2956241946(1)
34	0.5838999588(1)	-4.34185341(2)	0.29564458501(9)
35	0.5841482212(1)	-4.33812276(2)	0.29566377458(9)
36	0.58438269528(9)	-4.33460363(2)	0.29568186633(8)
37	0.58460449874(9)	-4.33127852(2)	0.29569895186(7)
38	0.58481463172(8)	-4.32813183(2)	0.29571511284(7)

Table 4.2: The $\langle p^2 \rangle$, $\langle r^2 \rangle$, and $\langle \frac{1}{r} \rangle$ transition matrix elements from the $1s2s\ {}^3S_1$ state to the $1s^2\ {}^1S_0$ state transition for nuclear charge $Z = 19$ through $Z = 38$ as calculated from the $\frac{1}{Z}$ expansion. All results are recorded in atomic units. The uncertainty in these calculations is given in parentheses for each individual calculation.

Z	$\frac{p^2}{Z^2}$	$\frac{r^2}{Z^2}$	$\frac{1}{Zr}$
39	0.58501399176(7)	-4.32514957(1)	0.29573042235(6)
40	0.58520338667(7)	-4.32231917(1)	0.29574494596(6)
41	0.58538354546(6)	-4.31962933(1)	0.29575874266(6)
42	0.58555512772(6)	-4.31706983(1)	0.29577186571(5)
43	0.58571873168(6)	-4.31463143(1)	0.29578436326(5)
44	0.58587490119(5)	-4.31230572(1)	0.29579627899(5)
45	0.58602413179(5)	-4.31008506(1)	0.29580765263(4)
46	0.58616687592(5)	-4.307962512(9)	0.29581852033(4)
47	0.58630354750(4)	-4.305931700(9)	0.29582891512(4)
48	0.58643452601(4)	-4.303986805(9)	0.29583886721(4)
49	0.58656015990(4)	-4.302122488(8)	0.29584840430(4)
50	0.58668076981(4)	-4.300333843(8)	0.29585755182(3)
51	0.58679665117(4)	-4.298616356(7)	0.29586633315(3)
52	0.58690807675(3)	-4.296965861(7)	0.29587476985(3)
53	0.58701529870(3)	-4.295378516(7)	0.29588288183(3)
54	0.58711855050(3)	-4.293850763(6)	0.2589068748(3)
55	0.58721804866(3)	-4.292379308(6)	0.29589820382(3)
56	0.58731399422(3)	-4.290961097(6)	0.29590544666(3)
57	0.58740657413(3)	-4.289593291(5)	0.29591243064(2)
58	0.58749596243(3)	-4.288273249(5)	0.29591916942(2)

Table 4.3: The $\langle p^2 \rangle$, $\langle r^2 \rangle$, and $\langle \frac{1}{r} \rangle$ transition matrix elements from the $1s2s\ ^3S_1$ state to the $1s^2\ ^1S_0$ state transition for nuclear charge $Z = 39$ through $Z = 58$ as calculated from the $\frac{1}{Z}$ expansion. All results are recorded in atomic units. The uncertainty in these calculations is given in parentheses for each individual calculation.

Z	$\frac{p^2}{Z^2}$	$\frac{r^2}{Z^2}$	$\frac{1}{Zr}$
59	0.58758232137(3)	-4.286998512(5)	0.29592567566(2)
60	0.58766580239(2)	-4.285766788(5)	0.29593196122(2)
61	0.58774654699(2)	-4.284575935(5)	0.29593803713(2)
62	0.58782468757(2)	-4.283423954(4)	0.29594391370(2)
63	0.58790034808(2)	-4.282308969(4)	0.29594960059(2)
64	0.58797364477(2)	-4.281229229(4)	0.29595510684(2)
65	0.58804468670(2)	-4.280183088(4)	0.29596044092(2)
66	0.58811357635(2)	-4.279169001(4)	0.29596561078(2)
67	0.58818041006(2)	-4.278185517(4)	0.29597062389(2)
68	0.58824527853(2)	-4.277231272(4)	0.29597548727(2)
69	0.58830826718(2)	-4.276304982(3)	0.29598020753(2)
70	0.58836945655(2)	-4.275405434(3)	0.29598479090(1)
71	0.58842892267(2)	-4.274531489(3)	0.29598924324(1)
72	0.58848673731(2)	-4.273682067(3)	0.29599357010(1)
73	0.58854296833(2)	-4.272856151(3)	0.29599777672(1)
74	0.58859767993(1)	-4.272052780(3)	0.29600186802(1)
75	0.58865093286(1)	-4.271271041(3)	0.29600584869(1)
76	0.58870278470(1)	-4.270510073(3)	0.29600972316(1)
77	0.58875329001(1)	-4.269769060(3)	0.29601349562(1)
78	0.58880250059(1)	-4.269047225(3)	0.29601717003(1)

Table 4.4: The $\langle p^2 \rangle$, $\langle r^2 \rangle$, and $\langle \frac{1}{r} \rangle$ transition matrix elements from the $1s2s\ ^3S_1$ state to the $1s^2\ ^1S_0$ state transition for nuclear charge $Z = 59$ through $Z = 78$ as calculated from the $\frac{1}{Z}$ expansion. All results are recorded in atomic units. The uncertainty in these calculations is given in parentheses for each individual calculation.

Z	$\frac{p^2}{Z^2}$	$\frac{r^2}{Z^2}$	$\frac{1}{Zr}$
79	0.58885046559(1)	-4.268343835(3)	0.29602075021(1)
80	0.58889723172(1)	-4.267658191(2)	0.29602423970(1)
81	0.58894284335(1)	-4.266989630(2)	0.29602764191(1)
82	0.58898734273(1)	-4.266337521(2)	0.29603096008(1)
83	0.58903077005(1)	-4.265701265(2)	0.29603419728(1)
84	0.58907316359(1)	-4.265080290(2)	0.29603735644(1)
85	0.58911455983(1)	-4.264474053(2)	0.296040440350(9)
86	0.58915499356(1)	-4.263882034(2)	0.296043451668(9)
87	0.58919449795(1)	-4.263303740(2)	0.296046392925(9)
88	0.58923310468(1)	-4.262738699(2)	0.296049266539(9)
89	0.58927084402(1)	-4.262186460(2)	0.296052074816(9)
90	0.58930774486(1)	-4.261646593(2)	0.296054819961(8)
91	0.589343834839(9)	-4.261118686(2)	0.296057504078(8)
92	0.589379140401(9)	-4.260602348(2)	0.296060129180(8)
93	0.589413686843(9)	-4.260097201(2)	0.296062697192(8)
94	0.589447498388(9)	-4.259602886(2)	0.296065209956(8)
95	0.589480598238(8)	-4.259119058(2)	0.296067669237(7)
96	0.589513008632(8)	-4.258645387(2)	0.296070076724(7)
97	0.589544750888(8)	-4.258181556(2)	0.296072434037(7)
98	0.589575845458(8)	-4.257727262(2)	0.296074742727(7)
99	0.589606311963(8)	-4.257282213(2)	0.296077004283(7)
100	0.589636169244(8)	-4.256846131(1)	0.296079220135(7)

Table 4.5: The $\langle p^2 \rangle$, $\langle r^2 \rangle$, and $\langle \frac{1}{r} \rangle$ transition matrix elements from the $1s2s$ $^3S_1$ state to the $1s^2$ $^1S_0$ state transition for nuclear charge $Z = 79$ through $Z = 100$ as calculated from the $\frac{1}{Z}$ expansion. All results are recorded in atomic units.

Z	$A\left(1s2s\ ^3S \to 1s^2\ ^1S\right)\ (\mathrm{s}^{-1})$	$\tau\ (\mathrm{s})$
19	$8.1874513625(1)\times10^{6}$	$1.22138130137(2)\times10^{-7}$
20	$1.38285449347(2)\times10^{7}$	$7.23141881320(9)\times10^{-8}$
21	$2.27542401966(3)\times10^{7}$	$4.39478528555(6)\times10^{-8}$
22	$3.65664332006(4)\times10^{7}$	$2.73474854525(3)\times10^{-8}$
23	$5.75132959130(6)\times10^{7}$	$1.73872838294(2)\times10^{-8}$
24	$8.87010312380(9)\times10^{7}$	$1.12738260880(1)\times10^{-8}$
25	$1.34360867789(1)\times10^{8}$	$7.44264320746(8)\times10^{-9}$
26	$2.00181533401(2)\times10^{8}$	$4.99546578054(5)\times10^{-9}$
27	$2.93720696819(3)\times10^{8}$	$3.40459494625(3)\times10^{-9}$
28	$4.24907768878(4)\times10^{8}$	$2.35345190943(2)\times10^{-9}$
29	$6.06657201333(5)\times10^{8}$	$1.64837736666(1)\times10^{-9}$
30	$8.55604184227(7)\times10^{8}$	$1.168764737756(9)\times10^{-9}$
31	$1.192992172491(9)\times10^{9}$	$8.38228467092(7)\times10^{-10}$
32	$1.64572301247(1)\times10^{9}$	$6.07635666768(5)\times10^{-10}$
33	$2.24760521166(2)\times10^{9}$	$4.44917993077(3)\times10^{-10}$
34	$3.04082276830(2)\times10^{9}$	$3.28858363738(3)\times10^{-10}$
35	$4.07764890887(3)\times10^{9}$	$2.45239357862(2)\times10^{-10}$
36	$5.42245985865(4)\times10^{9}$	$1.84418147126(1)\times10^{-10}$
37	$7.15404503010(5)\times10^{9}$	$1.397810603363(9)\times10^{-10}$
38	$9.3683071100(6)\times10^{9}$	$1.067428712792(7)\times10^{-10}$

Table 4.6: The M1 transition rate from the $1s2s\ ^3S_1$ state to the $1s^2\ ^1S_0$ state, and the lifetime, τ, of the metastable $1s2s\ ^3S_1$ state for nuclear charge $Z = 19$ through $Z = 38$ as calculated from the $\frac{1}{Z}$ expansion. The uncertainty in these calculations is given in parentheses for each individual calculation.

Z	$A\left(1s2s\ ^3S \to 1s^2\ ^1S\right)\ (\mathrm{s}^{-1})$	τ (s)
39	$1.218134016768(8)\times10^{10}$	$8.20927735565(6)\times10^{-11}$
40	$1.57329807219(1)\times10^{10}$	$6.35607465415(4)\times10^{-11}$
41	$2.01908511360(1)\times10^{10}$	$4.95273821428(3)\times10^{-11}$
42	$2.57549613650(2)\times10^{10}$	$3.88274703979(3)\times10^{-11}$
43	$3.26629191392(2)\times10^{10}$	$3.06157571446(2)\times10^{-11}$
44	$4.11958905531(3)\times10^{10}$	$2.42742658691(2)\times10^{-11}$
45	$5.16851651402(3)\times10^{10}$	$1.93479114807(1)\times10^{-11}$
46	$6.45197653870(4)\times10^{10}$	$1.549912641500(9)\times10^{-11}$
47	$8.01547426303(5)\times10^{10}$	$1.247586814185(8)\times10^{-11}$
48	$9.91206671235(7)\times10^{10}$	$1.008871337351(6)\times10^{-11}$
49	$1.220339806411(7)\times10^{11}$	$8.19443891567(5)\times10^{-12}$
50	$1.496088478728(9)\times10^{11}$	$6.68409665751(4)\times10^{-12}$
51	$1.82669931619(1)\times10^{11}$	$5.47435470709(3)\times10^{-12}$
52	$2.22166980735(1)\times10^{11}$	$4.50111891827(3)\times10^{-12}$
53	$2.69190355815(2)\times10^{11}$	$3.71484333817(2)\times10^{-12}$
54	$3.24989124394(2)\times10^{11}$	$3.07702604468(2)\times10^{-12}$
55	$3.90989793164(2)\times10^{11}$	$2.55761152205(1)\times10^{-12}$
56	$4.68818040156(3)\times10^{11}$	$2.13302371997(1)\times10^{-12}$
57	$5.60321638181(4)\times10^{11}$	$1.784689242498(9)\times10^{-12}$
58	$6.67596372042(4)\times10^{11}$	$1.497911076032(8)\times10^{-12}$

Table 4.7: The M1 transition rate from the $1s2s\ ^3S_1$ state to the $1s^2\ ^1S_0$ state, and the lifetime, τ, of the metastable $1s2s\ ^3S_1$ state for nuclear charge $Z = 39$ through $Z = 58$ as calculated from the $\frac{1}{Z}$ expansion. The uncertainty in these calculations is given in parentheses for each individual calculation.

Z	$A\left(1s2s\ {}^3S \to 1s^2\ {}^1S\right)\ (\mathrm{s}^{-1})$	τ (s)
59	$7.93013807284(5){\times}10^{11}$	$1.261012091864(7){\times}10^{-12}$
60	$9.39251890085(5){\times}10^{11}$	$1.064677122885(6){\times}10^{-12}$
61	$1.109328330436(5){\times}10^{12}$	$9.01446373057(5){\times}10^{-13}$
62	$1.306636848571(7){\times}10^{12}$	$7.65323587111(4){\times}10^{-13}$
63	$1.534986227838(8){\times}10^{12}$	$6.51471643110(3){\times}10^{-13}$
64	$1.798644209636(9){\times}10^{12}$	$5.55974324796(3){\times}10^{-13}$
65	$2.102382728118(1){\times}10^{12}$	$4.75650787378(3){\times}10^{-13}$
66	$2.451529328517(1){\times}10^{12}$	$4.07908642319(2){\times}10^{-13}$
67	$2.852020685069(2){\times}10^{12}$	$3.50628592996(2){\times}10^{-13}$
68	$3.310462295549(2){\times}10^{12}$	$3.02072614252(2){\times}10^{-13}$
69	$3.834191614089(2){\times}10^{12}$	$2.60811169772(1){\times}10^{-13}$
70	$4.431346378314(2){\times}10^{12}$	$2.25665049542(1){\times}10^{-13}$
71	$5.110937872332(3){\times}10^{12}$	$1.956588056790(9){\times}10^{-13}$
72	$5.882931962940(3){\times}10^{12}$	$1.699832679180(9){\times}10^{-13}$
73	$6.758331563342(3){\times}10^{12}$	$1.479655134744(8){\times}10^{-13}$
74	$7.749270978871(4){\times}10^{12}$	$1.290443969151(6){\times}10^{-13}$
75	$8.869111713807(4){\times}10^{12}$	$1.127508630254(6){\times}10^{-13}$
76	$1.0132548846689(5){\times}10^{13}$	$9.86918508986(5){\times}10^{-14}$
77	$1.1555721651207(6){\times}10^{13}$	$8.65372176817(4){\times}10^{-14}$
78	$1.3156336749395(6){\times}10^{13}$	$7.60090000012(4){\times}10^{-14}$

Table 4.8: The M1 transition rate from the $1s2s\ {}^3S_1$ state to the $1s^2\ {}^1S_0$ state, and the lifetime, τ, of the metastable $1s2s\ {}^3S_1$ state for nuclear charge $Z = 59$ through $Z = 78$ as calculated from the $\frac{1}{Z}$ expansion. The uncertainty in these calculations is given in parentheses for each individual calculation.

Z	$A\left(1s2s\ ^3S \to 1s^2\ ^1S\right)\ (\mathrm{s}^{-1})$	τ (s)
79	$1.4953794023291(7)\times10^{13}$	$6.68726611081(3)\times10^{-14}$
80	$1.6969325314503(8)\times10^{13}$	$5.89298620579(3)\times10^{-14}$
81	$1.9226138092472(9)\times10^{13}$	$5.20125256144(3)\times10^{-14}$
82	$2.174957448184(1)\times10^{13}$	$4.59779110086(2)\times10^{-14}$
83	$2.456727476829(1)\times10^{13}$	$3.60888941964(2)\times10^{-14}$
84	$2.770935553076(1)\times10^{13}$	$3.60888941964(2)\times10^{-14}$
85	$3.120859706067(2)\times10^{13}$	$3.20424528554(2)\times10^{-14}$
86	$3.510064628260(2)\times10^{13}$	$2.84895039239(1)\times10^{-14}$
87	$3.942421111274(2)\times10^{13}$	$2.53651239118(1)\times10^{-14}$
88	$4.422131238776(2)\times10^{13}$	$2.26135305807(1)\times10^{-14}$
89	$4.953750101888(2)\times10^{13}$	$2.018672681165(9)\times10^{-14}$
90	$5.542212208160(3)\times10^{13}$	$1.804333653135(9)\times10^{-14}$
91	$6.192856795124(3)\times10^{13}$	$1.614763643150(8)\times10^{-14}$
92	$6.911458437195(3)\times10^{13}$	$1.446872623321(7)\times10^{-14}$
93	$7.704253481399(4)\times10^{13}$	$1.297984291943(6)\times10^{-14}$
94	$8.577975736007(4)\times10^{13}$	$1.165776204988(6)\times10^{-14}$
95	$9.539885800390(4)\times10^{13}$	$1.048230577309(5)\times10^{-14}$
96	$1.0597809557856(5)\times10^{14}$	$9.43591215280(4)\times10^{-15}$
97	$1.1760172601587(6)\times10^{14}$	$8.50327655791(4)\times10^{-15}$
98	$1.3036042064110(6)\times10^{14}$	$7.67103999114(4)\times10^{-15}$
99	$1.4435164930956(7)\times10^{14}$	$6.92752735963(3)\times10^{-15}$
100	$1.5968013881966(7)\times10^{14}$	$6.26251960571(3)\times10^{-15}$

Table 4.9: The M1 transition rate from the $1s2s\ ^3S_1$ state to the $1s^2\ ^1S_0$ state, and the lifetime, τ, of the metastable $1s2s\ ^3S_1$ state for nuclear charge $Z = 79$ through $Z = 100$ as calculated from the $\frac{1}{Z}$ expansion.

This gives an approximate change in the energy of

$$\Delta E = -\frac{3Z^2}{8}\left[1 + \frac{11}{48}\alpha^2 Z^2\right].$$

(4.8)

Since the transition rate, Eq. (3.1) is dependent upon the energy to the fifth power, the lowest order correction is $\frac{55}{48}Z^2\alpha^2$. This value will be used as the estimation of the uncertainty of the current results.

In comparison with other theoretical work for the case of helium, most recently Łach and Pachucki (2001) [23] report the $1s2s\ ^3S_1 \rightarrow 1s^2\ ^1S_0$ M1 transition rate as 1.272426×10^{-4} s^{-1}, which is in complete agreement with the results presented in this thesis. Prior to this, Johnson et al. (1995) [21] used relativistic many body perturbation theory to calculate forbidden transitions in helium and heliumlike ions. Their results for the $1s2s\ ^3S_1 \rightarrow 1s^2\ ^1S_0$ M1 transition rate is 1.266×10^{-4} s^{-1}. The discrepancy, as pointed out by Łach and Pachucki, is attributed to the inclusion of some higher order terms while not accounting for electron correlations correctly. In addition, the current work agrees with the original calculation by Drake(1971) [18] with a reported value of 1.272×10^{-4} s^{-1}.

There have only been three experimental measurements of the $1s2s\ ^3S_1 \rightarrow 1s^2\ ^1S_0$ transition rate in helium. The first was by Moos and Woodsworth [25] in 1973, and was followed by a more precise measurement by the same authors in 1975 [26]. The latter experiment reported a transition rate of 1.11×10^{-4} s^{-1}, with an error of 30%. In 2009, Hodgman et al. [32] improved upon the measurement of Moos and Woodsworth, and gave more precise value for the transition rate of 1.27×10^{-4} s^{-1} with an error of 6.5%. The current work is well within error of these experimental measurements.

For heliumlike ions, there are several experiments that can be used to compare against the current theoretical calculations. For heliumlike lithium, ion trap measurements by Knight and Prior(1980) [56] found a lifetime of 58.6 ± 12.9 s. This value is in agreement with the value obtained in this work of $49.01(3)$ s.

High precision measurements of the transition rate of heliumlike carbon using an ion storage ring were performed by Schmidt et al. (1994) [57]. The results of this experiment were a transition rate of 48.57 ± 0.11 s^{-1} which is in excellent agreement with the value $48.6(1)$ s^{-1} obtained in this thesis.

Line emissions for this transition in heliumlike oxygen play an important role in plasma diagnostics. An electron beam ion trap measurement by Crespo López-Urrutia, Beiersdorfer, Savin, and Widmann(1998) [58], and determined the lifetime of the $1s2s\ ^3S_1$ state in heliumlike O^6+ as $955.9 \pm 3.5 \times 10^{-6}$ s. This is again within experimental error with the value obtained in the current work of $958(4) \times 10^{-6}$ s.

A precise measurement of the lifetime of heliumlike neon in the $1s2s\ ^3S_1$ state from electron beam ion trapping was performed by Träbert et al. (1999) [28], which was an improvement from the previous work by Wargelin, Beiersdorfer, and Khan(1993) [59]. The lifetime reported by Träbert, of $91.7 \pm 0.4 \times 10^{-6}$ s, is in excellent agreement with the current value of $92.0(6) \times 10^{-6}$ s.

For heliumlike sulfur, the lifetime of the $1s2s\ ^3S_1$ state was determined from an electron beam ion trap measurement by Crespo López-Urrutia, Beiersdorfer, and Widmann(2006) [60] was found to be $703 \pm 4 \times 10^{-9}$ s. This does agree, within error, with the current calculated value of $7.1(1) \times 10^{-9}$ s from this thesis. It should be noted that while these results do agree, this is the first experiment for which the current calculated nonrelativistic result of $710.404605610(5) \times 10^{-9}$ did not fit within error bounds of the experimental measurement without accounting for the order $(Z\alpha)^2)$ uncertainty. The comparison between theory and experiment is therefore sensitive to the relativistic correction.

In heliumlike chlorine, the triplet state lifetime was measured and found to be $3.54 \pm 0.24 \times 10^{-7}$ s, by Bednar et al. [61]. This is measurement agrees with the current results of $3.81(7) \times 10^{-7}$ s.

While measurements for heliumlike sulfur and chlorine disagreed with the current calculation, measurements by Hubricht and Träbert [62] determined the lifetime of heliumlike argon to be $2.03 \pm 0.13 \times 10^{-7}$ s, which does agree, within experimental error, with the current calculation of $2.12(4) \times 10^{-7}$ s.

The triplet state lifetime of heliumlike titanium was found to be $2.58 \pm .13 \times 10^{-8}$ s by Gould et al. [63] in 1973. Their experimental value is in agreement with the value obtained in the current calculation of $2.73(8) \times 10^{-8}$ s.

The lifetimes of heliumlike vanadium and iron were measured by Gould et al. [64] in

1974. The lifetime of heliumlike vanadium was determined to be $1.69 \pm 0.07 \times 10^{-8}$ s which is compared with the current calculation of $1.74(6) \times 10^{-8}$ s. The lifetime of heliumlike iron was found to be $4.8 \pm 0.6 \times 10^{-9}$ s and is compared with the current calculation of $5.0(2) \times 10^{-9}$ s. Both of these results agree within experimental error.

Measurements by Dunford et al. [65] in 1990 determined the lifetime of heliumlike bromine to be $2.241 \pm 0.071 \times 10^{-10}$ s. Comparing this to the the current calculation of $2.5(2) \times 10^{-10}$ s again shows agreement at order $(Z\alpha)^2$.

Heliumlike krypton was studied by Cheng et al. [66] in 1994, and determined a triplet state lifetime of $1.710 \pm 0.022 \times 10^{-10}$ s. This measurement can be additionally be seen to show agreement with the current calculation of $1.8(2) \times 10^{-10}$ s at order $(Z\alpha)^2$.

The triplet state lifetime of heliumlike niobium was measured also measured in 1994 by Simionovici et al. [67]. The result of this measurement was a lifetime of $4.545 \pm 0.016 \times 10^{-11}$ s which also agrees with the current calculation of $5.0(5) \times 10^{-11}$ s.

in 1993, heliumlike silver was studied by Birkett et al. [68] and a lifetime $1.11 \pm 0.02 \times 10^{-11}$ s was measured. This is compared and seen to be in agreement with the current value of $1.2(2) \times 10^{-11}$ s.

Currently the ion with the largest nuclear charge for which the lifetime of the metastable triplet state has been measured is heliumlike xenon. This measurement, performed by Marrus et al. [69] determined the lifetime to be $2.554 \pm 0.076 \times 10^{-12}$ s. This again can be seen toagree with the current measurement of $3.0(6) \times 10^{-12}$ s at the order $(Z\alpha)^2$)

From these comparisons, it can be seen, as expected, that with increasing nuclear charge the relativistic effects play a greater role. As mentioned before, the accuracy of the nonrelativisitc approximation of the current calculation is of order $(Z\alpha)^2$. That is, the error in the value of the transition rate A_Z, where the subscript Z labels the nuclear charge of the ion, can be estimated to be $\frac{55}{48} A_Z (Z\alpha)^2$. At this order all of the experimental measurements agree with the current calculation.

The comparisons of the current work and other theoretical calculations and experimental measurements are summarized in Tables (4.10), (4.11), and (4.12). Figure (4.1) shows the ratio of the experimental lifetimes to the theoretical lifetimes for different nuclear charges.

The errors bars in Figure (4.1) correspond to the experimental error from each experiment. The red curve is the current theoretical value plus the partial relativistic correction due to the transition energy.

4.2 Future Work

This work can be extended in several ways. Firstly, the largest source of error in these calculations, when compared with experimental results, is that these are nonrelativistic transition rates and are correct only to order $(Z\alpha)^2$. For helium and light heliumlike ions, this approximation is very good and the agreement between these nonrelativistic decay rates and the experimentally measured values are very good. As Z increases, this approximation worsens as can be seen by the disagreement for heliumlike sulfur. Therefore, the next step in these calculations would be to account for higher order relativistic effects. This can be accomplished by taking additional Foldy-Wouthuysen transformations of the Hamiltonian, which as discussed in Sec. (1.3.2) allows any Hamiltonian to be written out to a desired order of $(Z\alpha)^2$, and then retaining higher order terms that appear in the interaction operator $\vec{\alpha}\cdot\vec{A}$.

This work can be extended in several ways. Firstly, the largest source of error in these calculations, when compared with experimental results, is that these are nonrelativistic transition rates and are correct only to order $(Z\alpha)^2$. For helium and light heliumlike ions, this approximation is very good and the agreement between these nonrelativistic decay rates and the experimentally measured value are very good. As Z increases, this approximation worsens as can be seen by the disagreement for heliumlike sulfur. Therefore, the next step in these calculations would be to account for higher order relativistic effects. This can be accomplished by taking additional Foldy-Wouthuysen transformations of the Hamiltonian, which as discussed in Sec. (1.3.2) allows any Hamiltonian to be written out to a desired order of $(Z\alpha)^2$, and then retaining higher order terms that appear in the interaction operator $\vec{\alpha}\cdot\vec{A}$.

The variational Hylleraas wave functions used in this work could be improved upon by increasing the basis size, or by adding a third, and potentially fourth set of nonlinear variational parameters to Eq. (2.43). The nonlinear variational parameters in Eq. (2.43) set the distance scale for the electron coordinates. By introducing a third set of variational

Z	$A(2\ ^3S_1 \to 2\ ^1S_0)$	units	Theory/Experiment	Source
2	1.2724(3)	$\times 10^{-4}\ \text{s}^{-1}$	Theory	Current work
	1.272	$\times 10^{-4}\ \text{s}^{-1}$		Drake [18]
	1.266	$\times 10^{-4}\ \text{s}^{-1}$		Johnson et al. [21]
	1.272426	$\times 10^{-4}\ \text{s}^{-1}$		Łach and Pachucki [23]
	1.11(33)	$\times 10^{-4}\ \text{s}^{-1}$	Experiment	Moos and Woodworth [26]
	1.270(83)	$\times 10^{-4}\ \text{s}^{-1}$		Hodgman et al. [32]
3	2.0400(9)	$\times 10^{-2}\ \text{s}^{-1}$	Theory	Current work
	1.71(38)	$\times 10^{-2}\ \text{s}^{-1}$	Experiment	Knight and Prior [56]
6	4.86(1)	$\times 10^{1}\ \text{s}^{-1}$	Theory	Current work
	4.857(11)	$\times 10^{1}\ \text{s}^{-1}$	Experiment	Schmidt et al. [57]
8	1.044(4)	$\times 10^{3}\ \text{s}^{-1}$	Theory	Current work
	1.046(4)	$\times 10^{3}\ \text{s}^{-1}$	Experiment	Crespo López-Urrutia et al. [58]
10	1.087(6)	$\times 10^{4}\ \text{s}^{-1}$	Theory	Current work
	1.0905(48)	$\times 10^{4}\ \text{s}^{-1}$	Experiment	Träbert et al. [28]

Table 4.10: Comparison of M1 decay rates from other theoretical calculations and experimental measurements of the $^3S_1$ state with decay rates from the present calculation for $Z = 2$ to $Z = 10$. The values in parentheses are the uncertainties in the decay rates if given in the corresponding literature.

Z	$A(2\,^3S_1 \rightarrow 2\,^1S_0)$	units	Theory/Experiment	Source
16	1.41(2)	$\times 10^6$ s^{-1}	Theory	Current work
	1.422(8)	$\times 10^6$ s^{-1}	Experiment	Crespo López-Urrutia et al. [60]
17	2.62(4)	$\times 10^6$ s^{-1}	Theory	Current work
	2.82(19)	$\times 10^6$ s^{-1}	Experiment	Bednar et al. [61]
18	4.71(8)	$\times 10^6$ s^{-1}	Theory	Current work
	4.93(29)	$\times 10^6$ s^{-1}	Experiment	Hurbricht and Träbert [62]
22	3.66(9)	$\times 10^6$ s^{-1}	Theory	Current work
	3.88(20)	$\times 10^6$ s^{-1}	Experiment	Gould, Marrus, and Schmieder [63]
23	5.8(2)	$\times 10^6$ s^{-1}	Theory	Current work
	5.92(24)	$\times 10^6$ s^{-1}	Experiment	Gould, Marrus, and Mohr [64]
26	2.00(7)	$\times 10^8$ s^{-1}	Theory	Current work
	2.08(26)	$\times 10^8$ s^{-1}	Experiment	Gould, Marrus, and Mohr [64]
35	4.0(3)	$\times 10^9$ s^{-1}	Theory	Current work
	4.46(14)	$\times 10^9$ s^{-1}	Experiment	Dunford et al. [65]

Table 4.11: Comparison of M1 decay rates from other theoretical calculations and experimental measurements of the $^3S_1$ state with decay rates from the present calculation for $Z = 16$ to $Z = 35$. The values in parentheses are the uncertainties in the decay rates if given in the corresponding literature.

Z	$A(2\,^3S_1 \rightarrow 2\,^1S_0)$	units	Theory/Experiment	Source
36	5.4(4)	$\times 10^9$ s^{-1}	Theory	Current work
	5.848(75)	$\times 10^9$ s^{-1}	Experiment	Cheng et al. [66]
41	2.0(2)	$\times 10^{10}$ s^{-1}	Theory	Current work
	2.1954(68)	$\times 10^{10}$ s^{-1}	Experiment	Simionovici et al. [67]
47	8.0(9)	$\times 10^{10}$ s^{-1}	Theory	Current work
	9.01(16)	$\times 10^{10}$ s^{-1}	Experiment	Birkett et al. [68]
54	3.3(5)	$\times 10^{11}$ s^{-1}	Theory	Current work
	3.92(12)	$\times 10^{11}$ s^{-1}	Experiment	Marrus et al. [69]

Table 4.12: Comparison of M1 decay rates from other theoretical calculations and experimental measurements of the $^3S_1$ state with decay rates from the present calculation for $Z = 36$ to $Z = 54$. The values in parentheses are the uncertainties in the decay rates if given in the corresponding literature.
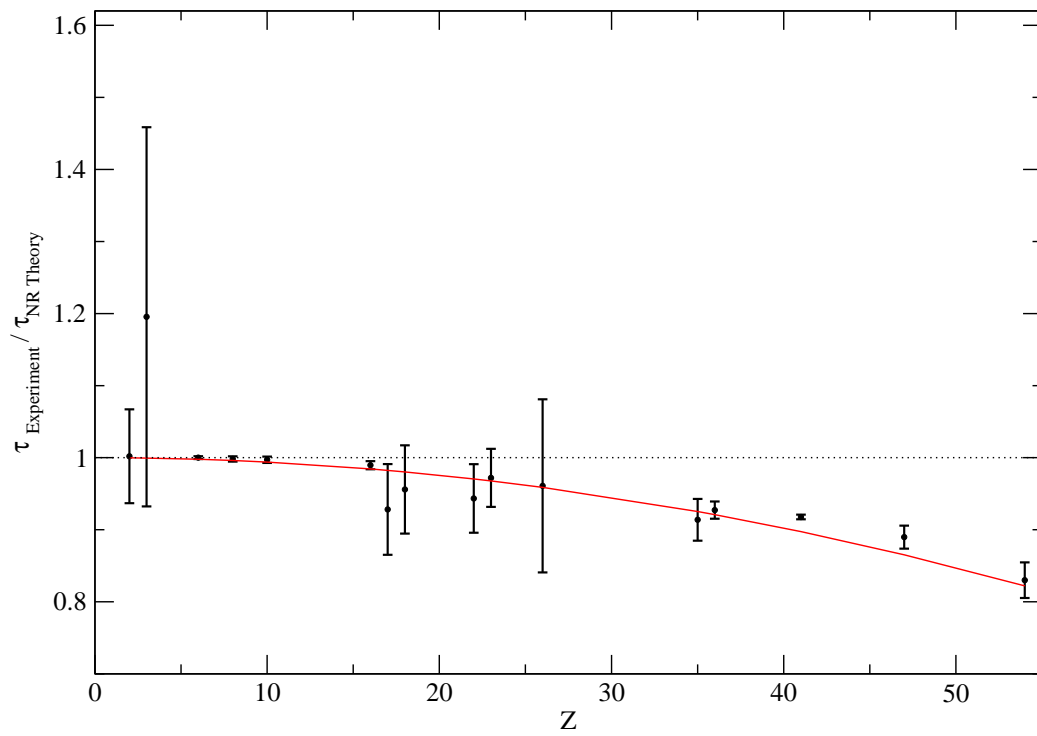
Figure 4.1: The ratio of experimental measurements of the lifetimes of the metastable triplet state to the current theoretical calculation. The error bars correspond to the experimental uncertainty of the experiment. The red curve is the nonrelativistic theoretical calculation minus a partial relativistic correction due to the transition energy.

parameters, the distance scale would be divided up into close, asymptotic, and intermediate range regimes. This would improve the accuracy of the wave functions used in these calculations.

While the results from this thesis agree with the recently most accurate theoretical results of Łach and Pachucki, as well as all the lower nuclear charge heliumlike ions, there is still some discrepancy with the results of experimental measurements for heliumlike sulfur. There is currently no explanation for this difference, and further study is required.

The theoretical works by Łach and Pachucki, and Johnson et al. have also been used to determine the transition rate and lifetimes of other forbidden transitions, such as the $3\,^3S_1 \rightarrow 2\,^3S_1$, $2\,^3P_2 \rightarrow 1\,^1S_0$, $2\,^3P_1 \rightarrow 1\,^1S_0$, and $2\,^1P_1 \rightarrow 2\,^3S_1$ transitions. The methods used in this thesis would extend directly to the calculation of these transitions as well. The dipole transition operators would need to be derived.

The determination of the zeroth and first order coefficients in the $\frac{1}{Z}$ expansion used in this work is a lowest order approximation. This is because it was constructed using a product of two noninteracting nonrelativistic solutions to the hydrogen Hamiltonian as the unperturbed helium solutions. It would be possible to use relativistic wave functions to evaluate numerically these first two coefficients.

When calculating the first order coefficients of the $\frac{1}{Z}$ expansions, it was required to determine the first order solutions to the corresponding perturbation equations. This was accomplished numerically by using the pseudo state method described in Sec. (2.5). It is possible, following the work of Dalgarno and Parkinson(1967) [50] for the $1snp\,^1P \rightarrow 1s^2\,^1S$ electric dipole transition, to solve these perturbation equations analytically. The choice to use numerically determined wave functions is justified because these calculations were carried out in quadruple precision and the resulting first order coefficients converged with a numerical accuracy of the same order as the data points used in the curve fitting. An attempt to solve these perturbation equations for analytic solutions was made, however it was never completed. As a further step, analytic solutions similar to the ones found for the dipole transition by Dalgarno and Parkinson should be determined and used to calculate the first order coefficients in the $\frac{1}{Z}$ expansions of the matrix elements.

Finally, an attempt to improve the accuracy of the results can be achieved by using more powerful computational resources . This work was completed in quadruple precision on the Shared Hierarchical Academic Research Computing Network (SHARCNet). Higher precision results would require computational resources that are capable of storing information with higher than quadruple precision.

Appendix A

Parahelium and Orthohelium

Helium is a two electron system and electrons, being fermions, must obey the Pauli exclusion principle. The Pauli exclusion principle asserts that no two identical fermions may occupy the same quantum state simultaneously. Therefore the wave function for helium will have restrictions based upon the spin configuration of its electrons. Due to the Pauli exclusion principle, the total wave function must therefore be antisymmetric. The wave function for helium can be written, in terms of a spatial wave function and a spin wave function, as follows

$$\Psi(1,2) = \begin{cases} \Psi^S\left(\mathbf{r}_1, \mathbf{r}_2\right) \chi^A(1,2) \\ \qquad \text{or} \\ \Psi^A\left(\mathbf{r}_1, \mathbf{r}_2\right) \chi^S(1,2) \end{cases} \tag{A.1}$$

where $\Psi^S\left(\mathbf{r}_1, \mathbf{r}_2\right)$ and $\Psi^A\left(\mathbf{r}_1, \mathbf{r}_2\right)$ are the symmetric and antisymmetric spatial wavfunctions, and $\chi^S(1,2)$ and $\chi^A(1,2)$ are the the symmetric and antisymmetric spin wave functions. The spatial wave functions are written

$$\Psi^S\left(\mathbf{r}_1, \mathbf{r}_2\right) = \frac{1}{\sqrt{2}}\left[\Psi\left(\mathbf{r}_1, \mathbf{r}_2\right) + \Psi\left(\mathbf{r}_2, \mathbf{r}_1\right)\right] \tag{A.2}$$

$$\Psi^A\left(\mathbf{r}_1, \mathbf{r}_2\right) = \frac{1}{\sqrt{2}}\left[\Psi\left(\mathbf{r}_1, \mathbf{r}_2\right) - \Psi\left(\mathbf{r}_2, \mathbf{r}_1\right)\right], \tag{A.3}$$

and it can be seen that the symmetric spatial wave function, Eq. (A.2) remains unchanged under the exchange of particle labels, whereas the antisymmetric spatial wave function, Eq. (A.3) is modified by a factor of (-1).

For two electrons, there are four possible configurations which will be labeled according to their symmetries as

$$\chi^S = \begin{cases} |\frac{1}{2}\,\frac{1}{2}\rangle \\ \frac{1}{\sqrt{2}}\left[|\frac{1}{2}\,\frac{-1}{2}\rangle + |\frac{-1}{2}\,\frac{1}{2}\rangle\right] \\ |\frac{-1}{2}\,\frac{-1}{2}\rangle, \end{cases} \tag{A.4}$$

$$\chi^A = \frac{1}{\sqrt{2}}\left[|\frac{1}{2}\,\frac{-1}{2}\rangle - |\frac{-1}{2}\,\frac{1}{2}\rangle\right], \tag{A.5}$$

where the symmetric spin function Eq. (A.4) is known as the *triplet* state, and the antisymmetric spin function Eq. (A.5) is known as the *singlet* state. When the electrons are in a triplet state (consequently with an antisymmetric spatial wave function), the helium atom is referred to as *orthohelium*. When the electrons are in the singlet state, the helium atom is referred to as *parahelium*.

The orthohelium levels have a lower energy in comparison to their parahelium counterparts, and this is a consequence of the symmetry of the spatial part of the wave function and the Coulomb repulsion of the two electrons. When in an orthohelium configuration, the electrons are in a symmetric triplet state, and to maintain the antisymmetry of the total wave function, the spatial part of the wave function must be antisymmetric. In parahelium, the symmetric form of the spatial wave function allows the electrons, on average, to be located in closer proximity than with the antisymmetric spatial wave function. Since the energy associated with the Coulomb potential is proportional to inverse square of the separation, the orthohelium states, with a larger average separation, clearly have a lower energy[1].

---

[1]The entire argument can be seen also be seen as an example of Hund's first rule.

Appendix B

Foldy-Wouthuysen Trasnformation:
Electron in an External Field

As an example, the Foldy-Wouthuysen transformation can be applied to a single electron in a electrostatic central potential. The Dirac Hamiltonian for such a system is

$$H = \beta m + e\phi + \alpha \cdot (\mathbf{p} - e\mathbf{A}), \tag{B.1}$$

where ϕ is the electrostatic potential. In this appendix, multiple Foldy-Wouthuysen transformations will be carried out and terms will be kept up to order $(\frac{v}{c})^2$ in the nonrelativisitic limit.

As with the free particle, the odd term in the Hamiltonian Eq. (B.1) is $\alpha \cdot (\mathbf{p} - e\mathbf{A})$, were all other terms in this Hamiltonian are even. This suggests that the unitary operator we choose would be

$$U_{\text{FW}} = e^{\frac{\beta}{2m}\mathcal{O}}, \tag{B.2}$$

with

$$\mathcal{O} = \alpha \cdot (\mathbf{p} - e\mathbf{A}).$$

Including time dependence, the Foldy-Wouthuysen transformation to be undertaken is

$$H' = U_{\text{FW}} \left(H - i\frac{\partial}{\partial t} \right) U_{\text{FW}}^{\dagger}. \tag{B.3}$$

This can be evaluated by use of the operator identity for any two operators A and B

$$
\begin{aligned}
e^A B e^{-A} &= B + [A, B] + \frac{1}{2}[A, [A, B]] + \frac{1}{3!}[A, [A, [A, B]]] + \dots \\
&\quad + \frac{1}{n!}[A, [A, \dots [A, [A, B]] \dots]] + \dots,
\end{aligned}
\tag{B.4}
$$

where the final term is taken to mean n commutators.

To obtain H' one must evaluate commutators of $\mathcal{O}$ with H and the time derivative. In this example we will retain only relativistic corrections up to order $(\frac{v}{c})^4$. With the commutation relations

$$[\beta, \mathcal{O}] = 2\beta\mathcal{O} \tag{B.5}$$

and

$$[\beta, e\phi] = 0 \tag{B.6}$$

the necessary commutators involving H can be written as

$$
\begin{aligned}
[\frac{\beta}{2m}\mathcal{O}, H] &= [\frac{\beta}{2m}\mathcal{O}, \beta m] + [\frac{\beta}{2m}\mathcal{O}, e\phi] + [\frac{\beta}{2m}\mathcal{O}, \mathcal{O}] \\
&= \frac{\beta}{m}\mathcal{O}^2 + \frac{\beta}{2m}[\mathcal{O}, e\phi] - \mathcal{O},
\end{aligned}
\tag{B.7}
$$

$$
\begin{aligned}
[\frac{\beta}{2m}\mathcal{O}, [\frac{\beta}{2m}\mathcal{O}, H]] &= [\frac{\beta}{2m}\mathcal{O}, \frac{\beta}{m}\mathcal{O}^2 + \frac{\beta}{2m}[\mathcal{O}, e\phi] - \mathcal{O}] \\
&= -\frac{1}{m^2}\mathcal{O}^3 - \frac{1}{4m^2}[\mathcal{O}, [\mathcal{O}, e\phi]] - \frac{\beta}{m}\mathcal{O}^2,
\end{aligned}
\tag{B.8}
$$

$$
\begin{aligned}
[\frac{\beta}{2m}\mathcal{O}, [\frac{\beta}{2m}\mathcal{O}[\frac{\beta}{2m}\mathcal{O}, H]]] &= [\frac{\beta}{2m}, \frac{1}{m^2}\mathcal{O}^3 - \frac{1}{4m^2}[\mathcal{O}, [\mathcal{O}, e\phi]] - \frac{\beta}{m}\mathcal{O}^2] \\
&= \frac{1}{m^2}\mathcal{O}^3 - \frac{1}{m^3}\beta\mathcal{O}^4,
\end{aligned}
\tag{B.9}
$$

and

$$
\begin{aligned}
[\frac{\beta}{2m}\mathcal{O}, [\frac{\beta}{2m}\mathcal{O}, [\frac{\beta}{2m}\mathcal{O}[\frac{\beta}{2m}\mathcal{O}, H]]]] &= [\frac{\beta}{2m}\mathcal{O}, \frac{1}{m^2}\mathcal{O}^3 - \frac{1}{m^3}\beta\mathcal{O}^4] \\
&= \frac{\beta}{m^3}\mathcal{O}^4.
\end{aligned}
\tag{B.10}
$$

The commutators required from the time derivative can be derived by first performing the derivative

$$e^{\frac{\beta}{2m}\mathcal{O}}\frac{\partial}{\partial t}e^{\frac{-\beta}{2m}\mathcal{O}} = e^{\frac{\beta}{2m}\mathcal{O}}(-\frac{\beta}{2m}\dot{\mathcal{O}})e^{\frac{-\beta}{2m}\mathcal{O}} \tag{B.11}$$

and then expanding with in the same manner using Eq. (B.4) such that

$$e^{\frac{\beta}{2m}\mathcal{O}}\frac{\partial}{\partial t}e^{\frac{-\beta}{2m}\mathcal{O}} \approx \frac{i\beta}{2m}\dot{\mathcal{O}} + i\left[\frac{\beta}{2m}, -\frac{\beta}{2m}\dot{\mathcal{O}}\right] + \dots, \tag{B.12}$$

where the first commutator can be expressed as

$$[\frac{\beta}{2m}\mathcal{O}, -\frac{\beta}{2m}\dot{\mathcal{O}}] = -\frac{1}{4m^2}[\mathcal{O}, \dot{\mathcal{O}}]. \tag{B.13}$$

Using the commutator identity Eq. (B.4) to expand the Foldy-Wouthuysen transformation Eq. (B.3) with Eqns. (B.7), (B.8), (B.9), (B.10), and (B.13) gives, after simplification

$$
\begin{aligned}
H' &= \beta m + e\phi + \frac{\beta}{2m}\mathcal{O}^2 - \frac{\beta}{8m^3}\mathcal{O}^4 - \frac{1}{8m^2}[\mathcal{O}, [\mathcal{O}, e\phi]] - \frac{i}{8m^2}[\mathcal{O}, \dot{\mathcal{O}}] \\
&\quad + \frac{\beta}{2m}[\mathcal{O}, e\phi] - \frac{1}{3m^2}\mathcal{O}^3 + \frac{i\beta}{2m}\dot{\mathcal{O}}.
\end{aligned} \tag{B.14}
$$

The first line of Eq. (B.14) contains only even operators and the second line of Eq. (B.14) contains only odd operators which are higher order than $\mathcal{O}$. We can write these operators as

$$\Lambda = e\phi + \frac{\beta}{2m}\mathcal{O}^2 - \frac{\beta}{8m^3}\mathcal{O}^4 - \frac{1}{8m^2}[\mathcal{O}, [\mathcal{O}, e\phi]] - \frac{i}{8m^2}[\mathcal{O}, \dot{\mathcal{O}}] \tag{B.15}$$

and

$$\mathcal{O}' = \frac{\beta}{2m}[\mathcal{O}, e\phi] - \frac{1}{3m^2}\mathcal{O}^3 + \frac{i\beta}{2m}\dot{\mathcal{O}}, \tag{B.16}$$

such that

$$H' = \beta m + \Lambda + \mathcal{O}'. \tag{B.17}$$

The odd operator $\mathcal{O}'$ can be canceled in the same fashion as before by performing a second Foldy-Wouthuysen transformation

$$H'' = e^{\frac{\beta}{2m}\mathcal{O}'}\left(H' - i\frac{\partial}{\partial t}\right)e^{-\frac{\beta}{2m}\mathcal{O}'}. \tag{B.18}$$

The result of this second Foldy-Wouthuysen transformation is

$$
\begin{aligned}
H'' &= \beta m + \Lambda + \frac{\beta}{2m}[\mathcal{O}', \Lambda] + \frac{i\beta}{2m}\dot{\mathcal{O}}'] \\
&= \beta m + \Lambda + \mathcal{O}'',
\end{aligned} \tag{B.19}
$$

where $\mathcal{O}''$ is again a higher order correction. To eliminate $\mathcal{O}''$, a third Foldy-Wouthuysen transformation is applied

$$H''' = e^{\frac{\beta}{2m}\mathcal{O}''}\left(H'' - i\frac{\partial}{\partial t}\right)e^{-\frac{\beta}{2m}\mathcal{O}''}. \tag{B.20}$$

The result of this third Foldy-Wouthuysen transformation is, after keeping only terms up to order $\mathcal{O}^4$,

$$
\begin{aligned}
H''' &\approx \beta m + \Lambda \\
&\approx \beta m + e\phi + \frac{\beta}{2m}\mathcal{O}^2 - \frac{\beta}{8m^3}\mathcal{O}^4 - \frac{1}{8m^2}[\mathcal{O},[\mathcal{O},e\phi]] - \frac{i}{8m^2}[\mathcal{O},\dot{\mathcal{O}}] \\
&\approx \beta m + e\phi + \frac{\beta}{2m}(\vec{\sigma}\cdot\vec{\pi})^2 - \frac{e}{8m^2}[(\vec{\sigma}\cdot\vec{\pi}),[(\vec{\sigma}\cdot\vec{\pi}),\phi]] - \frac{\beta}{8m^3}(\vec{\sigma}\cdot\vec{\pi})^4.
\end{aligned} \tag{B.21}
$$

Appendix C

First Order Correction to the Hydrogen Wavefunction: Dipole Polarizability

By treating the dipole interaction $r \cos \theta$ as a perturbation, the hydrogen Hamiltonian is written, in atomic units,

$$H = H_0 + r \cos \theta, \tag{C.1}$$

with the expansions

$$\Psi = \Psi^{(0)} + \lambda \Psi^{(1)} + \lambda^2 \Psi^{(2)} + \dots, \tag{C.2}$$

$$E = E^{(0)} + \lambda E^{(1)} + \lambda^2 E^{(2)} + \dots, \tag{C.3}$$

where λ is an expansion parameter that will be set to one at the end of the calculation, H_0 is the unperturbed hydrogen Hamiltonian with energy $E_0 = -1/2$, and $\Psi^{(0)}$ is the ground state hydrogen wave function. Using the above definitions in the Schrödinger equation, and collecting terms of like order, up to first order, gives

$$H_0 \Psi^{(0)} = E^{(0)} \Psi^{(0)} \tag{C.4}$$

and

$$(H_0 - E^{(0)}) \Psi^{(1)} + r \cos \theta \Psi^{(0)} = E^{(1)} \Psi^{(0)}. \tag{C.5}$$

The first order perturbation equation (C.5) can be simplified by using $E^{(1)} = 0$ (as discussed in Sec. (2.5.1)) as

$$(H_0 - E^{(0)})\Psi^{(1)} + r\cos\theta\Psi^{(0)} = 0. \tag{C.6}$$

To solve Eq. (C.6), the form of $\Psi^{(1)}$ is taken to be

$$\Psi^{(1)} = \sum_k b_k r^r \cos\theta e^{-r}, \tag{C.7}$$

and is then substituted into Eq. (C.6). Explicitly acting on $\Psi^{(1)}$ by H_0 yields

$$H_0\Psi^{(1)} \;=\; -\frac{1}{2}\left[\frac{1}{r^2}\frac{\partial}{\partial r}\left(r^2\frac{\partial}{\partial r}\Psi^{(1)}\right) + \frac{1}{r^2\sin\theta}\frac{\partial}{\partial\theta}\left(\sin\theta\frac{\partial}{\partial\theta}\Psi^{(1)}\right)\right] - \frac{1}{r}\Psi^{(1)}, \tag{C.8}$$

where the derivatives with respect to the azimuthal angle have been omitted since they do not contribute. Inspection of the second term in Eq. (C.8) shows

$$\frac{1}{r^2\sin\theta}\frac{\partial}{\partial\theta}\left(\sin\theta\frac{\partial}{\partial\theta}\Psi^{(1)}\right) \;=\; \frac{1}{r^2\sin\theta}\frac{\partial}{\partial\theta}\sum_k b_k r^k e^{-r}\left(-\sin^2\theta\right) \tag{C.9}$$

$$=\; \frac{-2}{r^2}\sum_k b_k\cos\theta r^k e^{-r}$$

$$=\; \frac{-2}{r^2}\Psi^{(1)},$$

which is precisely $-\frac{l(l+1)}{r^2}\Psi^{(1)}$, with $l = 1$, as expected for a p-state solution.

Direct substitution of Eq. (C.7) into Eq. (C.6), yields

$$0 \;=\; -\frac{1}{2}\sum_k\left[b_k k(k+1)r^{k-2} - 2b_k(k+1)r^{k-1} - b_k r^k - 2b_k r^{k-2}\right] \tag{C.10}$$

$$-\sum b_k r^{k-1} - E^{(0)}\sum_k b_k r^k + r\frac{1}{\sqrt{\pi}},$$

where the entire equation has been multiplied by $\frac{e^r}{\cos\theta}$. By relabeling the index of the first term with $k \to k+1$,

$$0 \;=\; -\frac{1}{2}\left[\sum_k b_{k+1}(k+2)(k+1)r^{k-1} - 2b_k(k+1)r^{k-1} - b_k r^k - 2b_k r^{k-2}\right] \tag{C.11}$$

$$-\sum_k b_k r^{k-1} - E^{(0)}\sum_k b_k r^k + \frac{r}{\sqrt{\pi}}.$$

Collecting terms of like powers of r gives an infinite set of equations. For powers of order $\mathcal{O}\left(r^{-2}\right) \to \mathcal{O}\left(r^3\right)$, these equations are

$$\mathcal{O}\left(r^{-2}\right): \quad 0 = -\frac{1}{2}2b_0 \tag{C.12}$$

$$\mathcal{O}\left(r^{-1}\right): \quad 0 = -\frac{1}{2}\left[2b_1 - 2b_0 - 2b_1\right] - b_0 \tag{C.13}$$

$$\mathcal{O}\left(r^0\right): \quad 0 = -\frac{1}{2}\left[6b_2 - 4b_1 + b_0 - 2b_2\right] - b_1 - E^{(0)}b_0 \tag{C.14}$$

$$\mathcal{O}\left(r\right): \quad 0 = -\frac{1}{2}\left[12b_3 - 6b_2 + b_1 - 2b_3\right] - b_2 - E^{(0)}b_1 + \frac{1}{\sqrt{\pi}} \tag{C.15}$$

$$\mathcal{O}\left(r^2\right): \quad 0 = -\frac{1}{2}\left[20b_4 - 8b_3 + b_2 - 2b_4\right] - b_3 - E^{(0)}b_2. \tag{C.16}$$

$$\mathcal{O}\left(r^3\right): \quad 0 = -\frac{1}{2}\left[30b_5 - 10b_4 + b_3 - 2b_5\right] - b_4 - E^{(0)}b_3 \tag{C.17}$$

Immediately, from Eq. (C.12) the the zeroth order expansion coefficient is determined as $b_0 = 0$. While Eq. (C.13) gives no new information, from Eq. (C.14) it is found that

$$b_2 = \frac{1}{2}b_1. \tag{C.18}$$

Further simplification of Eqns. (C.15), (C.16), and (C.17) gives

$$-5b_3 + 2b_2 + \frac{1}{\sqrt{\pi}} = 0 \tag{C.19}$$

$$-3b_4 + b_3 = 0 \tag{C.20}$$

$$7b_5 + 2b_4 = 0. \tag{C.21}$$

The perturbation term is only present in Eq. (C.15), and therefore we look for a recursion relation for the coefficients with k larger than 4. By relabeling the index $k \to k + 4$, the equations of order $\mathcal{O}\left(r^3\right)$ and higher are

$$-\frac{1}{2}b_{k+5}(k + 5)(k + 6) + b_{k+4}(k + 4) = 0, \tag{C.22}$$

which yields the recursion relation

$$b_{k+5} = 2b_{k+4}\frac{k + 4}{(k + 5)(k + 6)}. \tag{C.23}$$

In the limit of large k Eq. (C.23) goes like

$$b_{k+5} \approx b_{k+4}\frac{1}{k}, \tag{C.24}$$

which leads to $\Psi^{(1)}$ diverging as $r \to \infty$. This means that there must be some value of $k = k_{max}$ such that $b_{k_{max}+1} = 0$. The value of k_{max} can be found by applying this condition to Eq. (C.24),

$$0 = \frac{k_{max} + 4}{(k_{max} + 5)(k_{max} + 6)}. \tag{C.25}$$

Therefore, $k_{max} = 4$, and any value coefficient b_k with $k > 4$ must be zero. Including this result into Eqns. (C.19), (C.20), and (C.21) gives

$$b_4 = 0, \quad b_3 = 0, \quad b_2 = -\frac{1}{2}\frac{1}{\sqrt{\pi}}, \quad \text{and} \quad b_1 = -\frac{1}{\sqrt{\pi}}. \tag{C.26}$$

By writing $\cos\theta = Y_1^0\sqrt{\frac{4\pi}{3}}$, the wave function Eq. (C.7) is then found to be

$$\Psi^{(1)} = -\frac{1}{\sqrt{3}}\left(2r + r^2\right)e^{-r}Y_1^0. \tag{C.27}$$

Appendix D

$\frac{1}{Z}$ *Expansion: Matrix Elements*

Following the form of Eq. (2.105) we can write the wavefuntion to first order in the perturbation Eq. (2.99)

$$\psi = \psi^{(0)} + \frac{1}{Z}\psi^{(1)}, \tag{D.1}$$

with the orthonormalization conditions

$$\langle \psi^{(0)}|\psi^{(1)} \rangle \quad = \quad 0 \tag{D.2}$$

$$\text{and}$$

$$\langle \psi^{(0)}|\psi^{(0)} \rangle \quad = \quad 1. \tag{D.3}$$

For any atomic property L, a power series expansion of the wave function given in Eq. (2.105) implies that a power series expansion can be written for the atomic property. For the purpose of showing the general method of finding the first order correction terms used in this work, all discussion shall be restricted to single electron operators; however, many body operators can be expanded similarly, given that the operator remains homogenous under the scale transformation of Eq. (2.100) [51].

D.1   Diagonal Elements

The diagonal matrix elements for an operator $\mathbf{L}$ and state ψ_i can be written [51]

$$
\begin{aligned}
\langle L \rangle &= \langle \psi_i | L | \psi_i \rangle \\
&= \left[\frac{L^{(0)} + \frac{1}{Z} L^{(1)} + \left(\frac{1}{Z}\right)^2 L^{(2)} + \dots}{1 + \frac{1}{Z} S^{(1)} + \left(\frac{1}{Z}\right)^2 S^{(2)} + \dots} \right],
\end{aligned}
\tag{D.4}
$$

where $L^{(i)}$ and $S^{(i)}$ are defined

$$
L^{(n)} = \sum_{m=0}^{n} \langle \psi^{(m)} | L | \psi^{(n-m)} \rangle
\tag{D.5}
$$

and

$$
S^{(n)} = \sum_{m=0}^{n} \langle \psi^{(m)} | \psi^{(n-m)} \rangle.
\tag{D.6}
$$

To first order, due to Eq. (D.2) and Eq. (D.3), $S^{(1)} = 0$. It is also always possible to choose normalization conditions such that all $S^{(n)} = 0$. To first order, the diagonal matrix elements are

$$
\langle L \rangle = L^{(0)} + \frac{1}{Z} L^{(1)}.
\tag{D.7}
$$

Direct substitution of Eq. (D.1) into Eq. (D.5) for $n = 0, 1$ yields expressions for the zeroth and first order terms of the diagonal matrix elements

$$
L^{(0)} = \langle \psi^{(0)} | L | \psi^{(0)} \rangle
\tag{D.8}
$$

and

$$
\begin{aligned}
L^{(1)} &= \langle \psi^{(0)} | L | \psi^{(1)} \rangle + \langle \psi^{(1)} | L | \psi^{(0)} \rangle \\
&= 2 \langle \psi^{(0)} | L | \psi^{(1)} \rangle.
\end{aligned}
\tag{D.9}
$$

By invoking the Dalgarno Interchange theorem [50] [51] [52] explained in Sec. (2.6.1), it is also possible to write

$$
L^{(1)} = 2 \langle \psi^{(0)} | H^{(1)} | \phi^{(1)} \rangle,
\tag{D.10}
$$

where $H^{(1)} = \frac{1}{r_{12}}$ is the electron-electron interaction term, and $|\phi^{(1)}\rangle$ satisfies the first order pertubation equation

$$
(H_0 - E_0) |\phi^{(1)}\rangle + \left(L - L^{(0)} \right) \psi^{(0)} = 0
\tag{D.11}
$$

with

$$\langle\phi^{(1)}|\psi^{(0)}\rangle = 0. \tag{D.12}$$

D.2 Off-Diagonal Elements

The process to calculate off-diagonal matrix elements of an operator L between the initial and final states $|\psi_i\rangle$ and $|\psi_f\rangle$ is similar to procedure for calculating diagonal elements. Based on Cohen (1988) we can write the matrix element

$$\langle\psi_f|L|\psi_i\rangle = \left[\frac{T^{(0)} + \frac{1}{Z}T^{(1)} + \left(\frac{1}{Z}\right)^2 T^{(2)} + \dots}{\left(1 + \frac{1}{Z}S_f^{(1)} + \left(\frac{1}{Z}\right)^2 S_f^{(2)} + \dots\right)^{1/2}\left(1 + \frac{1}{Z}S_i^{(1)} + \left(\frac{1}{Z}\right)^2 S_i^{(2)} + \dots\right)^{1/2}}\right], \tag{D.13}$$

where

$$T^{(n)} \quad = \quad \sum_{m=0}^{n}\langle\psi_f^{(n)}|L|\psi_i^{(n-m)}\rangle, \tag{D.14}$$

$$S_f^{(n)} \quad = \quad \sum_{m=0}^{n}\langle\psi_f^{(n)}|\psi_f^{(n-m)}\rangle, \tag{D.15}$$

and

$$S_i^{(n)} \quad = \quad \sum_{m=0}^{n}\langle\psi_i^{(n)}|\psi_i^{(n-m)}\rangle. \tag{D.16}$$

With the othorgonality Eq. (D.2), to first order the denomintor in Eq. (D.13) reduces to unity. By substitution of Eq. (D.1) into Eq. (D.14) the zeroth and first order correction terms can be written

$$T^{(0)} \quad = \quad \langle\psi_f^{(0)}|L|\psi_i^{(0)}\rangle \tag{D.17}$$

and

$$T^{(1)} \quad = \quad \langle\psi_f^{(1)}|L|\psi_i^{(0)}\rangle + \langle\psi_f^{(0)}|L|\psi_i^{(1)}\rangle. \tag{D.18}$$

Using the Dalgarno Interchange theorem the first order term can be rewritten

$$T^{(1)} = \langle\phi_f^{(1)}|H^{(1)}|\psi_i^{(0)}\rangle + \langle\phi_i^{(1)}|H^{(1)}|\psi_f^{(0)}\rangle, \tag{D.19}$$

where $\phi_i^{(1)}$ and $\phi_f^{(1)}$ are the solutions to the equations

$$\left(H_0 - E_f^{(0)}\right)\phi_f^{(1)} + L\psi_i^{(0)} \quad = \quad T^{(0)}\psi_f^{(0)} \tag{D.20}$$

and

$$\left(H_0 - E_i^{(0)}\right)\phi_i^{(1)} + L\psi_f^{(0)} \quad = \quad T^{(0)}\psi_i^{(0)}, \tag{D.21}$$

and satisfy

$$\langle\phi_f^{(1)}|\psi_f^{(0)}\rangle = \langle\phi_i^{(1)}|\psi_i^{(0)}\rangle = 0. \tag{D.22}$$

Bibliography

[1] G. W. F. Drake. *Phys. Rev. A*, 9(6):2799–2801, 1974.

[2] R. Shankar. *Principles of Quantum Mechanics.* Plenum Press, New York, second edition, 1994.

[3] W. R. Johnson. *Phys. Rev. Lett.*, 29:1123–1126, 1972.

[4] S. P. Goldman and G. W. F. Drake. *Phys. Rev. A*, 24:183–191, 1981.

[5] W. L. Wiese and J. R. Fuhr. *J. Phys. Chem. Ref. Data*, 38(3), 2009.

[6] J. J. Brehm and W. J. Mullin. *Introduction to the Structure of Matter.* Wiley & Sons, Inc., 1989.

[7] G. W. F. Drake and W. C. Martin. *Canadian Journal of Physics*, 76(9):679–698, 1998.

[8] A. H. Gabriel and C. Jordan. *Monthly Notices Roy. Astron. Soc.*, 145:241, 1969.

[9] G. W. F. Drake G. R. Blumenthal and W. H. Tucker. *Astrophys. J.*, 172:205, 1972.

[10] J. S. Mathis. *Astrophys. J.*, 125:328, 1957.

[11] J. S. Mathis. *Astrophys. J.*, 125:318, 1957.

[12] M. Robberto, R. C. O'Dell, L. A. Hillenbrand, M. Simon, D. Soderblom, E. Feigelson, J. Krist, P. McCullough, M. Meyer, R. Makidon, J. Najita, N. Panagia, F. Palla, M. Romaniello, I. N. Reid, J. Stauffer, K. Stassun, K. Smith, B. Sherry, L. E. Bergeron, V. Kozhurina-Platais, M. McMaster, and E. Villaver. *An overview of the HST Treasury Program on the Orion Nebula*, volume 37 of *Bulletin of the American Astronomical Society.* 2005.

[13] G. Breit and E. Teller. *Astrophys. J.*, 91:215, 1940.

[14] G. W. F. Drake and A. Dalgarno. *Astrophys. J. Letters*, 152(L121), 1968.

[15] O. Bely and P. Faucher. *Astron. Astrophys.*, 1:37, 1969.

[16] G. W. F. Drake, G. A. Victor, and A. Dalgarno. *Phys. Rev.*, 180, 1969.

[17] A. H. Gabriel and C. Jordan. *Nature*, 221:947, 1969.

[18] G. W. F. Drake. *Phys. Rev. A*, 3(3):908, 1971.

[19] G. Feinberg and J. Sucher. *Phys. Rev. Lett.*, 26, 1971.

[20] W. R. Johnson and C. Lin. *Phys. Rev. A*, 9, 1974.

[21] W. R. Johnson, D. R. Plante, and J. Sapirstein. *Adv. At. Mol. Phy.*, 35:225–329, 1995.

[22] J. Krause. *Phys. Rev. A*, 34, 1986.

[23] G. Łach and K. Pachucki. *Phys. Rev. A*, 64:042510, 2001.

[24] R. Marrus and R. W. Schmieder. *Phys. Rev. A*, 5, 1972.

[25] H. W. Moos and J. R. Woodworth. *Phys. Rev. Lett.*, 30, 1973.

[26] J. R. Woodworth and H. W. Moos. *Phys. Rev. A*, 12, 1975.

[27] J. R. Crespo López-Urrutia, P. Beiersdorfer, D. W. Savin, and K. Widmann. *Phys. Rev. A*, 58, 1998.

[28] E. Träbert, P. Beiersdorfer, G. V. Brown, A. J. Smith, S. B. Utter, M. F. Gu, and D. W. Savin. *Phys. Rev. A*, 60, 1999.

[29] J. R. Crespo López-Urrutia, P. Beiersdorfer, and K. Widmann. *Phys. Rev. A*, 74:012507, 2006.

[30] H. T. Schmidt, P. Forck, M. Grieser, D. Habs, J. Kenntner, G. Miersch, R. Repnow, U. Schramm, T. Schüssler, D. Schwalm, and A. Wolf. *Phys. Rev. Lett.*, 72, 1994.

[31] E. Träbert. *J. Phys. B: At. Mol. Opt. Phys.*, 43(074034), 2010.

[32] S. S. Hodgman, R. G. Dall, L. J. Byron, K. G. H. Baldwin, S. J. Buckman, and A. G. Truscott. *Phys. Rev. Lett.*, 103:053002, 2009.

[33] D. M. Brink and G. R. Satchler. *Angular Momentum.* Claredon Press, Oxford, third edition, 1993.

[34] L. L. Foldy and S. A. Wouthuysen. *Phys. Rev.*, 78, 1950.

[35] A. Messiah. *Quantum Mechanics Vol. II.* New York : Wiley, 1962.

[36] A. I. Akhiezer and V. B. Berestetskii. *Quantum Electrodynamics.* Interscience, New York, 1965.

[37] H. A. Bethe and E. E. Salpeter. *Quantum Mechanics of One- and Two-Electron Atoms.* Springer, Berlin, 1957.

[38] H. Goldstein. *Classical Mechanics.* Addison-Wesley, second edition, 1983.

[39] E. A. Hylleraas and B. Undheim. *Z. Phys*, 65:759, 1930.

[40] J. K. L. MacDonald. *Phys. Rev.*, 43(830), 1933.

[41] E. A. Hylleraas. *Z. Phys*, 48(469), 1928.

[42] E. A. Hylleraas. *Z. Phys*, 54(347), 1929.

[43] G. W. F. Drake. *Long Range Casimir Forces: Theory and Recent Experiments in Atomic Systems*. Plenum Press, 1993.

[44] G. W. F. Drake. *Atomic, Molecular and Optical Physics Handbook*. AIP Press, 1996.

[45] H. Margenau and G. M. Murphy. *The Mathematics of Physics and Chemistry*. Princeton, N.J. : Van Nostrand, 1964.

[46] G. B. Arfken and H. J. Weber. *Mathematical Methods for Physicists*. Academic Press, 4th edition edition, 1995.

[47] D. J. Griffiths. *Introduction to Quantum Mechanics*. Prentice Hall, third edition, 1995.

[48] G. W. F. Drake. *Phys. Rev. A*, 18:820–826, 1978.

[49] G. W. F. Drake. *Encyclopedia of Applied Physics*, 23, 1998.

[50] A. Dalgarno and E.M. Parkinson. *Proc. Roy. Soc. A.*, 301:253–260, 1967.

[51] M. Cohen. *Adv. At. Mol. Phy.*, 25:195–220, 1988.

[52] M. Cohen and A. Dalgarno. *Proc. R. Soc. A*, 280:258–270, 1964.

[53] B. Klahn and W. A. Bingel. *Theoretica chimica acta*, 44:27–43, 1977.

[54] A. Dalgarno and E. M. Parkinson. *Proc. Roy. Soc. A*, 301:253–260, 1967.

[55] D. C. Montgomery and E. A. Peck. *Introduction to linear regression analysis*. New York : Wiley, second edition, 1992.

[56] R. D. Knight and M. H. Prior. *Phys. Rev. A*, 21:179–187, Jan 1980.

[57] H. T. Schmidt, P. Forck, M. Grieser, D. Habs, J. Kenntner, G. Miersch, R. Repnow, U. Schramm, T. Schüssler, D. Schwalm, and A. Wolf. *Phys. Rev. Lett.*, 72:1616–1619, Mar 1994.

[58] J. R. Crespo López-Urrutia, P. Beiersdorfer, D. W. Savin, and K. Widmann. *Phys. Rev. A*, 58:238–241, Jul 1998.

[59] B. J. Wargelin, P. Beiersdorfer, and S. M. Kahn. *Phys. Rev. Lett.*, 71:2196–2199, Oct 1993.

[60] J. R. Crespo López-Urrutia, P. Beiersdorfer, and K. Widmann. *Phys. Rev. A*, 74:012507, Jul 2006.

[61] J. A. Bednar, C. L. Cocke, B. Curnutte, and R. Randall. *Phys. Rev. A*, 11(460), 1975.

[62] G. Hurbricht and E. Träbert. *Z. Phys. D*, 7(243), 1987.

[63] H. Gould, R. Marrus, and R. W. Schmieder. *Phys. Rev. Lett.*, 31(504), 1973.

[64] H. Gould, R. Marrus, and P. J. Mohr. *Phys. Rev. Lett.*, 33(676), 1974.

[65] R. W. Dunford, D. A. Church, C. J. Liu, H. G. Berry, M. L. Raphaelian, M. Hass, and L. J. Curtis. *Phys. Rev. A*, 41(4109), 1990.

[66] S. Cheng, R. W. Dunford, C. J. Liu, B. J. Zabransky, A. E. Livingston, and L. J. Curtis. *Phys. Rev. A*, 49(2347), 1994.

[67] A. Simionovici, B. B. Birkett, R. Marrus, P. Charles, P. Indelicato, Dietrich D. D., and K. Finlayson. *Phys. Rev. A*, 49(3553), 1994.

[68] B. B. Birkett, J. P. Briand, P. Charles, D. D. Dietrich, K. Finlayson, P. Indelicato, D. Liesen, R. Marrus, and A. Simionovici. *Phys. Rev. A*, 47(R2454), 1993.

[69] R. Marrus, P Charles, P. Indelicato, L. de Billy, C. Tazi, J. P. Briand, A. Simionovici, D. D. Dietrich, F. Bosch, and D. Liesen. *Phys. Rev. A*, 39(3725), 1989.

VITA AUCTORIS

Name:	Lauren Isolde Moffatt
Place of Birth:	Calgary, Alberta
Year of Birth:	1980
Education:	St. Francis High School, Calgary, Alberta
	1995 - 1998
	University of Alberta, Edmonton, Alberta
	1998 - 2002, B.Sc. Hons.
	University of Alberta, Edmonton, Alberta
	2002 - 2004 M.Sc.